Study of the physical and biogeochemical variability of water masses in the Mediterranean Sea

Félix Margirier

THÈSE DE DOCTORAT
DE SORBONNE UNIVERSITÉS

Spécialité : Océanographie Physique

École doctorale : « Sciences de l'Environnement d'Île-de-France »

réalisée au

Laboratoire d'Océanographie et du Climat
Expérimentations et Approches Numériques

présentée par

Félix MARGIRIER

pour obtenir le grade de :

DOCTEUR DE SORBONNE UNIVERSITÉ

Étude de la variabilité physique et biogéochimique des masses d'eaux en Mer Méditerranée

soutenue le 29/11/2018

devant le jury composé de :

M^me^	Pascale BOURUET-AUBERTOT	LOCEAN UPMC, Paris	*Présidente*
M^me^	Karina VON SCHUCKMANN	Mercator Ocean, Toulouse	*Rapportrice*
M.	Bruno ZAKARDJIAN	MIO TLN, Toulon	*Rapporteur*
M^me^	Emma HESLOP	IOC UNESCO, Paris	*Examinatrice*
M.	Gabriel JORDÀ	UIB, Palma de Majorque	*Examinateur*
M.	Daniele IUDICONE	SZN, Naples	*Examinateur*
M.	Laurent MORTIER	ENSTA, Paris	*Directeur de thèse*
M.	Pierre TESTOR	CNRS LOCEAN, Paris	*Co-encadrant de thèse*

"Je ne sais pas parler de la mer. Tout ce que je sais c'est qu'elle me débarrasse soudain de toutes mes obligations. Chaque fois que je la regarde, je deviens un noyé heureux."

Romain Gary

Acknowledgements

Je voudrais tout d'abord remercier Pierre et Laurent de m'avoir accompagné tout le long de cette thèse en me laissant beaucoup de liberté pour orienter mon travail comme je le voulais. Je voudrais aussi vous remercier de m'avoir permis de partir en Mer et en Conférences de nombreuses fois tout au long de la thèse !

Un grand merci également à Karina Von Schuckmann et Bruno Zakardjian qui ont accepté de rapporter mon travail ainsi qu'à Emma Heslop, Gabriel Jordà et Daniele Iudicone qui ont accepté de faire partie de mon jury après m'avoir suivi durant cette thèse.

Je voudrais également remercier Thomas, qui m'a beaucoup aidé avec NEMO, et Blandine, qui m'a souvent aiguillé dans la bonne direction également. Je voudrais remercier tout particulièrement Anthony, qui m'a co-encadré à mes débuts et avec qui les conversations ont toujours étées riches en idées. Il a été un des nombreux co-bureaux que je dois citer ici : Martin la flèchette, Dimitri, Cinthia, Keerthi, Laurent, Yona, Marine, Benjamin, Siny et les nombreux stagiaires squatteurs. Un gros merci à Katia qui m'aura accompagné durant ces trois ans et avec qui j'ai autant travaillé que rigolé dans ce bureau 427.

Un grand merci à tout le LOCEAN, du service administratif au personnel embarqués en passant par la fine équipe de thésards (et associés), on aura bien rigolé ! Une petite mention pour la team cantine, très diverse et qui a jalloné ces trois années. Merci à ma famille de m'avoir soutenu et supporté tout ce temps. Un immense merci à Anda.

Scientific activities during the thesis

Teaching

– Teaching fellow at Université Pierre et Marie Curie in "M1 Introduction to ocean dynamics", "L2 Sutainable Development" and "L1 Geosciences", 196h over 3 years.

Courses and Summer Schools

– PLOCAN GliderScool, Oceanic Platform of the Canary Islands, Spain. 1 week in November 2017, 50h.

– "Climate change and impacts" ED129 doctoral course, 21h.

Oceanographic Cruises

– MOOSE-GE 2018 cruise, 12 days on-board the ATALANTE - 0-4 watch leader. CTD, LADCP and SADCP data processing.

– MOOSE-GE 2017 cruise, 25 days on-board the ATALANTE - 0-4 watch leader. CTD, LADCP and SADCP data processing.

– MOOSE-GE 2016 cruise, 24 days on-board the ATALANTE - Coordination and management of the Cruise web server.

Scientific colloquiums

– Colloque de Liège , Belgium, May 2018 (oral presentation)

– EGU, Vienna, Austria, April 2018 (PICO presentation)

– HYMEX, Barcelona, Spain, July 2017 (oral presentation)

– LEFE-GMMC, Brest, France, June 2017 (oral and poster presentations)

– EGU, Vienna, Austria, April 2017 (poster presentation)

– CIESM, Kiel, Germany, October 2016 (PICO presentation)

– EGO confernce, Southampton, England, September 2016 (oral and poster presentations)

– EGU, Vienna, Austria, April 2016 (poster presentation)

Résumé

Étude de la variabilité physique et biogéochimique des masses d'eaux en Mer Méditerranée

L'explosion du nombre d'observations in-situ collectées en Mer Méditerrranée au cours des 15 dernières années offre de nouveaux moyens d'analyse et de suivi des masses d'eaux. L'accent a été mis sur la Méditerranée Nord-Occidentale, siège du phénomène dit de convection profonde et plus intensément observée. Notemment grâce aux observations à hautes résolutions temporelles et spatiales de gliders, un réchauffement et une salinification intense des Eaux Levantines Intermédiaires (LIW) a été mis en évidence. Des indicateurs de variabilité de la LIW ont été construits et sa circulation a été détaillée. En l'absence de convection profonde depuis l'hiver 2012/2013, le bassin a été envahi par ces eaux non diluées dans les eaux profondes et un nouvel état du bassin est observé. Afin de mieux comprendre comment la convection profonde régule la Méditerranée Occidentale, une étude de processus a été effectuée et les importances relatives du préconditionnement océanique et des flux atmosphériques ont été évaluées afin de discuter la possibilité d'évènements convectifs profonds futurs. Pour la première fois, les propriétés physiques et biogéochimiques des plumes convectives ont été caractérisées et s'inscrivent dans le nouveau paradigme de la convection profonde proposé.

Mots-clés: Mer Méditerranée, convection profonde, series temporelles, gliders, plumes convectives, vitesses verticales, observations oceanographiques in-situ.

Abstract

Study of the physical and biogeochemical variability of water masses in the Mediterranean Sea

The numerous in-situ observations collected in the Mediterranean Sea over the past 15 years enable a new analysis, and the monitoring of water masses is now possible. A focus has been put on the North-Western Mediterranean Sea where deep convection occurs. Thanks to the numerous high resolution temporal and spatial data collected notably by gliders, an intense warming and salinification of the Levantine Intermediate Water (LIW) was evidenced. Indexes have been built to monitor the LIW and its spreading pattern was further described. This warming and salinification concurs with the absence of deep convective events since winter 2012/2013 and the basin has been invaded at intermediate depth by the new waters. The interplay between the key deep convection phenomenon and the warming at intermediate levels was explored through the mixing agents: for the first time, the physical and biogeochemical properties of convective plumes were characterised and have been integrated in the new paradigm for deep convection. In order to better understand how the deep convective events regulate the basin, the relative importance of oceanic preconditioning and of atmospheric fluxes, as well as the possibility of future deep convective events were discussed.

Keywords: Mediterranean Sea, deep convection, time series, gliders, convective plumes, vertical velocities, oceanographic in-situ observations.

Contents

List of Figures

List of Abbreviations

AW	**A**tlantic **W**ater
mAW	**m**odified **A**tlantic **W**ater
WIW	**W**inter **I**ntermediate **W**ater
LIW	**L**evantine **I**ntermediate **W**ater
WMDW	**W**estern **M**editerranean **D**eep **W**ater
EMDW	**E**astern **M**editerranean **D**eep **W**ater
NC	**N**orthern **C**urrent
NBF	**N**orth **B**alearic **F**ront
WCC	**W**estern **C**orsican **C**urrent
GoL	**G**ulf **o**f **L**ions
MOOSE	**M**editerranean **O**cean **O**bserving **S**ystem for the **E**nvironment
OSSE	**O**bserving **S**ystem **S**imulation **E**xperiment
EGO	**E**veryone's **G**liding **O**bservatories
CTD	**C**onductivity-**T**emperature-**D**epth
XBT	**E**xpandable **B**athy**t**hermograph
MBT	**M**echanical **B**athy**t**hermograph
Argo	**A**rray for **r**eal-time **g**eostrophic **o**ceanography
MLD	**M**ixed **L**ayer **D**epth
SCV	**S**ubmesoscale **C**oherent **V**ortex
SCVs	**S**ubmesoscale **C**oherent **V**ortices

Introduction

Contents

0.1 Global Ocean

About 71% of the Earth's surface is covered by water, making the oceans not only key in the study of the climate system but also full of unknown physical processes and biological mysteries[1].

With a mean depth of 3800 m, the oceans form a very thin layer on the globe and the vertical dimensions have to be exaggerated in order to represent the vertical structure of the water column [Fieux, 2010], which plays an essential role in the thermohaline circulation. The surface layer can be decomposed into two parts: into the upper mixed layer where air-sea exchanges take place and into the stratified zone where vertical gradients (temperature, salinity, oxygen, nutrients...) are strong. The ocean-atmosphere exchanges drive the ocean circulation at a global scale through wind forcing [Sverdrup, 1947], which together with the buoyancy fluxes are also responsible for vertical mixing (overturning being induced by heat loss and evaporation), restratification (heat gain and rainfall lightening the surface waters), and a thermohaline circulation, as presented Figures 0.1 and 0.2. Figure 0.1 diplays the complex array of physical and biogeochemical processes taking place in the oceans, showing its key role notably for the rapid heat and salt transfer to the deep ocean, they are "stored" on those short time scales and will get released on longer time scales and larger spatial scales.

The global ocean circulation (idealised scheme represented in Figure 0.2) transports heat from the tropics to the high latitudes, where heat is transferred to the atmosphere

[1] 2000 new marine species are discovered each year [World Register of Marine Species, http://www.marinespecies.org/photogallery.php].

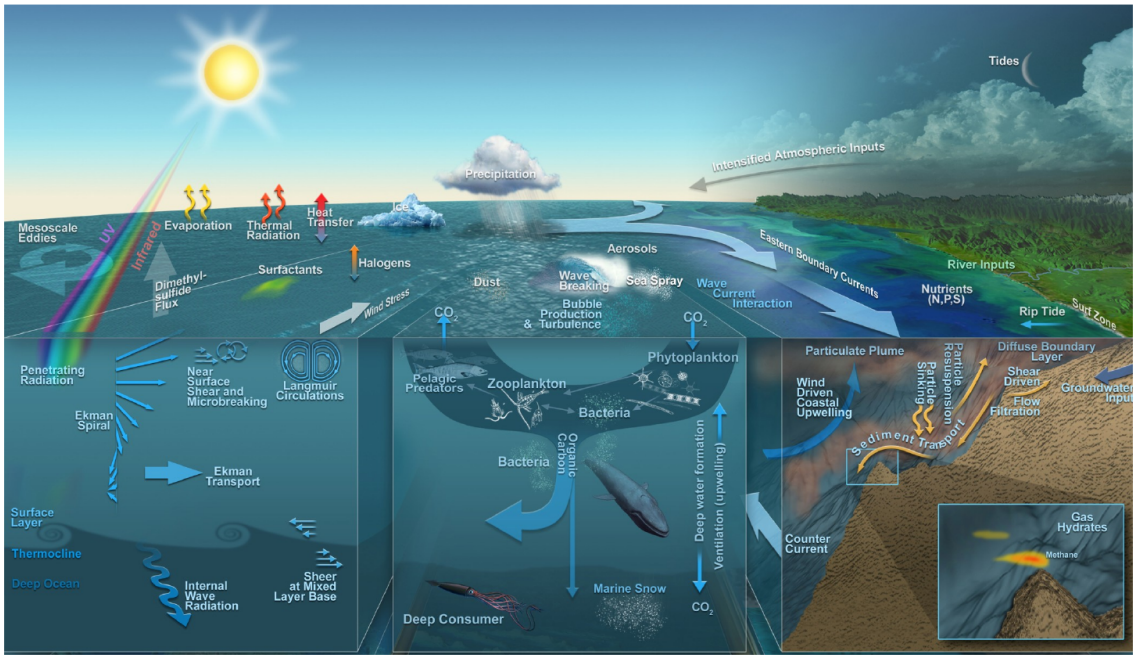

FIGURE 0.1: Upper Ocean physical and biogeochemical main processes. Illustration designed by John Delaney and Mark Stoermer; created by the Center for Environmental Visualization (CEV) for the NEPTUNE Program, University of Washington, Seattle.

and intermediate and deep waters are formed. The vertical stratification is highly variable depending on the region and the time of the year, and, in extreme cases, the mixed layer can reach great depths. This phenomenon of open-ocean deep convection will be discussed in depth in Section 0.3. In those regions, there is no stable pycnocline and deep waters can be formed down to the ocean floor. This rare phenomenon only happens in a select few locations: in addition to polar regions such as the Labrador Sea [Gascard and Clarke, 1983], the Greenland and Norwegian Seas, the Weddell and Ross Seas [Killworth, 1983]; open-ocean deep convection also takes place in the East Japan Sea and in the Mediterranean Sea [MEDOC-Group, 1970]. The mean circulation time scale has been estimated at 1000 years and changes in the decadal variability modes could have many impacts on the climate system.

Although water masses are mainly identified by their temperature and salinity, non-conservative properties such as dissolved oxygen and nutrients (e.g. nitrates, phosphates, silica) are also characteristic of regions and formation periods, and play an important biogeochemical role.

0.2 The Mediterranean Sea: a miniature global ocean

The Mediterranean Sea is often referred to as a miniature global ocean, as it exhibits all the processes at play in the global ocean circulation with nowadays the exception of ice related processes (the Mediterranean area was covered by glaciers a long time ago). Its

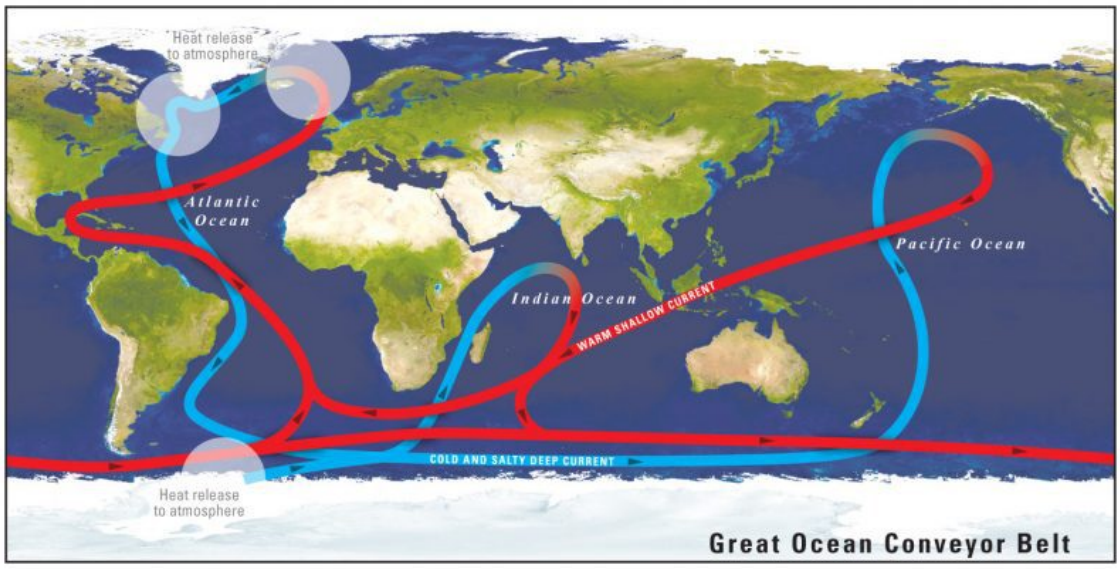

FIGURE 0.2: Simplified scheme of the global circulation and overturning. The white spots indicate locations of deep water formation. The mean surface circulation is in red and the deep circulation pattern is in blue. Illustration from United States Geological Survey[2], after Broecker (1991).

reduced size and accessibility make it an ideal laboratory for impact studies: the Mediterranean is both under important anthropogenic pressure and more responsive to changes [Giorgi, 2006; Somot et al., 2006; Vaquer-Sunyer and Duarte, 2013], as its general circulation time is estimated to be around 100 years, 10 times less than that of the global ocean [Durrieu de Madron et al., 2011]. It also has a global impact, as it exchanges water masses with the Atlantic and influences its hydrology by injecting salt at intermediate depths.

0.2.1 Mediterranean geography, hydrology and climate

The Mediterranean Sea, a semi-enclosed sea confined between the mountainous continental masses of Europe, Africa and Asia, is a deep interior concentration basin extending from 6°W to 36°E (over 4000 km) and 30°N to 46°N (over 800 km). With an average depth of 1500 m and a maximum depth of 5000 m, it is connected to the Atlantic Ocean via the Gibraltar Strait (300 m deep) and to the Black Sea via the Dardanelles Strait (100 m deep). It is composed of two main basins separated by the Sicily Channel (400 m deep): the Western Mediterranean and the Eastern Mediterranean. The two basins are themselves divided in sub-basins: From East to West, the Alboran Sea, the Balearic Sea, the Algerian Basin, the Northwestern Mediterranean Sea and the Tyrrhenian Sea in the Western Mediterranean; and the Adriatic Sea, the Ionian Basin, the Aegean Sea and the Levantine Basin in the Eastern Mediterranean (see Figure 0.3).

The Mediterranean is classified as antiestuarine and accumulative, as evaporation dominates [Sanchez-Gomez et al., 2011] and the influx of **A**tlantic **W**ater (AW) through

the Stait of Gibraltar (0.81 Sv[3]) is counterbalanced by the export of colder (on average) and more saline waters at depth into the Atlantic (0.78 Sv) [Soto-Navarro et al., 2015]. Along its circulation pathway, the AW is modified through ocean-atmosphere interactions and mixing with environing waters, gradually becoming more saline and denser.

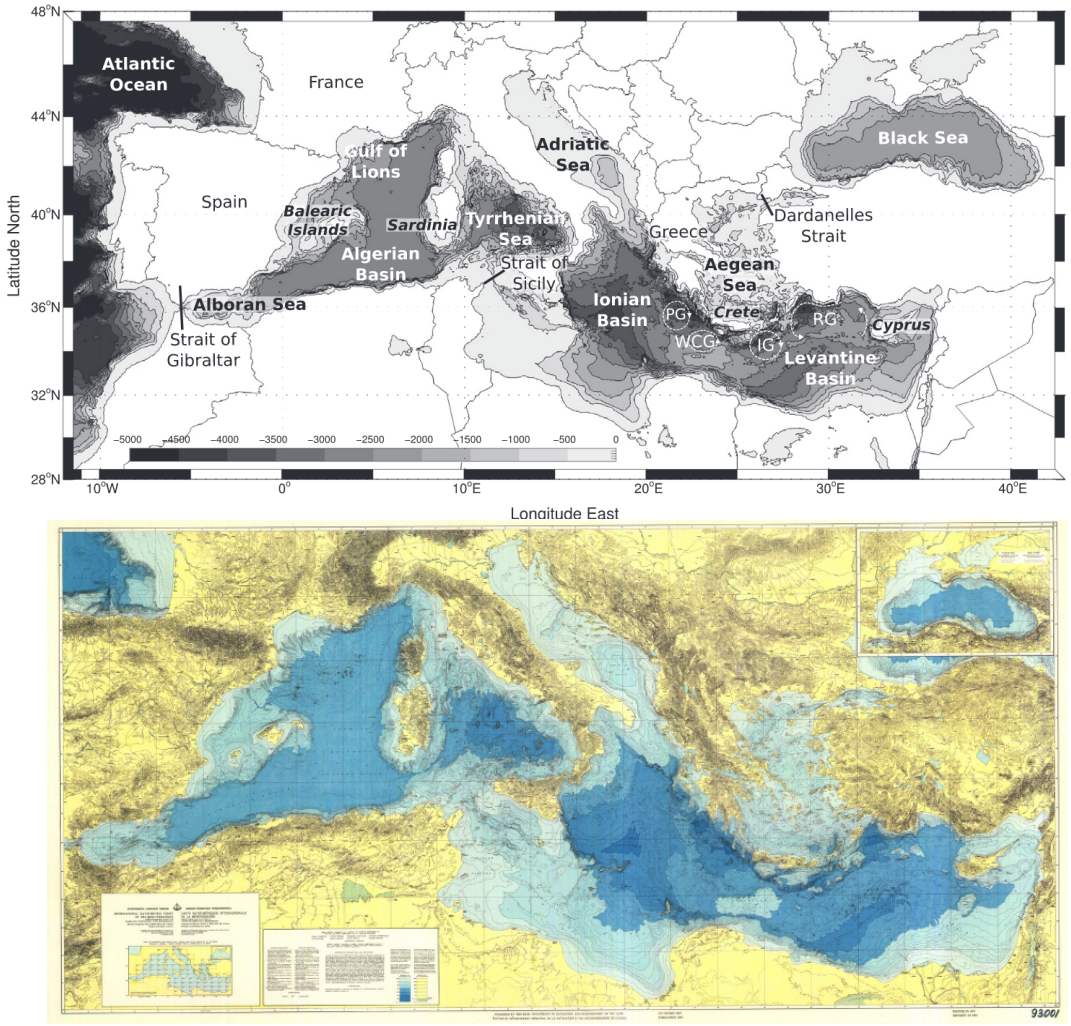

FIGURE 0.3: (top) Bathymetry and main sub-basins of the Mediterranean Sean, from Houpert et al. (2015), (bottom) Mediterranean bathymetry and the surrouding mountainous topography, from the International Bathymetric Chart of the Mediterranean.

The mountainous surroundings of the Mediterranean make it subject to various northern cold and dry catabatic winds. In winter, winds such as the Mistral and the Tramontane in the Gulf of Lions, the Bora in the Adriatic Sea, and the Etesian winds in the Aegean Sea trigger heat losses at the surface of the ocean that can locally reach more than 1000 W.m^2. This strong forcing triggers an intense vertical mixing activity and a higher seasonality in the **M**ixed **L**ayer **D**epth (MLD) compared to that of the global ocean [Houpert et al., 2015; D'Ortenzio et al., 2005]. These dynamics are crucial both for the water mass transformations and for the phytoplanktonic activity through the injection

[3] $1\ SV = 10^6\ m^3.s^{-1}$

of nutriments in the surface layer, controlling the marine ecosystems [D'Ortenzio and Ribera d'Alcalà, 2008; Lavigne et al., 2013; D'Ortenzio et al., 2014].

0.2.2 The Mediterranean biogeochemical stakes

Not only is the Mediterranean Sea a miniature global ocean, it is also subjected to intense anthropogenic forcing. The Mediterranean Basin is a very highly populated area (see Figure 0.4) and undergoes intense marine traffic and pollutions. Monitoring the changes in the region is key for the tourism industry but also for fisheries [Sánchez-Muros et al., 2018].

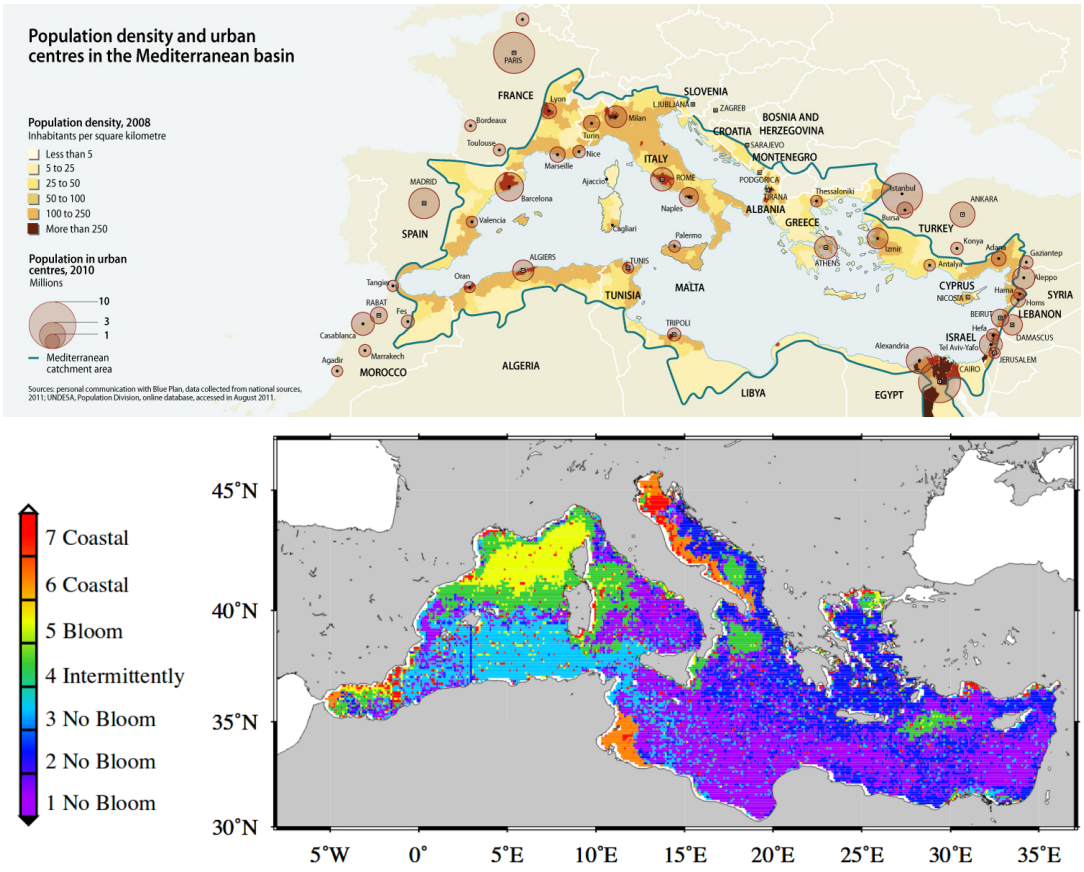

FIGURE 0.4: (top) Population density and urban centres in the Mediterranean basin, retrieved from GRID-Arendal [http://www.grida.no/resources/5900], (bottom) Mediterranean bioregions determined with the k-means on the seasonal cycle, from D'Ortenzio and Ribera d'Alcalà (2008).

The marine trophic chain begins in the upper ocean where the phytoplankton lives, controlled by light and nutrient availability [Mann and Lazier, 2005]. The light is rapidly attenuated in the surface (only 10% of the surface light is transmitted to 90 m depth in a clear ocean), and the nutrient concentration is generally low near the surface due to rapid consumption by the phytoplankton. This explains why, most of the time, the phytoplankton concentration maximum is observed in the subsurface. The deep chlorophyll maximum is usually observed within a layer of density stratification, the pycnocline,

which usually coincides with the nutricline. As phytoplankton account for 50% of the photosynthetic activity on Earth, this phenomenon is part of the ocean biological pump, which is estimated to absorb half of the anthropogenic carbon [Sabine et al., 2004]. The Mediterranean is no exception to this phenomenon and presents a wide array of biogeochemical behaviours that can be found in the global ocean, as presented in Figure 0.4. The Mediterranean is indeed host of various biogeochemical regimes ranging from blooming to oligotrophical regimes: despite its small surface, the Mediterranean hosts up to 4-18% of the total marine diversity [Bianchi and Morri, 2000]. Deep convective processes also have impacts on the benthic life and deep organisms [Marco Luna et al., 2016; Rastelli et al., 2018].

Therefore, the Mediterranean is key to explaining some global processes, as it is easily accessible, and observing its response to anthropogenic forcing may provide a first important step towards protecting the global ocean.

0.2.3 The Mediterranean water masses

The Mediterranean circulation is described by a three layer system comprised of three main water masses: surface waters, intermediate waters and deep waters. The Mediterranean Waters and their circulation have been thoroughly described [see reviews Pinot and Ganachaud, 1999; Pinardi and Masetti, 2000; Malanotte-rizzoli, 2001; Millot and Taupier-Letage, 2005a; López-Jurado et al., 2005; Schroeder et al., 2012; Jordà et al., 2017], and a brief summary of the main characteristics is presented in the following.

The Surface Waters

The surface layer (down to ∼250 m) of the Mediterranean is comprised of AW. As its name indicates, the AW enters the Mediterranean Sea at the Strait of Gibraltar, and follows a cyclonic pathway along the coast in the two basins (see Figure 0.5.A). Characterised by a salinity minimum (S∼36) as it enters the Mediterranean, it gradually salinifies through mixing and under the influence of evaporation to reach S∼39 in the Eastern Basin. The AW located in the main circulation vein, close to the coast, has a lower salinity than the surface waters in the centre of the basins, which have a higher residence time.

The main cyclonic circulation pathway of the surface waters is well known beacuase of its easier access through in-situ observation with drifting buoys and satellite altimetry [Birol et al., 2010; Poulain et al., 2012]. This mean circulation pattern is subject to a high variability controlling a great part of the coast/offshore exchanges:

- The Mediterranean exhibits a marked seasonal variability: the MLD can greatly vary between seasons and locations, and coastal currents intensify in winter when the density gradients between the coast and offshore are more significant (e.g. the **N**orthern **C**urrent (NC) gets thinner and deeper, reaching ∼0.5 cm.s^{-1} compared to ∼0.3 cm.s^{-1}) [Millot, 1999].

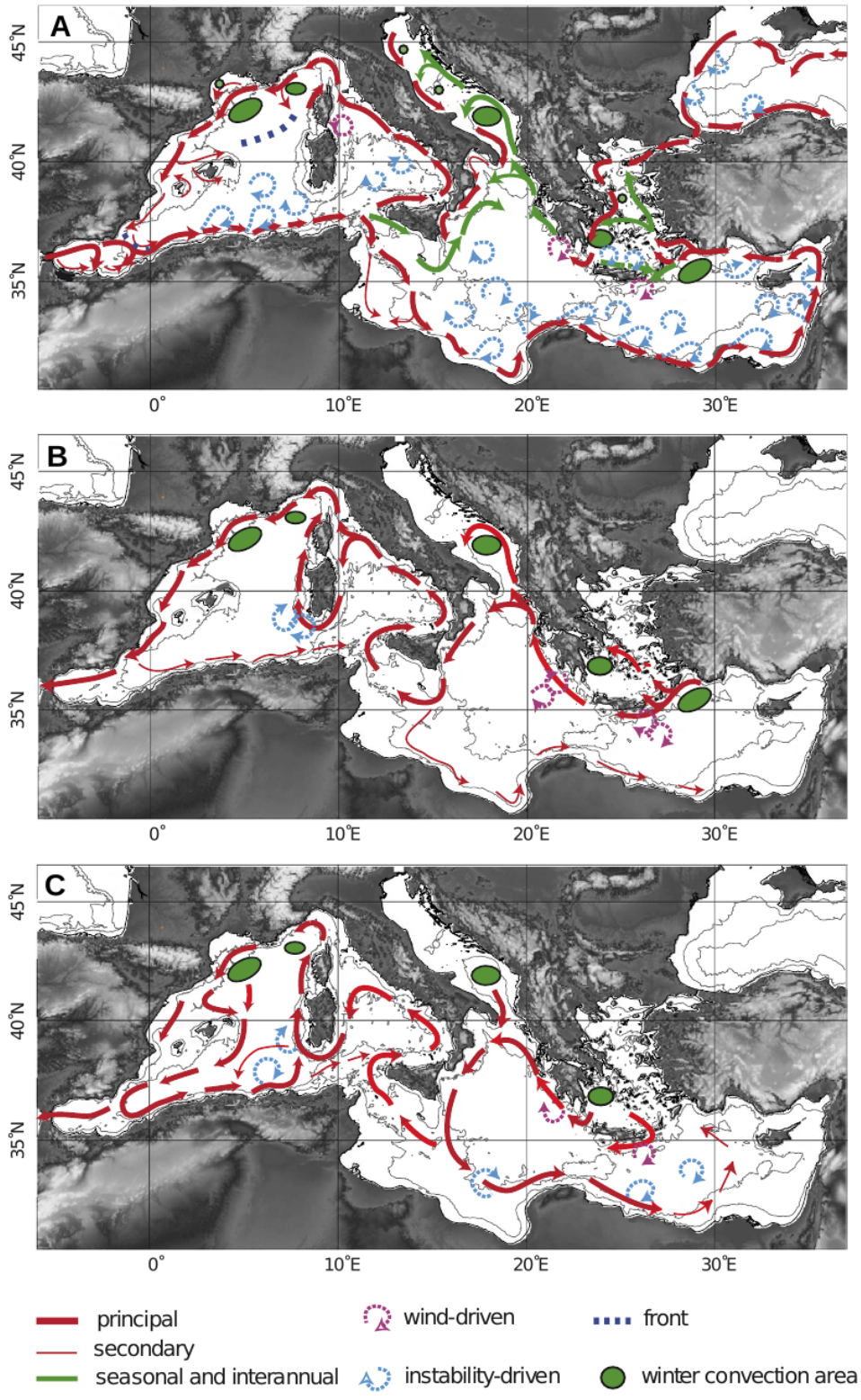

FIGURE 0.5: (a) Surface, (b) intermediate and (c) deep water masses circulation patterns in the Mediterranean Sea , from Durrieu de Madron et al. (2011) after Millot and Taupier-Letage (2005).

- Intense mesoscale activity (occurring at spatial scales of 10-100 km) has been extensively observed, for example in the Algerian meanders and eddies or in the oscillations associated with the Eastern Mediterranean Transient [Borzelli et al., 2009;

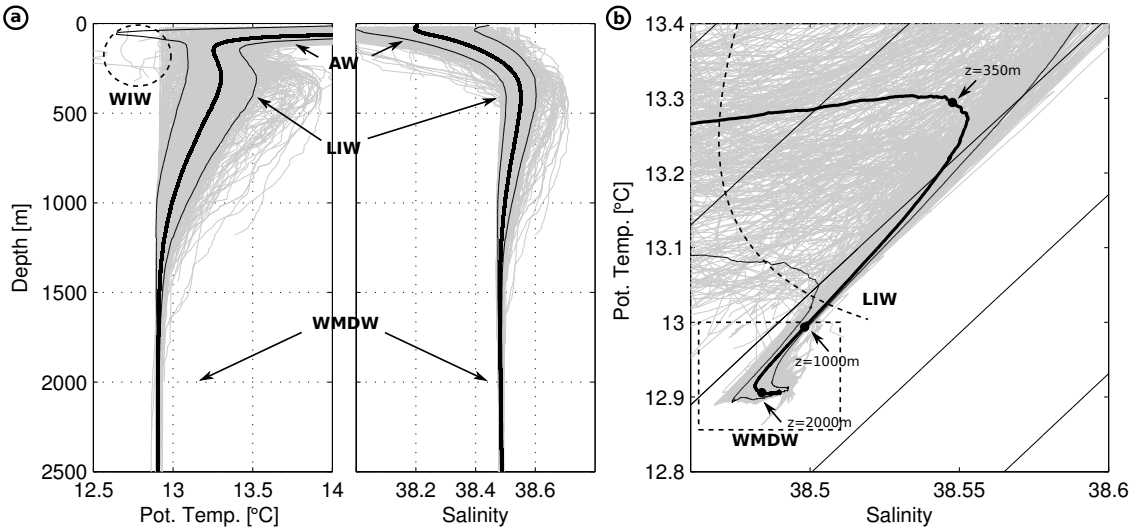

FIGURE 0.6: (a) Potential temperature and salinity profiles, (b) θ/S diagram. Built from reference CTD profiles collected in 2012 and 2013 in the Northwestern Mediterranean Sea . The water masses present in the region are annotated: **A**tlantic **W**ater (AW), **W**inter **I**ntermediate **W**ater (WIW), **L**evantine **I**ntermediate **W**ater (LIW), **W**estern **M**editerranean **D**eep **W**ater (WMDW), from Bosse, thesis, 2015

Gacic et al., 2010]. It can be generated by topographic waves or instabilities in the coastal current.

- Sub-mesoscale activity can occur in density fronts where filaments of high vertical velocities may form, and impact the primary production. Sub-mesoscale eddies (1-10 km) may also be formed and are key in the spreading of newly formed intermediate and deep waters [Bosse, thesis, 2015].

The Intermediate Waters

Intermediate waters (between $\sim 300 - 1000$ m) are formed by convection through ocean-atmosphere interactions. Significant surface heat losses induce buoyancy fluxes that lower the MLD through turbulent processes. This mixing induces a new water mass, usually referred to as "Mode Water". As the convection depth varies in place and time, reaching the ocean floor or not, the 'intermediate waters' denote waters formed at intermediate depths. Their circulation pattern is similar to that of the surface waters as they follow the coastal bathymetry in a cyclonic motion. They also spread to the center of the basins, for instance through sub-mesoscale eddies [Bosse et al., 2015].

The main intermediate water mass present in the Mediterranean is the LIW. Formed in the Eastern Basin, it results from the mixing of surface AW down to 500-1000 m in the Levantine Basin. The surface waters here are some of the saltiest waters found in the Mediterranean (S>39), due to intense evaporation in summer. The LIW formed with these warm and extremely saline surface waters is identified by a marked local temperature and/or salinity maximum at intermediate depths (typically between 300 and 800 m, see Figure 0.6 in the Western Basin). This sub-surface maximum is detected throughout

the Mediterranean, and as the LIW travels away from the Levantine Basin, its signature is attenuated as it mixes with environing waters. It mixes with the Cretan Intermediate Water [Millot, 2013] in the Eastern Basin before entering the Western Mediterranean through the Sicily Channel, where it undergoes significant mixing [Vladoiu et al., 2018]. In the Western Basin, the LIW is also marked by a local minimum of dissolved oxygen, due to the long time elapsed since the last contact with the atmosphere, illustrating its old formation compared to the surrounding waters. The LIW is even present at the Strait of Gibraltar, where it makes up half of the exiting waters [Gascard and Richez, 1985; Bryden et al., 1994]. It stores a significant amount of heat and salt at intermediate depths and is present throughout the Mediterranean Sea, playing a crucial role in the Mediterranean thermohaline circulation [Grignon et al., 2010]. It notably plays a key role in preconditioning the Northwestern Mediterranean for deep convective events.

Another significant intermediate water investigated in this thesis is the WIW. Formed in the Northwestern Mediterranean Sea in winter by intermediate offshore convection, it lies over the LIW and is marked by a local temperature minimum and a dissolved oxygen maximum. It can also be formed on the Gulf of Lions plateau [Juza et al., 2013] by localised mixing processes. It plays an important role in the Balearic Sea spring/summer circulaton right after its formation [Pinot et al., 1999; Heslop et al., 2012; Juza et al., 2018].

The Deep Waters

The deep waters, found below 1000 m, are formed in very specific regions in the Eastern (Adriatic and Aegean Seas) and Western (Gulf of Lions) basins. Their formation results from a complex combination of processes detailed in Section 0.3, which restricts their occurrence only to these specific regions.

The **E**astern **M**editerranean **D**eep **W**ater (EMDW) is mostly formed in the Adriatic Sea under the influence of the Bora winds (and occasionally through deep water cascading events [Ivanov et al., 2004]) but, during the 1990s, the meteorological conditions favoured the formation of slightly warmer, much saltier, and thus denser deep waters in the Aegean Sea [Roether et al., 1996; Lascaratos et al., 1999; Gačić et al., 2011]. These new waters then invaded the bottom Eastern Basin, causing what is now referred to as the Eastern Mediterranean Transient, interfering with the characteristics of the waters exported to the Western Mediterranean [Gasparini et al., 2005].

The WMDW is formed in the Northwestern Mediterranean Sea through winter deep convection. Its intermittent formation [Mertens and Schott, 1998; Schroeder et al., 2008a] also varies in terms of the volume of deep water formed, which is a key indicator that is difficult to estimate. The WMDW can also be formed through "dense water cascading" events close to the coast in the Gulf of Lions, but not as often and in smaller volumes [Durrieu de Madron et al., 2005]. Studies by Durrieu de Madron et al. (2013) and Schroeder et al. (2008) suggest that the Western Mediterranean underwent an intense renewal of its deep waters over the past decade. After having stable properties in the first half of the XXth century [Lacombe et al., 1985], the WMDW has been observed to salinify and

warm since the 1970s [Béthoux et al., 1990] until the present day [Schroeder et al., 2010; Houpert, 2013; Somot et al., 2016]. These deep waters form the other half of the exiting waters in the Gibraltar overflow, with waters as deep as 700-1300 m crossing the 300 m deep strait through the Bernoulli effect [Stommel et al., 1973; Kinder and Parrilla, 1987].

The Mediterranean outflow

Comprised of both intermediate and deep waters, the Mediterranean outflow sinks to its neutral buoyancy depth around 1100 m after exiting through the Strait of Gibraltar [Ambar and Howe, 1979]. It then spreads along isopycnals and can be traced throughout the Atlantic Basin [Fieux, 2010]. The outflow transports salt across the Atlantic in coherent vortices known as Meddies (Mediterranean Eddies) [Armi and Zenk, 1984; Armi et al., 1988] and thus has an important impact on the Atlantic water masses characteristics as well as on the thermohaline circulation and its variability [Candela, 2001][4]. As an increase in the temperature and salinity of intermediate and deep Mediterranean waters has been reported both in the Eastern Basin notably in Roether et al. (1996); Ozer et al. (2016)] and in the Western Basin notably in Béthoux et al. (1990); J. Rohling and L. Bryden (1992); Schroeder et al. (2010); Houpert (2013), this trend has also been evidenced in the Mediterranean outflow [Millot et al., 2006].

0.3 Deep convection in the Gulf of Lions

Deep convection was observed for the first time by the MEDOC-Group (1970) during the winter of 1969 in the Gulf of Lions, centered around 42°N 5°E. It is an intermittent phenomenon [Gascard, 1978; Somot et al., 2016] and presents wide variations in intensity and volume of new waters formed from year to year. Deep convection is usually depicted in three phases illustrated in Figure 0.7 [Marshall and Schott, 1999]:

FIGURE 0.7: The three phases of deep convection. **a.** preconditionning **b.** vertical mixing **c.** lateral exchanges and spreading, from Marshall and Schott (1999).

Preconditioning

The mean cyclonic circulation in the North of the Western Mediterranean induces a doming of the isopycnals, bringing deeper waters nearer to the surface and thus exposing less stratified waters to atmospheric forcing in the centre of the gyre. The deep layers are hence nearer to the surface in the centre of the dome and more easily reached by local

[4]Climate control needs a dam at the Gibraltar Strait to regulate the changes. [Gower, 2015]

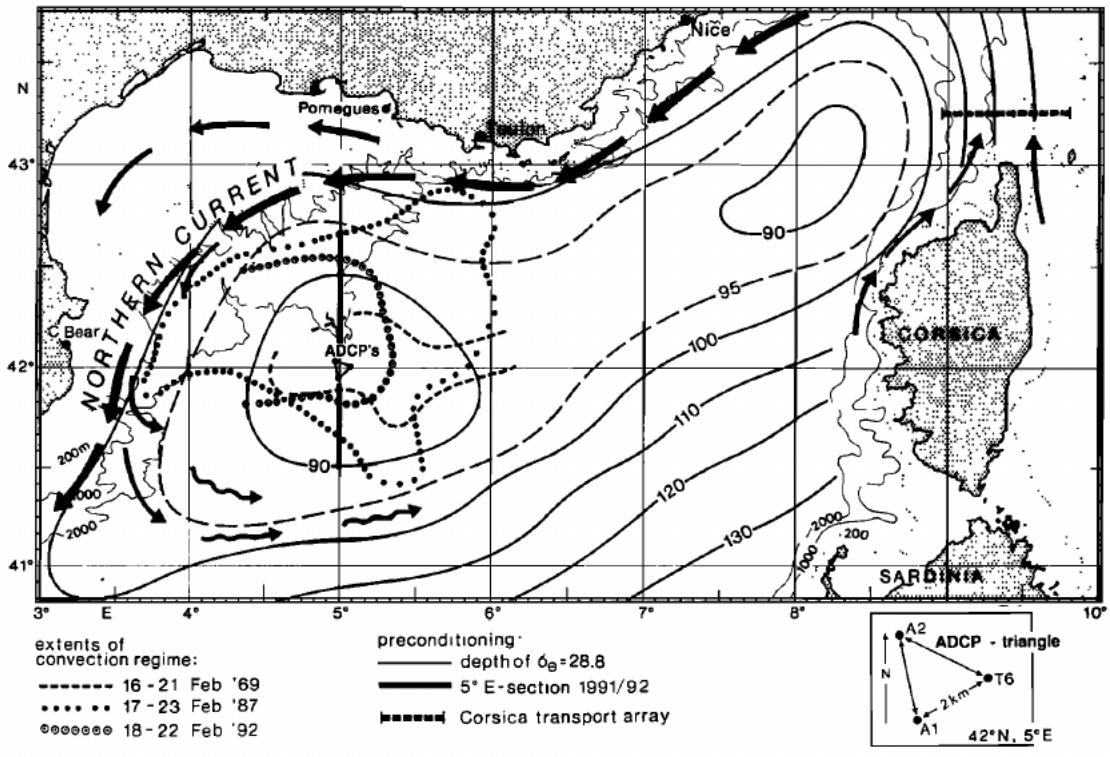

FIGURE 0.8: The preconditioning phase. Superimposed on the mean cyclonic circulation pattern are the depth of the 28.8kg.m^{-3} isopycnal (m) and the lateral extention of the convection area in 1969,1987 et 1992, from Marshall and Schott, 1999.

heat losses, less energy is necessary to reach those layers as seen in Figure 0.8. Moreover, the LIW is a key component in the preconditioning: when the mixing reaches the very salty LIW, there is a density gain and the mixing is enhanced [Lacombe et al., 1985; Madec et al., 1996; Grignon et al., 2010].

Vertical mixing

Depending both on the intensity of the atmospheric forcing and on the preconditioning, deep convection does not occur every year. Under the intense heat losses and evaporation (heat losses can easily reach -1000 W.m^{-2} [Mertens and Schott, 1998]), the stability of the water column is weakened in preconditioned areas, allowing the appearance of convective cells called plumes, O(1 km) in diameter and over the whole water column. In the downward plumes, the vertical velocities can reach 10 cm.s^{-1} [Leaman and Schott, 1991; Visbeck et al., 1996]. The mean vertical velocities being zero during the convective episodes, the plumes are more significant in terms of the mixing they induce than in terms of the transport to the deep waters. This violent vertical mixing phase produces a significant volume of mixed waters and renews the deep layers. The mixed patch (if it exists) varies both in shape and depth from year to year, and it is characterised by the different spatial scales depicted in Figure 0.9: plumes, eddies and gyre. Its typical radius is of 50–100 km and it presents horizontal inhomogeneities at meso- [Frajka-Williams et al., 2014] and submeso-scales [Marshall and Schott, 1999].

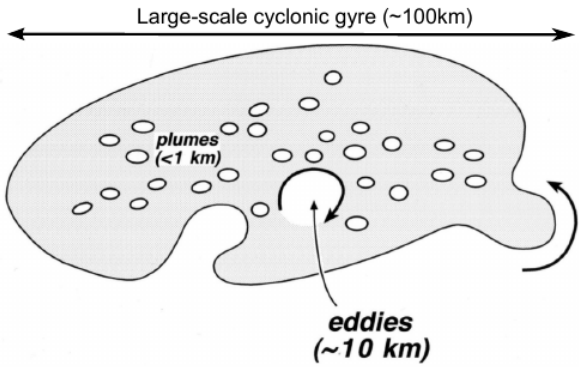

FIGURE 0.9: The different scales of deep convection, from Marshall and Schott, 1999.

Numerical experiments conducted by Marshall and Schott (1999) showed that the horizontal density gradient between the mixed patch and the surrounding waters was at equilibrium with a peripheral rim current around the mixed patch. This rim current is baroclinically unstable and generates eddies which in turn induce lateral fluxes [Gascard, 1978; Gascard and Clarke, 1983]. These experiments suggest that baroclinic instability acts against vertical mixing by restratifying and exporting the newly mixed waters out of the mixed patch, but also that it enhances the mixing by bringing deep waters nearer to the surface.

When the rim current component of the baroclinic instability may act against vertical mixing, the MEDOC-Group (1970) conjectured that the horizontal gradient component could act to maintain the mixing. The instability indeed injects surrounding waters in the mixed patch as it exports newly formed waters. These surrounding waters, as they get pushed nearer to the surface by oblique convection movements induced by the baroclinic instability, can be mixed through atmospheric forcing. This eddy producing process can also favour vertical mixing by preconditioning an area at mesoscale. This is in good agreement with numerical simulations which showed that the baroclinic instabilities and the atmospheric forcing act together and induce more vertical mixing than when considered independently [Legg and McWilliams, 2001; Straneo and Kawase, 1999].

Restratification, lateral exchanges and spreading

After the strong forcings, lateral energy exchanges reconquer the basin. Eddies form and spread under the influence of rotation and stratification [Visbeck et al., 1996; Jones and Marshall, 1997]. Send et al. (1996) observed temperature fluctuations on mooring line recordings along the Spanish coast, which could result from an incorporation of new waters in the coastal Northern Current. They estimated that 50% of the newly formed waters could "escape" in the coastal current. Numerical simulations conducted by Madec et al. (1991) also indicate such a mechanism. These waters would then follow the cyclonic circulation pattern all the way to the Tyrrhenian Sea, and would return to the mixing area 30 years later. Testor and Gascard (2006) estimate that another 50% of the newly formed waters can spread in the basin in the form of very coherent (lifespan $>$ 1.5 years) lenticular (h $\sim$ 1 km) deep mesoscale eddies (5–10 km in radius).

Naturally, these three phases overlap throughout the year and a memory feedback is observed as the restratification and the spreading patterns partly determine the following year's preconditioning.

This vision of deep convection will be completed and updated in Chapter 2, which presents a new understanding of deep convection thanks to an intense observational effort conducted in the Northwestern Mediterranean Sea in the winter 2012/2013.

0.4 Cascading of deep waters in the Gulf of Lions

Another source of WMDW results from the cascading of waters formed on the shallow (∼100 m) Gulf of Lions shelf. Dense shelfwater cascading can occur in shallow regions separated from the deep ocean by a steep slope [Ivanov et al., 2004; Durrieu de Madron et al., 2005], which precisely characterise the Gulf of Lions shelf. The four main phases of dense shelfwater cascading are described by Shapiro et al. (2003): first, dense water accumulates on the shelf during the preconditioning phase. Then, this density front propagates down the slope. A dense steady flow eventually forms along the slope and the dense waters finally reach their neutral buoyancy level where they spread (see Figure 0.10). The Gulf of Lions shelf is separated from the deep ocean by several canyons which act as natural corridors for the dense waters [Durrieu de Madron et al., 2005; Canals et al., 2006; Font et al., 2007].

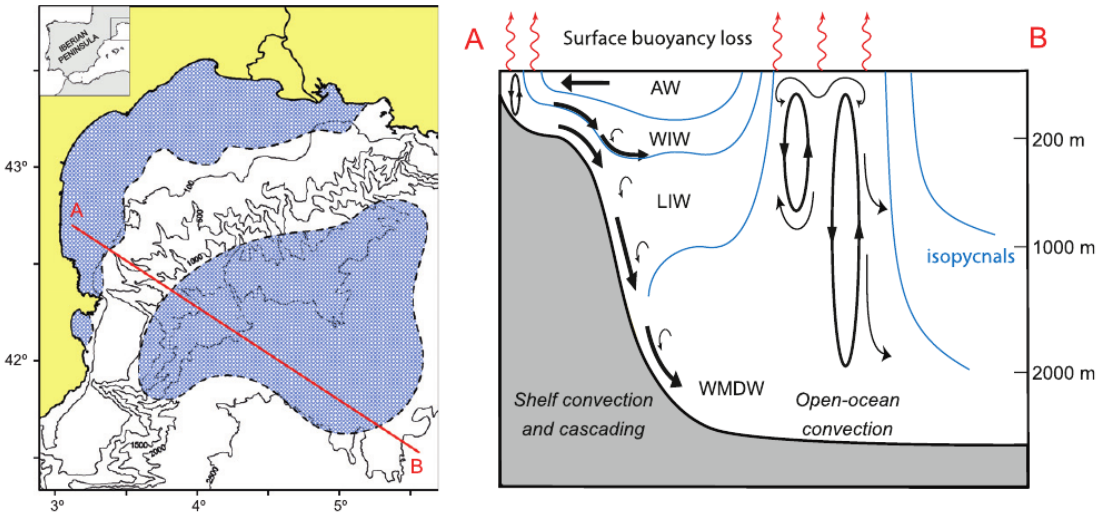

FIGURE 0.10: The interactions between cascading and open ocean convection in the Gulf of Lions. (left) Bathymetric map of the region, the dense water formation sites are in blue patches. (right) Vertical section in the convection area, from Puig et al. (2013).

Both deep water formation processes can occur simultaneously or separately, and the deep waters formed by both interact and lie at their respective neutral buoyancy depths, overlapping one another. Much like deep convection, dense shelfwater cascading

is intermittent and does not occur in the same proportions every year, if at all [Béthoux et al., 2002].

0.5 Motives and Objectives of the thesis

In this context of a changing Mediterranean Sea, threatened by various sources of anthropogenic forcings (global climate change, pollutions, spatial planning, tourism, fisheries), it is crucial to better understand this system. Crucial not only for better monitoring, but also for better model representations in order to anticipate the impacts of human activity and address the topical issues of climate change, environment protection, sustainable resources management and marine safety. With the revolutionary dataset collected in the Northwestern Mediterranean Sea in the past 10 years, we have the means to analyse key phenomena like deep convection, and to understand the long-lasting impact they have on the basin. Furthermore, the glider measurements of finescales during extremely hard to observe convective events –happening in remote regions of the globe in winter when sea conditions are harsh– provide a novel set of data in the convective patch.

The main scientific questions addressed in this work are listed below:

– Can we create relevant indexes and time series to monitor the hydrological state of the Northwestern Mediterranean ?

– Can these indexes help assess the performance of a numerical model in reproducing the state and variability on local and basin scales ? How can we in-turn use the models to assess the chosen sampling strategy ?

– How does the intermittent character of deep convection affect the rest of the basin ?

– Can we characterise the properties of the mixing agents of open ocean deep convection on a small temporal and spatial scale ?

After a general introduction to the Mediterranean Sea presented in Section 0, the revolutionary available dataset is introduced in Chapter 1. This dataset enables a better characterisation of deep convection presented in Chapter 2. Thanks to an intense observational effort during the winter 2012/2013, the properties of the waters in convective plumes were characterised for the first time and a revised paradigm for deep convection after the vision of Marshall and Schott (1999) is offered. Benefiting from this thorough description of deep convection, Chapter 3 presents time series of LIW over the past 10 years in the Northwestern Mediterranean Sea and investigates how deep convection not only forms new deep waters but also regulates the intermediate heat and salt content of the whole basin. A new state of the basin has been attained since 2013 in the absence of deep convective events. Chapter 3 also provides an analysis of the NEMO Med12 model's ability to track this phenomenon and, in an **O**bserving **S**ystem **S**imulation **E**xperiment (OSSE) framework, confirms that the sampling strategy adopted is relevant to monitor the changing basin. This leads to Chapter 4 which analyses the new state of the basin and considers the possibility of deep convection occurrence in the future by discussing the relative importance of the preconditioning versus the atmospheric forcing in determining deep convective years.

The main results of this work are finally put into perspective in the last Section 5.

Chapter 1

Oceanographic measurements in the Mediterranean Sea

Contents

1.1 The different observational platforms

The ocean can be a hostile environment, hard to observe and not easily accessible. Although some currents have been known since the antiquity[1], the vertical structure long remained a mystery. Thanks to the development of both theory and experimental devices, there now are numerous techniques at hand. Modellers are now able to use the huge provided observational datasets for comparison with their results. It is key to monitor the ocean in order to track the energy imbalance and changes [Von Schuckmann et al., 2016] and to unravel new physical processes. To do so, two complementary approaches

[1] Mostly surface currents, although it is worth noting that the deep outflow at Gibraltar was known to the Phoenicians 2000 years ago.

emerged: in-situ measurements over the water column and remote sensing of the surface. Here is a brief overview of the techniques and instruments employed.

1.1.1 Ship operations

Oceanographic vessels are usually used during at sea experiments to deploy the instruments (gliders, mooring lines, profiling floats, drifters, **C**onductivity-**T**emperature-**D**epth (CTD)s and others) and collect in-situ data and samples. Ships can also collect underway data with vessel-mounted devices such as the Acoustic Doppler Current Profiler (ADCP) and the thermosalinograph (measuring surface temperature, conductivity, salinity). The thermosalinograph can also be mounted on non-oceanographic vessels, providing a greater knowledge of surface data and the potential to help with designing at-sea experiments.

The main operation conducted on oceanographic cruises is usually the CTD, mounted on a rosette frame that may also have additional sensors installed. The rosette is lowered on a cable as data (conductivity, temperature, depth, fluorescence, oxygen, turbidity) is collected through the water column and made available for preview on the ship in real time. The ship repeats the operation at different locations and/or times in order to thoroughly cover the region of interest according to the objectives of the experiment. The water sampling bottles (Knudsen, Nansen and Niskin over time) attached to the rosette are remotely closed at different selected depths during the ascent, enabling the sampling of numerous physical and/or biogeochemical and/or biological properties of the water in the layers of interest.

1.1.2 Mooring lines

Mooring lines are fixed platforms, anchored on the ocean floor and comprised of a vertical cable that rises straight thanks to buoyant devices attached along its length. Usually not reaching the surface in order avoid interference with marine traffic, they are mounted with various instruments. They collect high resolution data (depending on the autonomy/time residence of the mooring line), and instruments can be fixed at any given depth, or can even move up and down the underwater line. Depending on the instruments attached, a mooring line usually records temperature, salinity, pressure, currents, sedimentation and biogeochemical quantities. Mooring lines may be attached to a surface buoy, in which case they may also record meteorological properties.

Mooring lines are deployed and recovered from oceanographic vessels, and although new technologies enable some data retrieval in real time, the data is most of the time only recovered when the instruments are back on-board. As the instruments can malfunction and/or be lost, mooring lines require regular maintenance, which can be problematic in remote or work hostile regions.

1.1.3 XBTs and MBTs

The **M**echanical **B**athy**t**hermograph (MBT) was originally designed in the late 1930s by the military to find the depth of the pycnocline (up to 275 m) for acoustic transmission applications. They were replaced in the 1970s by a deeper expandable version (the **E**xpandable **B**athy**t**hermograph (XBT)) that is not reusable but can be deployed underway. The deployed head of the device remains linked to the ship through a copper cable through which temperature is transmitted. When the cable breaks (hopefully at its full length), the profile ends. Some XCTDs with an added conductivity sensor were devised in the 1980s but remain poorly used due to their price and non-reusable characteristics.

1.1.4 Profiling floats

Profiling floats are passive autonomous platforms advected by the horizontal flow in the ocean interior. They only control their ascent and descent by modifying their volume. Argo is an international effort comprising an extensive global array of almost 4000 operating profiling floats. Argo floats usually sit at a given "parking" depth (400 m in the Mediterranean , 1000 m in the global ocean) during a predefined time (4 days in the Mediterranean, 10 days in the global ocean) before sampling. They then dive to 2000 m where they start their profile, sampling as they ascend to the surface. They then transmit the collected profile via satellite before sinking to their parking depth for another cycle (see Figure 1.1). The Argo mission aims to complement altimetry data from satellites, gridding the ocean with profiling floats.

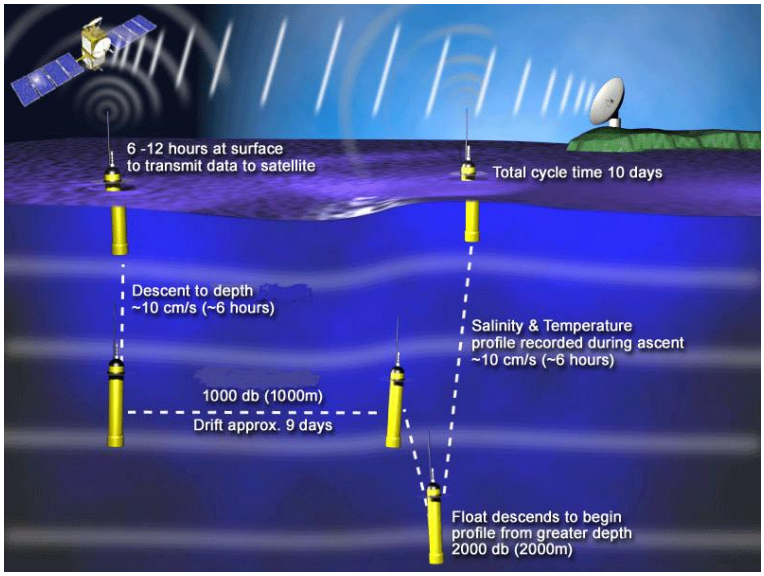

FIGURE 1.1: Schematic of the Argo operating and communicating method illustrating the 'park and profile' operation, from http://www.argo.ucsd.edu/HowArgofloats.html.

Profiling floats where first deployed in the 1990s and there now are 3948 active floats

gridding the global ocean, 68 of which in the Mediterranean as of September 2018[2]. Traditionally equipped with CTD sensors, some are now equipped with biogeochemical sensors, notably oxygen, and deep floats (profiling down to 4000-6000 m) are now being deployed. Their lifespan is of approximately 4 years, and a global effort is made to preserve this array which feeds data centres providing the free data in near-real time. This global coverage in time and space enables in turn a monitoring of the ocean health and provides data for model calibration and data assimilation. Argo floats are a key component in tracking the ocean changes in a climate change context [Roemmich et al., 2009].

1.1.5 Gliders

Imagined by Stommel (1989), gliders are programmable Autonomous Underwater Vehicles that "explore" the ocean without real time controlling on operators' part (communication is done when the glider surfaces). 1.5 m long, 20 cm in diameter and weighing approximately 50 kg, they have been gliding since the beginning of the 2000s, thanks to their wings and using the displacement of a ballast as they change volume by pumping or deflating a bladder. Unlike profiling floats, their wings allow them to transfer some of their vertical movement to the horizontal [Davis et al., 2002; Testor et al., 2010]. They are usually programmed to follow a course during which they follow a saw-tooth trajectory at an angle of 15-30°(as depicted in Figure 1.2), collecting data down to 1000 m along the way. Usually mounted with sensors such as conductivity, pressure and temperature, they can also be equipped with turbidity, oxygen and fluorescence sensors. More sensors are also being developed and adapted (nitrates, microstructure, miniature ADCPs [Wolk et al., 2009] and hydrophones [Cauchy et al., 2014; Cauchy et al., 2018]).

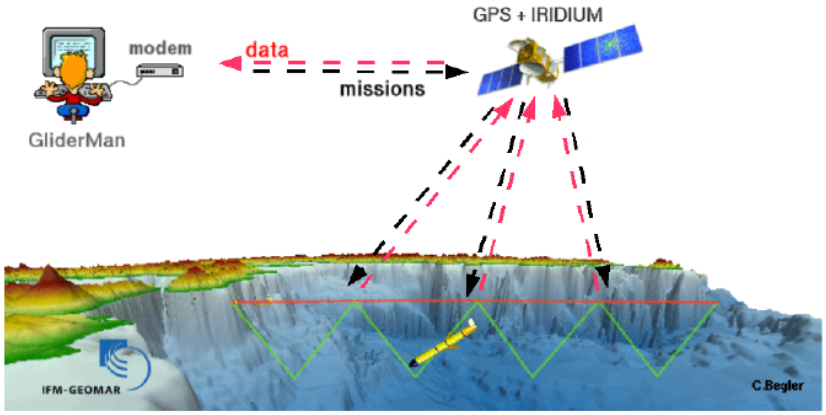

FIGURE 1.2: Glider operation principle, from IFM-GEOMAR

Gliders estimate a mean current between two surfacings and adapt their next direction to reach the aimed waypoint accordingly. They can be reprogrammed along the way and communicate via satellite when surfacing, enabling a close monitoring of the glider's vitals and adapting the sampling strategy. Covering some 15-35 km/day (at

[2]Mediterranean & Black Sea Argo Centre (MedArgo), http://nettuno.ogs.trieste.it/sire/medargo/active/index.php.

speeds between 20-40 cm.s^{-1}) and with an autonomy of up to several months, gliders provide high resolution temporal and spatial datasets. Their speed enables the monitoring of intense currents such as the Gulf Stream, or the study of (sub)-mesoscale structures such as eddies. Gliders are also relatively easy to deploy, as the record transatlantic crossing (7 months) glider was deployed and retrieved from a small rubber boat. New developments recently experimented glider measurements under sea ice, and down to 6000 m. Henry Stommel's revolutionary dream is coming true as underwater gliders are now becoming a key component of the ocean monitoring.

1.1.6 Remote sensing

The development of satellites was a revolution in oceanography, as they enable regular measurements and viewing of the data in near-real time. They assure a regular measurement and a regular monitoring of the oceans surface from a distance.

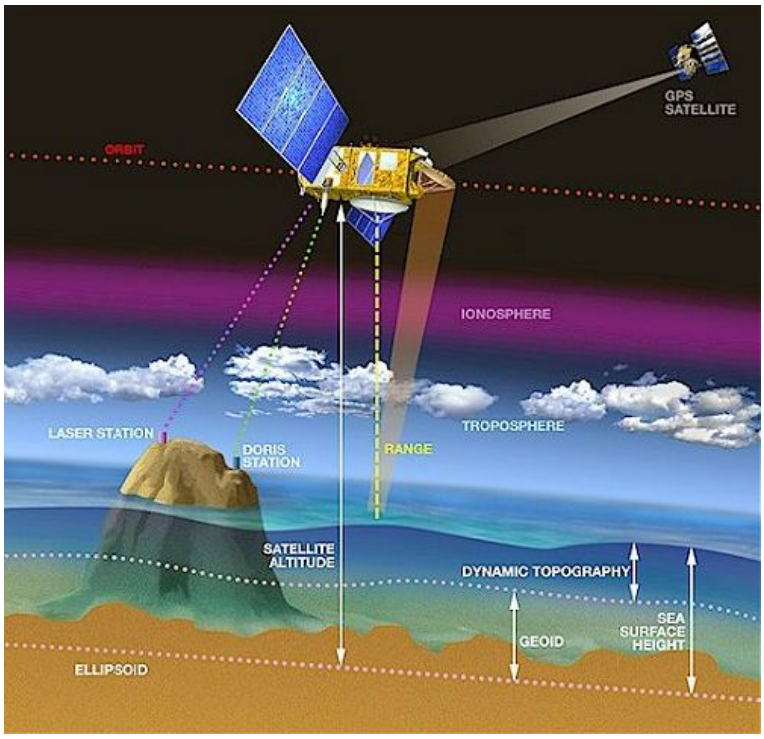

FIGURE 1.3: Schematic of altimetry operation, from CNES

Sea Surface Height

The Sea Surface Height (SSH) has been measured up to a centimetric resolution since 1992 and the TOPEX/POSEIDON missions. It corresponds to the difference in height measured between the water level and the reference ellipsoid adjusted with both the geoid and oceanic currents. Altimeters carried on-board satellites orbit around the ellipsoid and measure their distance to the sea surface, sending a high frequency signal and its reflection, thus directly measuring the SSH (see Figure 1.3). The satellite measurements have enabled the monitoring of the rising sea level linked to climate change (+$\sim$3 mm.year^{-1}),

and, combined with in-situ measurements, they allow the monitoring of geostrophic currents or eddy tracking. SSH is unfortunately not as precise near the coast, but several products have been devised to correct it in the Mediterranean [Sanchez-Roman et al., 2018].

Sea Surface Temperature

Sea Surface Temperature (SST) can also be obtained from satellites thanks to infrared scanners or microwave radiometers. Microwave radiometers have the advantage of not being affected by clouds, enabling complete sampling. The highest resolution products present a 1-4 km resolution in cloudless regions.

Chlorophyll-*a*

Chlorophyll-*a* can be derived from ocean colour observed data with complex algorithms. The surface colour of the ocean ranges from dark blue to green depending on the phytoplankton concentration. In clear weather, a 1-4 km resolution can be attained, which allows the identification and close monitoring of phytoplankton blooms, nutrient reserves and fishing areas.

1.1.7 Modelling tools – NEMO Med12

In parallel to the in-situ and remote sensing techniques for the observation of the oceans, oceanographers have developed numerical models aiming to complement the partial vision of in-situ measurements. In this thesis, the regional NEMO Med12 model configuration was used. It is based on the tagged version nemo-v3.2 of the global ocean circulation NEMO model[3] devised by Madec and NEMO Team (2008). NEMO Med12 covers the whole Mediterranean Sea plus a buffer zone including a part of the near Atlantic Ocean, from 30°N to 47°N, and from 11°W to 36°E.

Developed jointly by the CNRM, Mercator-Océan and ENSTA, NEMO Med12 has a 1/12°horizontal resolution (extracted from the global ORCA1/12 grid), corresponding to about 6-8 km throughout the basin. This resolution allows for the representation of most straits (although there are only 3 grid points the Gibraltar Strait) and for the resolving of mesoscale (the Rossby deformation radius R_d being of $\sim$15 km). Nonetheless, the region of interest of this thesis, the Northwestern Mediterranean, is rather well resolved at this resolution [Beuvier et al., 2012]. On the vertical, NEMO Med12 uses a 75 fixed z-levels grid with a thickness varying from 1 m near the surface to 130 m in the deep ocean. The bathymetry is extracted from ETOPO[4] [Smith and Sandwell, 1997] and the 'partial cells' are activated to adapt the thickness of the last level to the bathymetry.

The specific version used in this thesis was a freerun for the period 1979-2013 of the model, forced by the ALADIN (12 km resolution) atmospheric model using the Mercator-Océan assimilation system. The model was mainly chosen for its ability to reproduce deep convection [Waldman et al., 2016b] in order to assess its impact on the rest of the

[3]The code can be found here, http://www.nemo-ocean.eu/.
[4]https://www.ngdc.noaa.gov/mgg/global/

basin. Thus enabling the monitoring of the long term trends in relation with the observations and assessing the model ability to reproduce the water masses variability (see Chapter 3).

1.2 The MOOSE program

The **M**editerranean **O**cean **O**bserving **S**ystem for the **E**nvironment (MOOSE)[5] network aims at addressing the key scientific and environmental issues relevant for climate change in the Northwestern Mediterranean Sea. It has a long term monitoring role (from 2010 to 2020 at least) in the context of the climate change and anthropogenic pressures [Durrieu de Madron et al., 2011], and as such combines various approaches. As can be seen in Figures 1.5 and 1.4, it maintains a large integrated array of moorings, radars, surface buoys and atmospheric monitoring as well as ship, glider and Argo operations.

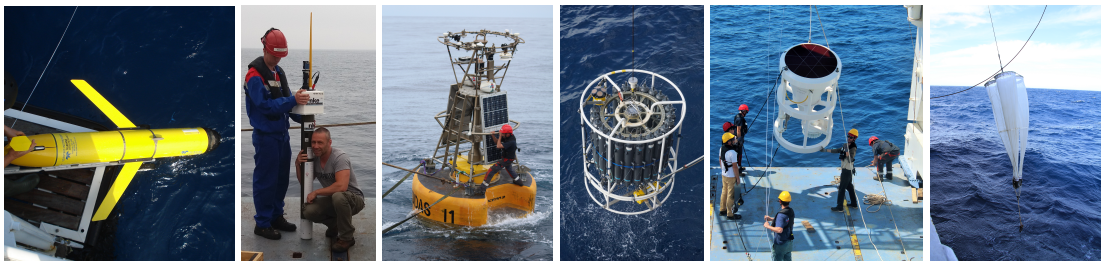

FIGURE 1.4: Various in-situ instruments part of the MOOSE program. From left to right: a slocum glider, an argo profiling float, a Météo France surface buoy, a CTD, mooring operations with a sediment trap and phytoplankton nets.

The MOOSE plan addresses five main scientific questions: the mesoscale circulation, the river inputs, the biogeochemical cycles and acidification, the biological communities and biodiversity, and the atmospheric depositions. As such, it aims at tracking and monitoring the Northern Current (notably with glider endurance lines), the coastal-offshore exchanges, as well as the deep water formation by cascading and open ocean deep convection (notably thanks to gliders, moorings and ship operations, see Durrieu de Madron et al. (2013); Houpert et al. (2016)). This tracking is not only made in a classical physical sense, as key biogeochemical parameters are also being measured (nitrate, phosphate, O_2, CO_2) to understand their relation to physical processes.
The three main components of the MOOSE program used in this thesis are:

– The annual and repeated oceanographic cruises the main component being the Moose-ge annual cruise. About 120 CTD casts are made each summer covering the Northwestern Mediterranean (see Figure 1.12), and the different mooring lines (LION, 42.04°N 4.68°E, and DYFAMED, 43.41°N 7.89°E, notably) as well as the Météo France surface buoys (LION, 42.06°N 4.64°E, and AZUR, 43.38°N 7.83°E) are also maintained. The monthly DYFAMED CTD casts near the Ligurian mooring location are also used.

– The repeated glider endurance lines comprising 3 trajectories: T00 between Nice and Calvi passing by the DYFAMED mooring, T01 outside Toulon and T02 in the Gulf

[5] http://www.moose-network.fr/

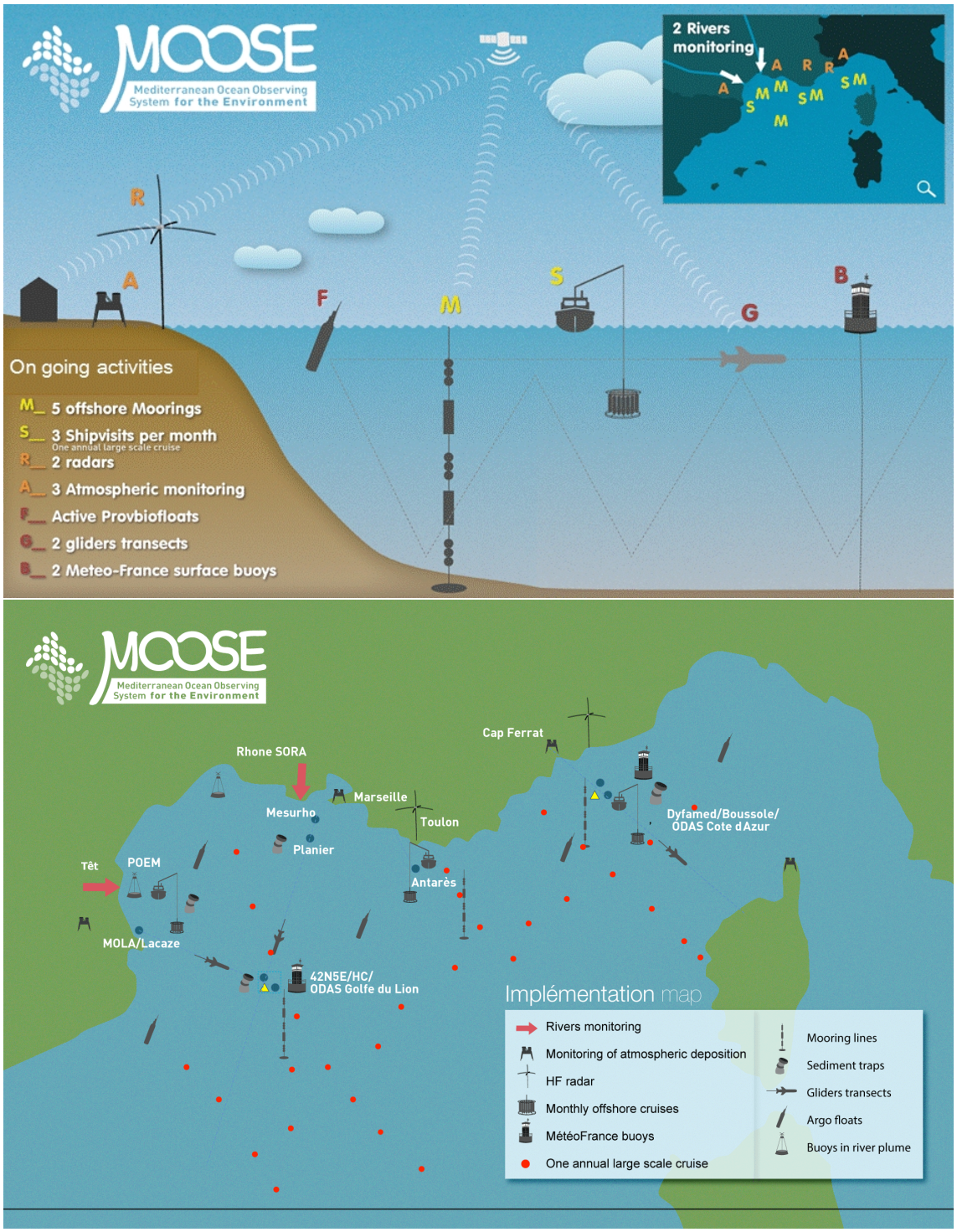

FIGURE 1.5: Schematics of the MOOSE network and the different monitoring techniques it encompasses, from the MOOSE website: http://www.moose-network.fr/.

of Lions between Marseille and Minorca through the LION mooring location (see Figure 1.12).

– The mooring lines. The two LION moorings in the in the Gulf of Lions , and the DYFAMED and AZUR moorings in the Ligurian Sea, as well as smaller lines in the canyons

of the Gulf of Lions . The mooring locations were chosen to track the deep water formation through open ocean convection [Houpert, 2013] and cascading [Durrieu de Madron et al., 2013].

See the figures in Section 1.3.4 to see the revolution that is the MOOSE program in terms of spatial and temporal resolution of data collected.

1.3 A meta-database for T/S profiles in the Mediterranean Sea

In this thesis, in addition to the key MOOSE dataset, all the available temperature and salinity profiles in the Mediterranean Sea have been assembled in a meta-database in order to track the changes in the water masses properties. The database is built on a first iteration by Houpert (2013)[6], storing the profile data in 0.5°longitude $\times$ 0.5°latitude boxes. The main sources of data come from the MOOSE dataset (cruises, gliders, floats...), the glider EGO-network[7], the CORIOLIS data centre[8], the Medar-MEDATLAS project [MEDAR, 2002] and the World Ocean Database [Conkright et al., 2002]. Additional smaller inputs come from Italian [D'Ortenzio et al., 2005] and Spanish oceanographic cruises [Puig et al., 2013], or from military releases of previously classified surveys (mostly XBT measurements).

1.3.1 Structure

After incorporating the different datasets in the 0.5°longitude $\times$ 0.5°latitude boxes, several quality checks are made and the different profiles are flagged along the process. The boxes are stored at each iteration of the process from BOXES_0 to BOXES_5, the number referring to the maturity level of the iteration. The first step is a duplicate removal check after which 600 223 temperature profiles are left (more than 2/3 of which also have salinity data). The next steps are calibrations (described in the next section in detail) after which MLD corrections and a seasonal outlier exclusion per region is done. The very basic structure of the database is presented in Figure 1.6, which also displays the final fields in the saved MATLAB structure, ensuring traceability. These fields are:

- CAMPAIGN, name of the cruise or deployment
- DATASOURCE, name of the source from which the data was retrieved
- IDINSTR, ID of the platform
- IDPF, name of the profile
- LAT, latitude of the profile

[6]The database was updated from 2013 to 2018, more than doubling the number of profiles, and additional calibrations and harmonisations were performed, see section 1.3.2.

[7]Everyone's Gliding Observatories.

[8]The Coriolis data centre collects data and does basic quality checks, data can be downloaded here: http://www.coriolis.eu.org/Data-Products/Data-Delivery/Data-selection.

- LON, longitude of the profile
- OP, name of the 'operator' who provided the data
- Pref, depth level of the profile
- SS, salinity profile
- SS_QC, salinity Quality Check value
- TIME, time of the profile, in Universal Time
- TP, potential temperature profile
- TP_QC, potential temperature Quality Check
- TYPINSTR, measurement platform ('CTD','GLIDER','ARGO','XBT','MBT','UNKNOWN'[9])

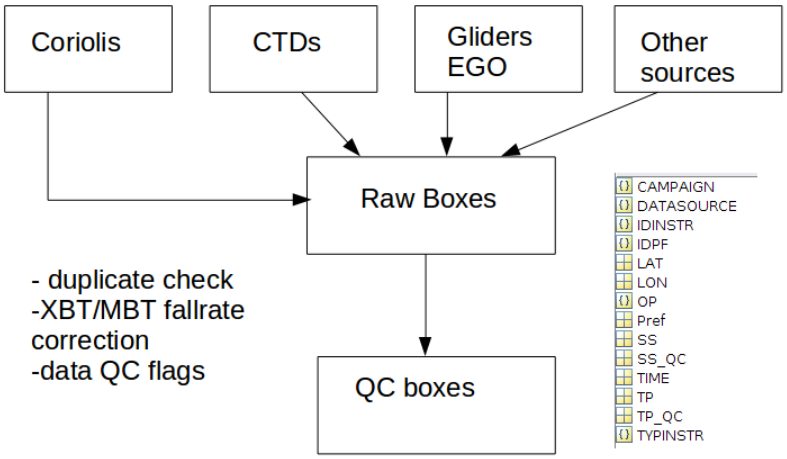

FIGURE 1.6: Schematic of the Mediterranean meta-database structure.

The performed Quality Checks are the same as the ones in the CORIOLIS database, and they include: 0 for no QC, 1 for Good, 2 for Probably Good[10], 3 for Probably Bad, 4 for Bad, 7 for error in time and/or position, 8 for No data. Several flags were also added for the different iterations in the BOXES: 10 for Good raw data, 11 for Good raw data adjusted by the principal investigator, 20 for probably good raw data and 41 for a problem in the surface data of the profile.

The database is accessed with a Matlab function to retrieve the data in a region and time of interest was devised:

$$dataDB = DBhisto\_loaddata(pathdb, arealimit, timeselect, minp, instrtyp, qcselec, qlvl)$$

where *pathdb* is the path of the desired BOXES to load, *arealimit* is a closed polygon of the area desired, *timeselect* the minimum and maximum time values of the desired time

[9]Most of the unknown instruments are military XBTs or MBTs that are not identified in the datasource.
[10]to be checked by a human operator.

period, *minp* the minimum depth of the desired profiles, *instrtyp* the type of instrument desired (note that 'ALL' is also accepted), *qcselec* is 1 if you want certain QCs only, 0 to load all the data and *qlvl* a vector with all the desired QCs, only used if *qcselec* is set to 1.

1.3.2 T/S calibration

Before a general treatment is applied to all profiles to render the database as homogeneous as possible, all the platforms are taken at the most mature corrections stage available. CTD data are for instance preferably retrieved after probe calibrations prior and post cruise, and after corrections were made by chief scientists of the cruise in question. For example, during the MOOSE cruise, a Seabird 911+ CTD is deployed and water samples are collected for standard salinity Autosal on-board measurements, which eventually guarantees an accurate and calibrated dataset (0.001°C in temperature and 0.003 in salinity[11]). Similarly, profiling floats data is also taken after any available cross-calibration (see Figure 1.7 for a cross-calibration of 3 Argo profiling floats during the MOOSE-GE 2016 cruise). Some platforms require extra attention:

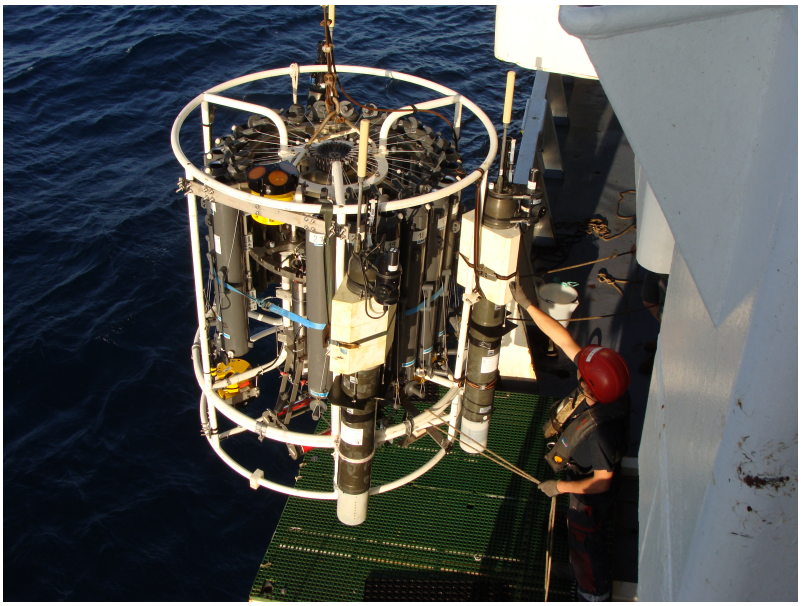

FIGURE 1.7: 3 Argo profiling floats cross-calibration during the MOOSE-GE 2016 cruise. Two of the floats had just been recovered and one was about to be deployed. They were attached to the rosette for cross-calibration with the calibrated ship CTD.

Gliders

Gliders have collected more profiles than any other platform, and have done so during the last 14 years. Because the data collected on the EGO-network is in a standard high resolution format, glider data is subject to various additional treatments before going through a database homogenisation scheme. The CTD probes mounted on gliders (pumped or un-pumped) require a thermal-lag correction due to the thermal capacity of the glider hull and the distance between sensors. When crossing important temperature

[11] All the numbers presented in this section are relative to the accuracy of the measurements, their resolution is consistently one order of magnitude lower.

fronts (δT >0.2°C), usually a seasonal thermocline (δT of 1-10°C over less than 10 m), the glider can produce artificial salinity spikes from the lag of the instrument measurement. The profiles were corrected using the method developed by Garau et al. (2011), and in our Mediterranean context, these corrections applied where only of second order elsewhere than in such strong thermoclines. Oxygen measurements were calibrated up to 2013. The values were recomputed using the temperature from the glider CTD instead of the optode temperature, and other corrections were applied to account for the difference in position between the glider CTD and the optode. For other oxygen measurements discussed in this work, only the relative values will be discussed as no calibration has been made yet. The fluorescence measurements were corrected using Ocean Colour measurements following the method described in Lavigne et al. (2012). It relies on an offsetting of the values to match 0 at depth, followed by a multiplication factor in order to match the surface values. The glider time series were finally sliced up in downcasts and upcasts, and interpolated every meter along the vertical to produce equivalent vertical profiles at the mean time and location of the casts.

XBTs and MBTs

XBT and MBT measurements have also been subjected to separate additional treatment, as recent studies have shown they are prone to a warm bias ranging from 0.2°C to 0.4°C due to errors in the fall rate equation [Domingues et al., 2008; Wijffels et al., 2008; Levitus et al., 2009; Ishii and Kimoto, 2009; Gouretski and Franco, 2010; Hamon et al., 2012]. These measurements constitute the major part of the historical dataset (pre-2000s and the Profiling floats and gliders), and as such are a key component of the database. The accuracy of MBT and XBT are respectively of 0.1°C and 0.2°C , and have a depth accuracy of about 5 m as specified by manufacturer technical sheets. To correct the biases previously mentioned, the depth calculation and temperature biases were processed with the Gouretski and Koltermann (2007)[12] method for MBT measurements, while XBT measurements were corrected with the Cowley et al. (2013) method[13], who used over 4100 side-by-side XBT and CTD measurements to separate the depth error form the temperature bias.

Database homogenisation

After those first step calibrations for the different instruments, an extra effort had to be made to render the database coherent. To achieve this, some measurements are considered 'reference' due to their known accuracy. The oceanographic cruises CTD casts are the first 'reference' with their accuracy of 0.001°C in temperature and 0.003 in salinity. As well as the CTD casts, the LION and DYFAMED mooring data are taken as reference. Their calibration indeed relies on oceanographic cruises (as is explained in the next Section 1.3.3), and their accuracy reaches 0.001°C in temperature and 0.005 in salinity.

Having these 'reference' profiles enables the cross-calibration of instruments passing nearby (in time and space). Other profiles can thus be calibrated up to the extent of the natural variability associated with the calibrating scales. This natural variability has been estimated to be lower than 0.01°C and 0.01 in salinity for scales of 2.5 km/18 h from 700

[12]The Gouretski and Koltermann (2007) updated values can be found here.
[13]A detail of the Cowley et al. (2013) correction steps can be found here.

to 1000 m (used for gliders) and of 15 km/3 days from 1500 to 2000 m (used for profiling floats) [Bosse et al., 2016]. The mooring locations in the Northwestern Mediterranean are key in this calibration, as they offer a profile every 30 minutes and the glider endurance lines make sure to pass by them. The calibration is realised with offsets in salinity and temperature, and the sensor drift or pressure induced errors are of one order of magnitude lower at the concerned depths if the instrument is not at sea for more than a year (unless exceptional sensor breakdown or biofouling, easily detected and discarded).

If the instrument does not come near a 'reference' measurement, a method has been devised for the Northwestern Mediterranean Sea where most of the profiles were sampled, and which is the focus region of this thesis. Thanks to the MOOSE-GE annual surveys covering the whole basin with about 100 'reference' CTD casts, a linear θ/S relationship representative of the basin status can be inferred every year at depths between 700-1500 m (see Figure 0.6). In this deep layer, the variability is weakest, and temperature and salinity compensate. The instruments left uncalibrated are then confronted with this linear relationship to determine a salinity offset as the temperature sensors are usually more reliable.

The final product is thus a coherent database with an accuracy of $\sim$0.1°C in temperature and $\sim$0.1 in salinity in the Northwestern Mediterranean Sea where reference measurements are numerous and of $\sim$0.15°C and $\sim$0.15 for the rest of the database.

1.3.3 Mooring lines complementary dataset

The mooring lines are not only important for the cross-calibration described previously, but they also complete the dataset. They indeed provide data at a high temporal resolution but in a fixed location and with a relatively low vertical resolution, complementarily to data provided by the instruments mentioned in the previous sections. The two offshore mooring lines of the MOOSE network are located at LION, 42.04°N 4.68°E, and DYFAMED, 43.41°N 7.89°E, and are equipped with CTD sensors (Seabird SBE37 microcats, some with additional oxygen sensors), temperature only sensors (Seabird SBE56), current-meters (Aquadopp) and sediment traps (see the mooring line configurations in Figures 1.8 and 1.9). The sensors are cross-calibrated before and after each mooring deployment with the ship CTD, by performing a high temporal resolution sampling cast with 30 min long timeseries at the fixed depths of 300 and 1000 m. This allows for a high accuracy of 0.001°C in temperature and 0.005 in salinity [Houpert, 2013]. First deployed in 09/2017, the LION mooring line has had at least 10 vertical levels from 150 to 2300 m since 2008 and the DYFAMED mooring at least 7 vertical levels from 200 to 2300 m since 2012 (first deployed in 10/2019).

Because of the harsh environmental conditions and intense marine traffic, these mooring lines stop below the surface. The Météo France surface buoys at LION, 42.06°N 4.64°E and AZUR, 43.38°N 7.83°E were used to complete the water column. Both buoys are indeed geographically close enough (3.8 km between the LION moorings, 5.8 km between the DYFAMED and AZUR moorings, compared to the $\sim$15 km Rossby radius in

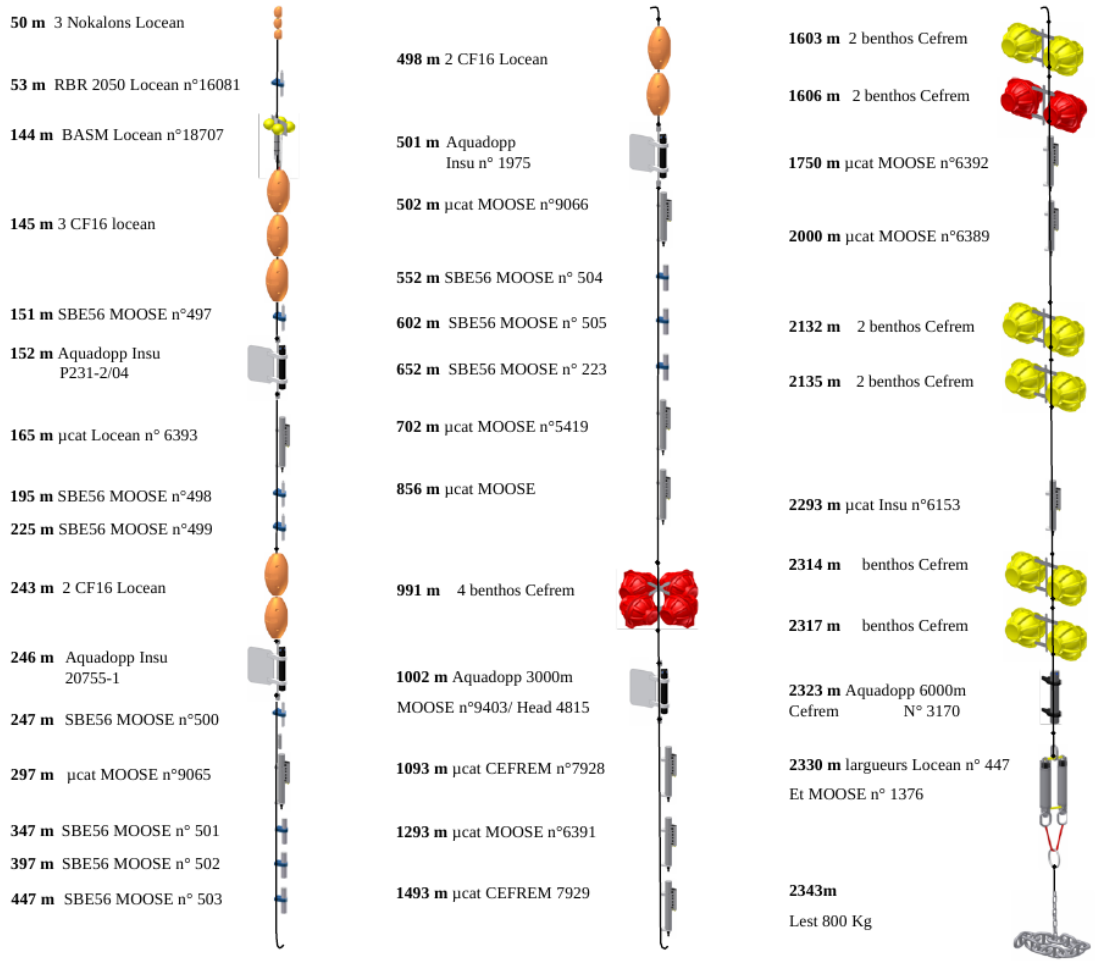

FIGURE 1.8: The LION mooring line configuration for the July 2012 deployment.

the region) to complete the profile, and have temperature sensors down to 250 m and 200 m depth respectively (20 NKE-SP2T and and SBE37 CTD just below the surface at 2 m depth). These sensors are also calibrated, and ensure the same sensor accuracies.

As a result of the various sampling rates of the instruments between the different mooring lines, 30 minutes time-series at the different depths are produced.

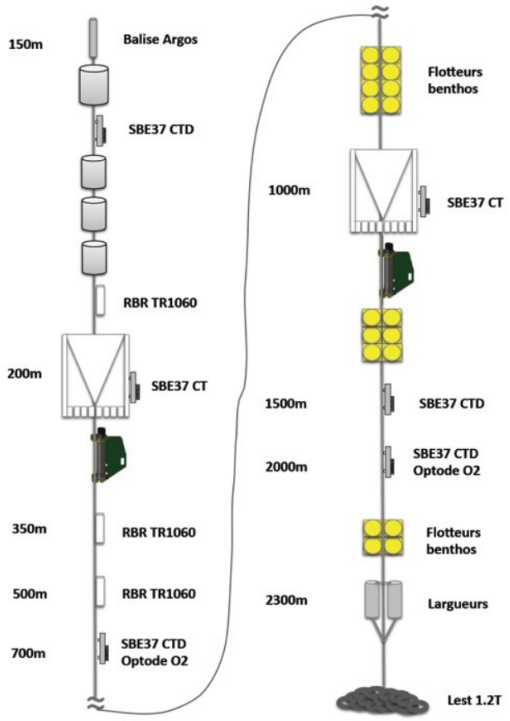

FIGURE 1.9: The DYFAMED mooring line configuration for the July 2015 deployment.

1.3.4 Description of the dataset

Starting in 1960, a total of 600223 profiles are in the BOXES (Figure 1.10). Over half of the profiles were sampled after the year 2000, showing how important the development of autonomous platforms has been in the observational effort. The glider measurements indeed represent more than a quarter of the profiles in under 10 years of activity. Not only are autonomous platforms collecting a very important number of profiles, they are also collecting data at greater depths, as gliders sample down to 1000 m and profiling floats down to 2000 m. Figure 1.10 also illustrates the rarity of deep measurements (less than 7% of the profiles are deeper than 1000 m), and how the trend has been changing since the 2000s. There is as well a huge disparity between the Eastern and Western Basins, especially since the 2000s and the numerous glider deployments in the Northwestern Mediterranean Sea.

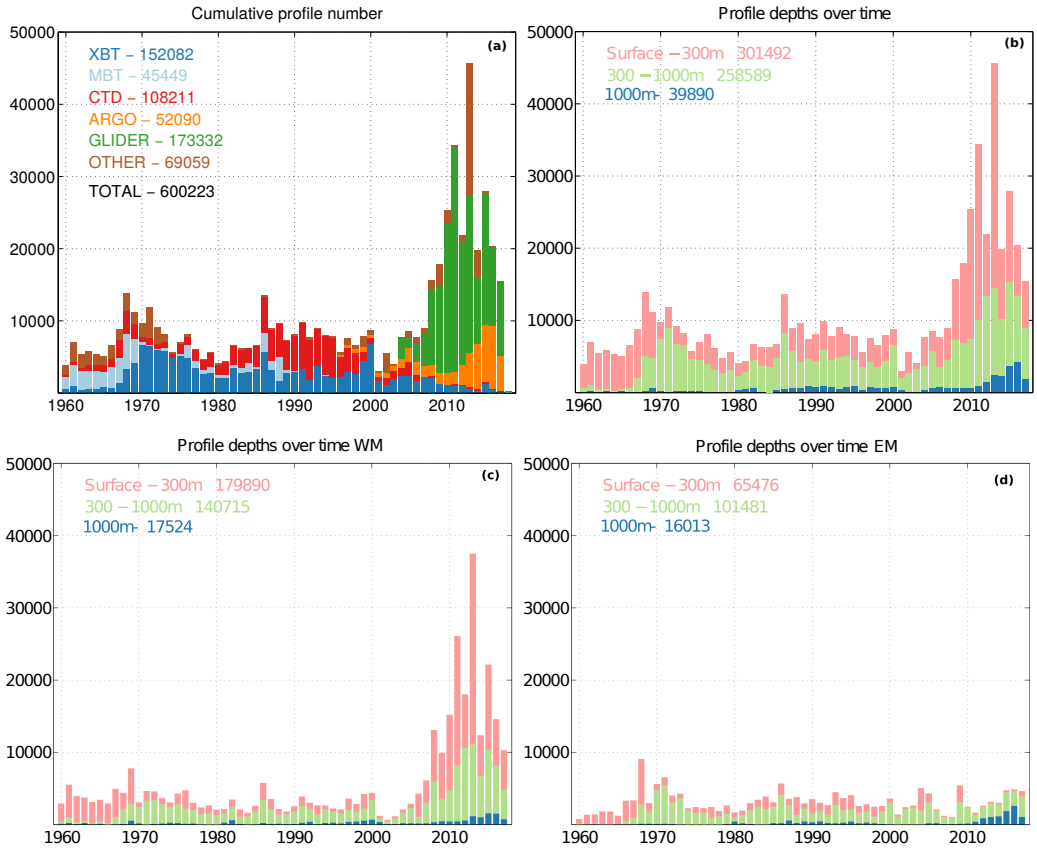

FIGURE 1.10: Meta-database contents (number of profiles) over time and depths: (a), yearly contents by platform type, (b), yearly contents by maximum depth, (c), yearly contents by maximum depth in the Western Mediterranean Basin, (d), yearly contents by maximum depth in the Eastern Mediterranean Basin.

This disparity is also on display in Figure 1.11, where the impact of the multi-year network of combined platforms that constitute the MOOSE program can clearly be seen. The regular glider deployments by SOCIB in the Balearic Islands and by the University of Cyprus in the South of Cyprus are also illustrated. The disparity between temperature and salinity measurements is also evidenced. This disparity is mostly due to historical

data, as most measurements were only of temperature.

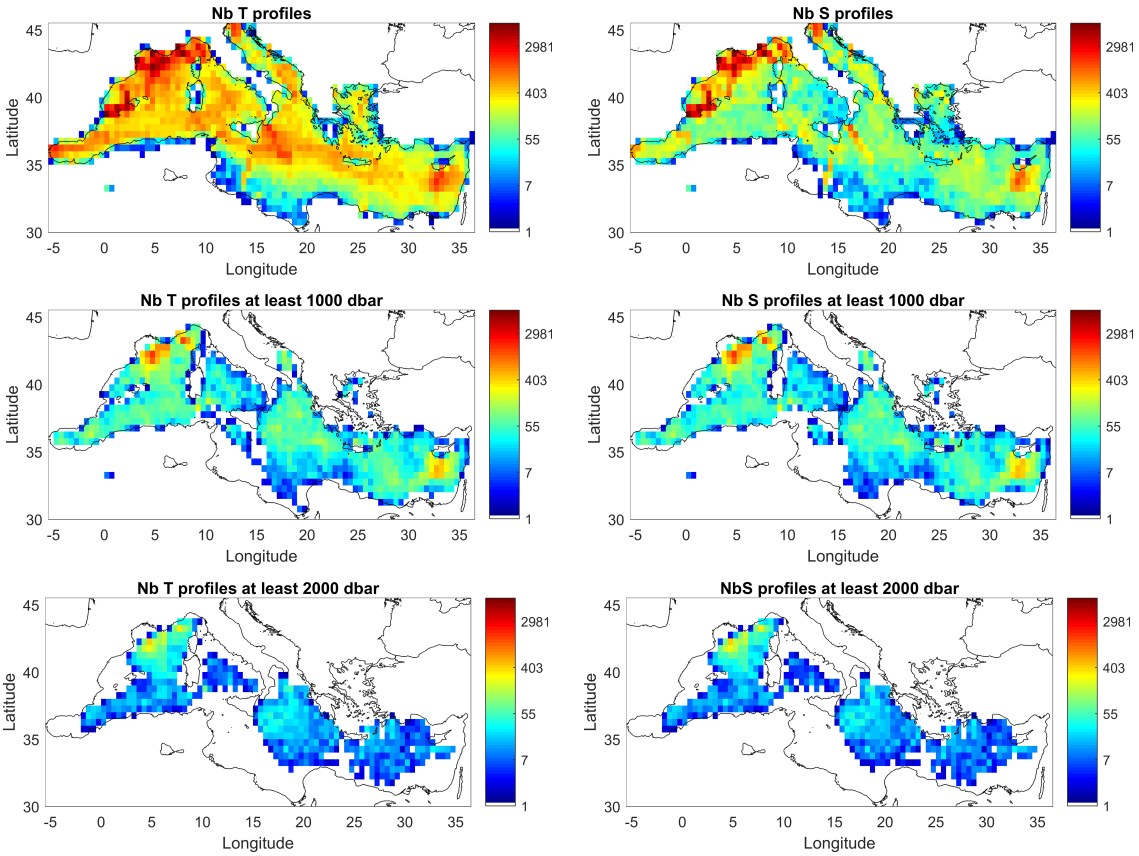

FIGURE 1.11: Spatial distribution of the meta-database contents per 0.5°longitude × 0.5°latitude box, on a logarithmic colour-scale. Number of temperature profiles on the left, number of salinity profiles on the right.

Figures 1.12 and 1.13 shows 4 typical yearly contents of the database. Mostly shallow MBT profiles were sampled in the early years until the 2000s, when the first profiling floats were deployed and when for a few years MBT transects were performed. The 2012 and 2017 panels clearly display the intensification of measurements thanks to gliders, especially in the Northwestern Mediterranean Sea where the glider endurance line as well as the yearly MOOSE-GE cruises appear. In particular, Figure 1.13 illustrates a working example of a sustained effort to collect regional in-situ observations, which proved essential to discovering new changes in water mass properties (see Chapter 3).

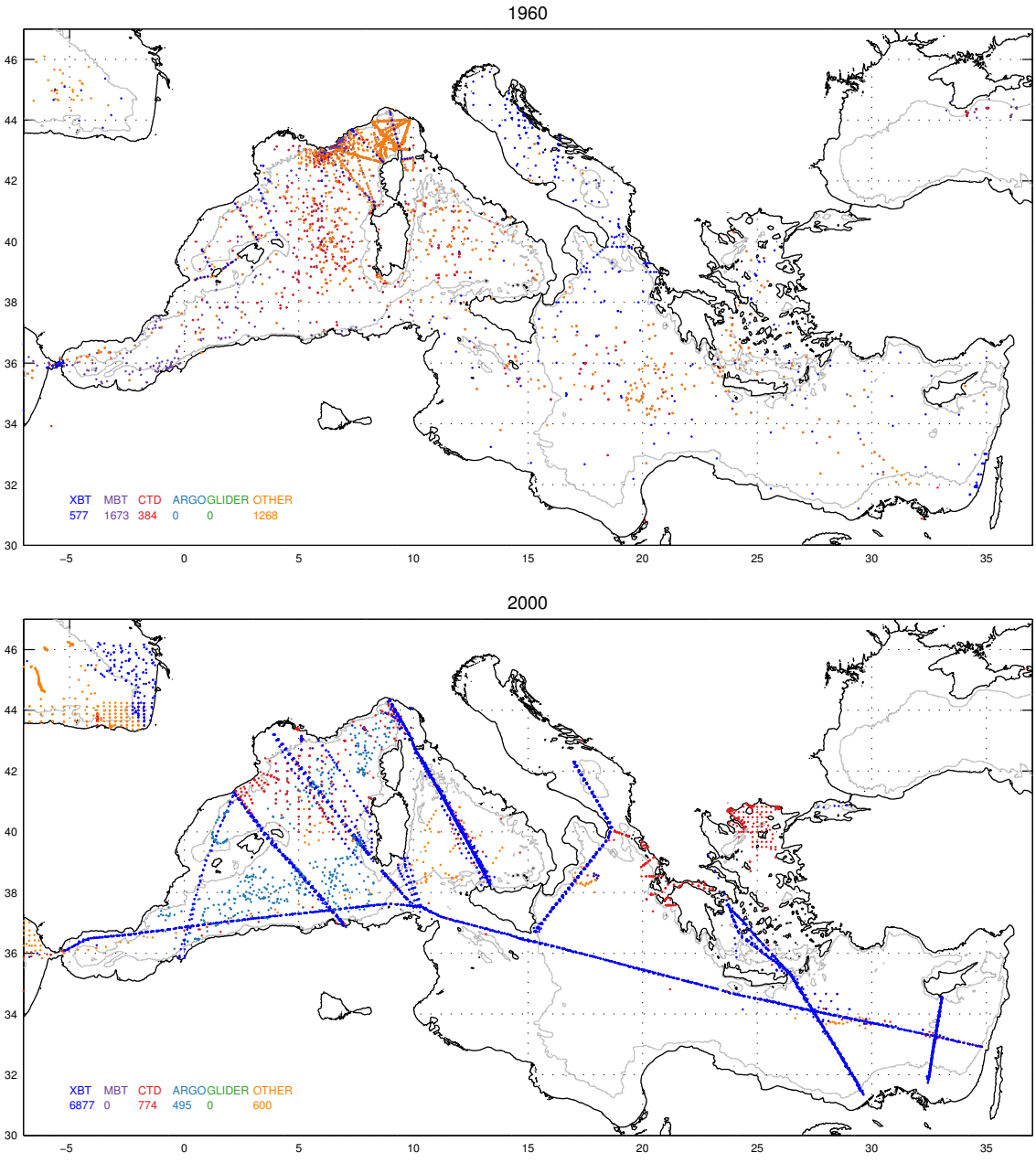

FIGURE 1.12: Temporal evolution of the data coverage of the Mediterranean by platform type. The number of profiles by platform type is annotated. Typical years are presented:1960 when most profiles where shallow MBT measurements, 2000 with the first profiling floats being deployed and the XBT surveys.

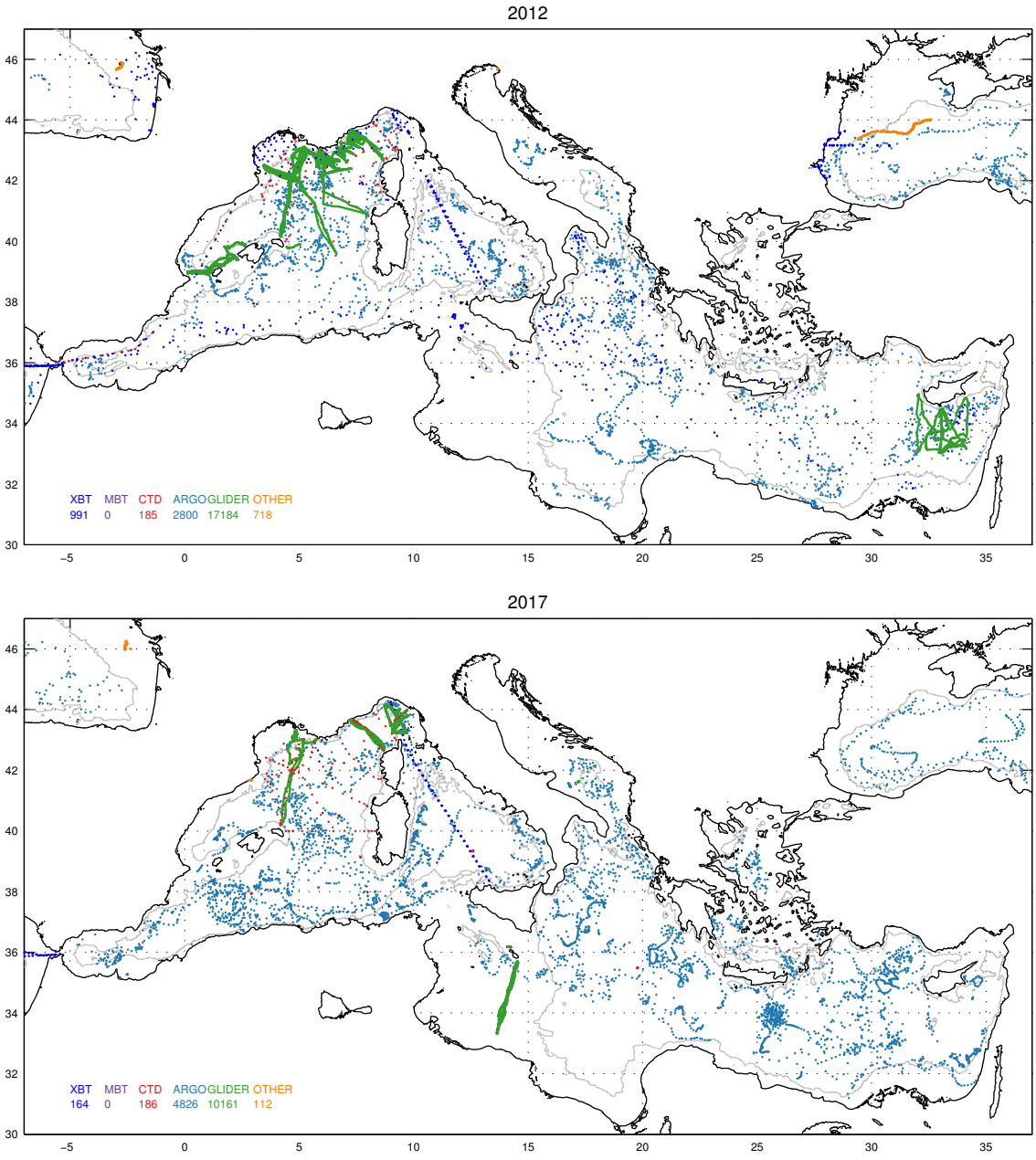

FIGURE 1.13: Temporal evolution of the data coverage of the Mediterranean by platform type. The number of profiles by platform type is annotated. Typical years are presented:2012 and 2017 to present the glider endurance lines and the overall impact of the thorough MOOSE sampling.

1.3.5 Examples of applications for the Database

Thanks to the meta-database, different diagnostics can be made: Houpert et al. (2015) derived seasonal heat budgets of the Mediterranean, and the warming and salinification trends of Mediterranean Waters observed by Béthoux et al. (1990); Béthoux et al. (1998) are also observed. The very quick computation of the θ/S diagram of deep waters (below 1000 m) in all the Mediterranean displayed in Figure 1.14 clearly shows the warming (0.004°C .year^{-1}) and salinification (0.002 year^{-1}) previously mentioned, which was more thoroughly investigated in Chapters 3 and 4.

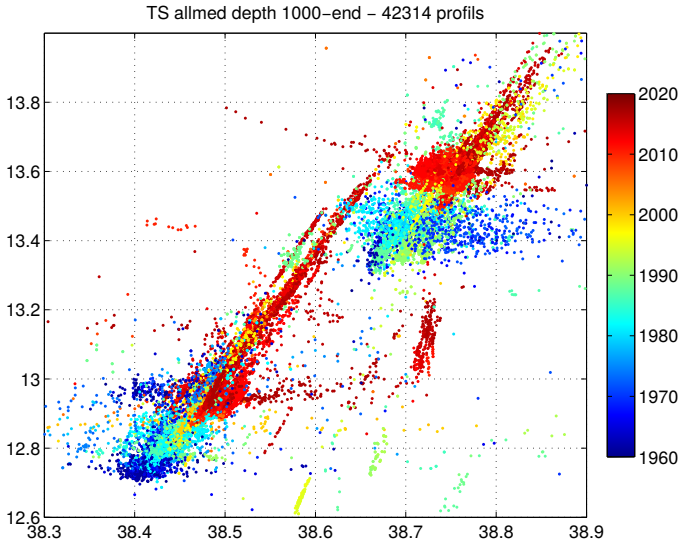

FIGURE 1.14: θ/S diagram of deep Mediterranean waters (under 1000 m) over time (represented in colour). The two patches correspond to the two basins: the Western Mediterranean on the bottom left, the warmer and saltier Eastern Mediterranean on the top right.

PERLE oceanographic cruise preparation

The meta-database can also be used for the preparation of new oceanographic projects. The PERLE[14] program aims at investigating the formation of LIW and the second cruise is currently ongoing. The Mediterranean meta-database was useful in determining the mooring location and the instrument depths thanks to the history of profiles collected in the region (see Figure 1.15).

[14]Updated information about the ongoing program can be found here

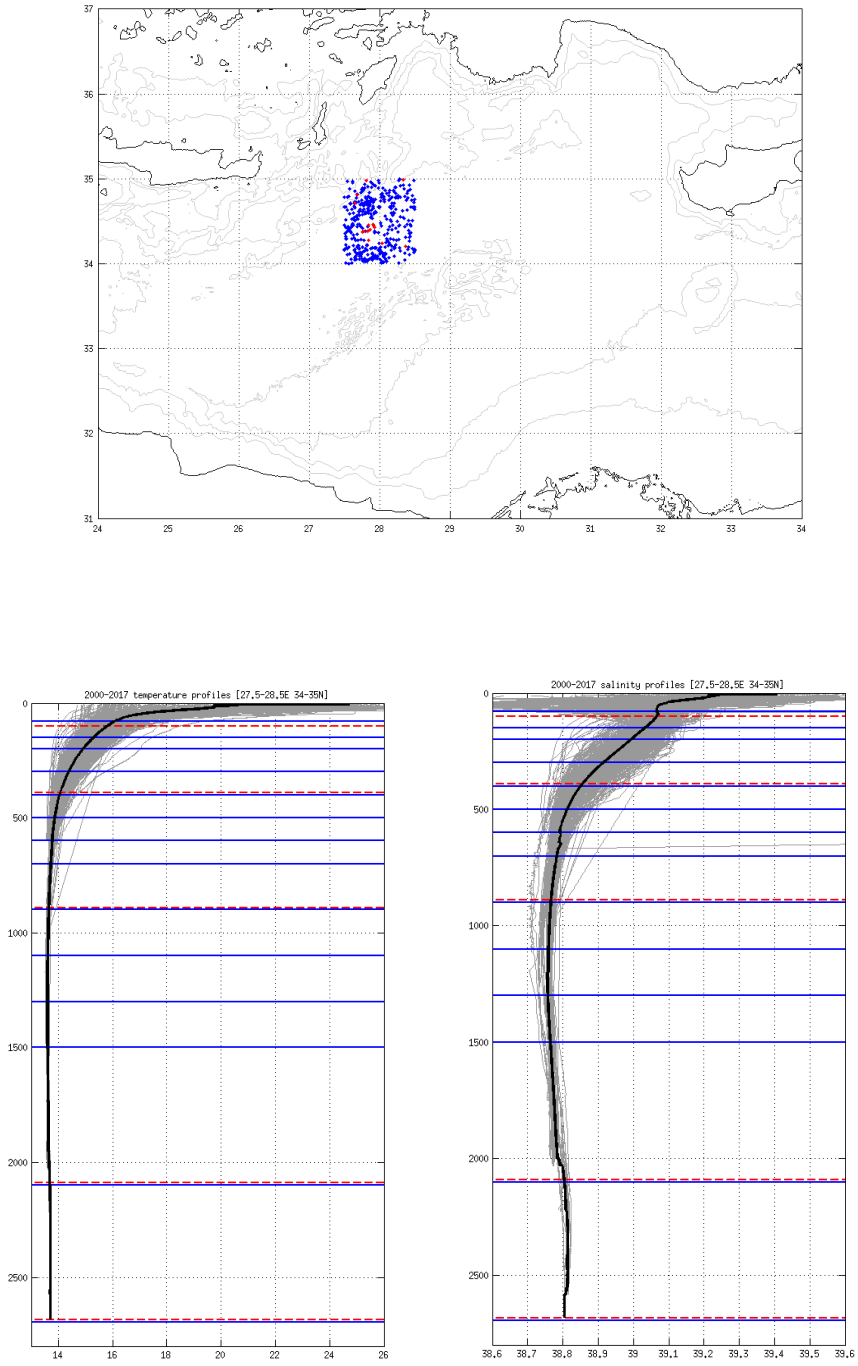

FIGURE 1.15: PERLE cruise preparation; left to right: map of the LIW supposed formation area where a mooring is to be deployed, the data collected in the region from 2000 up to 2017 in blue, the data from 2017 in red. Temperature and salinity from all profiles over the 2000-2017 period are represented in grey, in black is the mean profile and the horizontal lines represent the depths at which an instrument will be moored (blue for microcats, red for aquadopps).

Chapter 2

A new concept for deep convection

Contents

2.1 The 2012-2013 winter in the Gulf of Lions: an intense observational effort

The current framework for deep convection is that of Marshall and Schott (1999), a global view hinting at small scale processes. Deep convective events are characterised by an intricate sequence of interacting physical and biogeochemical processes (especially during the subsequent spring bloom), as particulate fluxes are constrained by both the biogeochemical cycles and the physical processes. What remains an open question is the scales and characteristics describing the variability of these phenomena.

Uncertainties arise mainly from the observational limitations as the mixed patch extends over 100 km, as the preconditioning, violent mixing and restratification phases overlap, as modulations at different scales come into play, and as the variability of the mixed patch is of very high temporal and spatial disparities. Numerous time and spatial scales are involved, and Durrieu de Madron et al. (2011) suggest that the bloom and the deep convection result from the succession of events starting 6 to 8 months prior to the event.

In order to overcome these limitations, this chapter relies on the 2012/2013 DEWEX[1] and ASICSMed experiments coordinating different projects for a more complete than

[1] DEnse Water EXperiment.

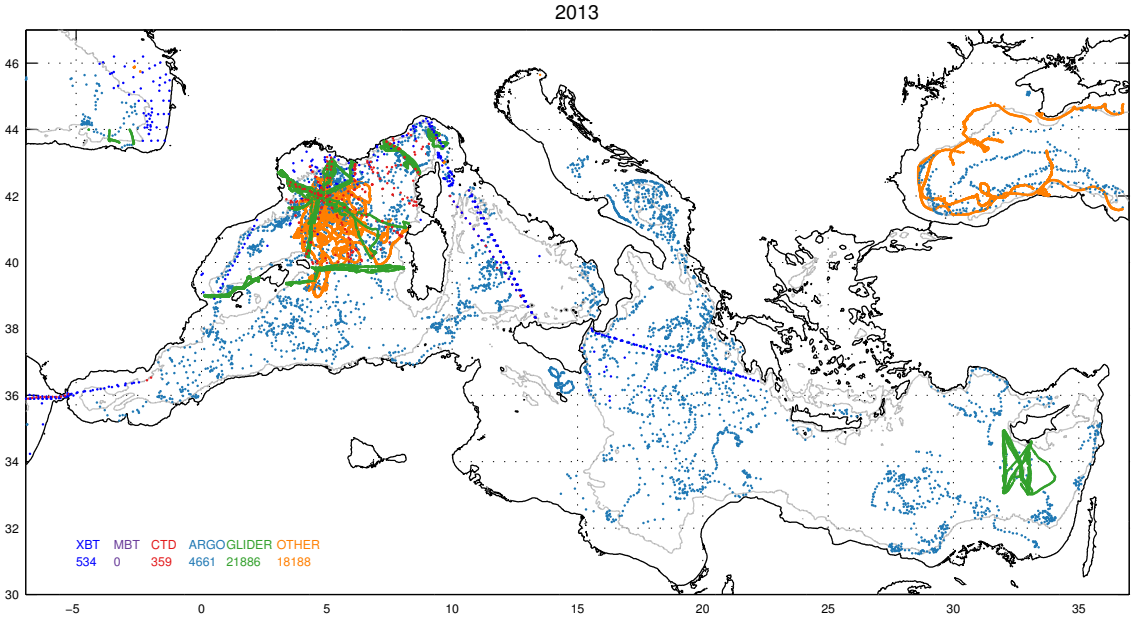

FIGURE 2.1: The intense observational effort in winter 2012/2013 in the Northwestern Mediterranean Sea compared to the rest of the basin.

ever description of the Northwestern Mediterranean Basin over the three different phases of deep convection [Estournel et al., 2016b].

2.1.1 An ideal case study

This DEWEX framework makes an ideal case study for deep convection. A first look at the density of observations collected relative to the yearly mean gives an idea of the density of the dataset (see Figure 2.1 compared to Figure 1.12). The experiment was conducted relying on the long-term MOOSE observational network carried out in the region. All the different observational platforms (research vessels, gliders, profiling floats, mooring lines, drifters) were combined to carry an extensive spatio-temporal coverage of the region from summer 2012 to summer 2013. Figure 2.2 presents in more detail all the data collected from July 2012 to October 2013, as well as the presence at sea of the different platforms over time. A number of 6 research cruises were completed to collect data during the different phases of deep convection, deploying and recovering moorings and autonomous platforms.

Key moments characterising the annual cycle where identified, and an intensive observation scheme was conducted to monitor these particular periods of the year. The sampling strategy was established jointly with the modelling community to ensure an observational scheme relevant to constrain modelling studies. A special care was also taken to record atmospheric variables (balloon and air tracks [Conan et al., 2018]) as they are central to the deep convective phenomena. Ship cruises where thus planned throughout the year, before, during, and after both the deep convection and the bloom events, while autonomous platforms (gliders, profiling floats and moorings) where responsible

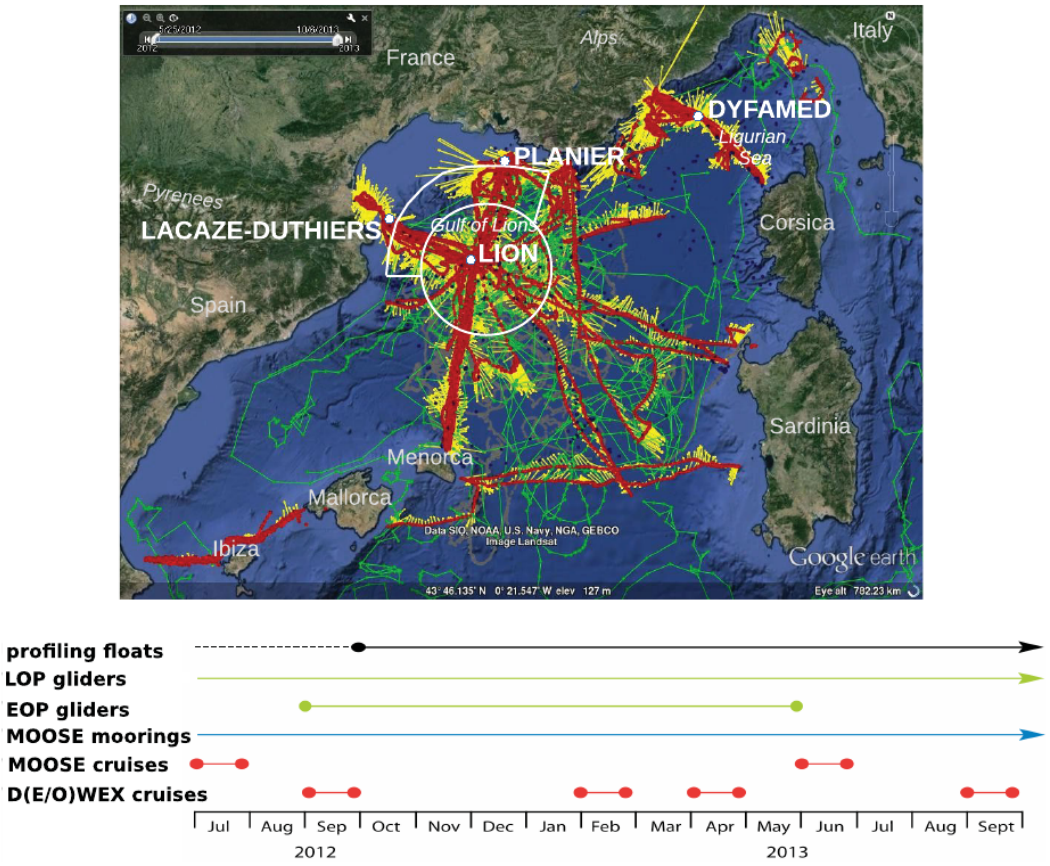

FIGURE 2.2: All observations carried out between the 1st of July 2012 and the 1st of October 2013. Gliders surface positions (red dots) and measured depth averaged currents (yellow arrows). Profiling floats surface positions and trajectories (green). CTD casts from research cruises (blue). Surface drifters trajectories (grey). Positions of the LION, LACAZE-DUTHIERS, PLANIER and DYFAMED moorings (white dots). From Testor et al. (2017).

for filling in the gaps and providing different observed scales. Physical sensors (temperature, salinity and current) as well as bio-optical ones (oxygen, chlorophyll-a, turbidity) allowed a continuous monitoring of the interactions between the physical forcings and the biogeochemical processes.

The combination of platforms and the coordination of sampling strategies ensured that the three phases were thoroughly observed. Maps of satellite derived surface chlorophyll-a concentration during each of the phases are shown in Figure 2.3. After a low phytoplankton content in late summer and fall, the mean concentration rises in winter around the "blue hole" that represents the mixed patch. A lagged bloom is observed in spring and then gradually fades out. But this description would not be complete without the vertical structure associated with these surface properties, and this is precisely what this

experiment enabled, providing about 40 profiles per day covering the whole Northwestern Mediterranean Basin[2].

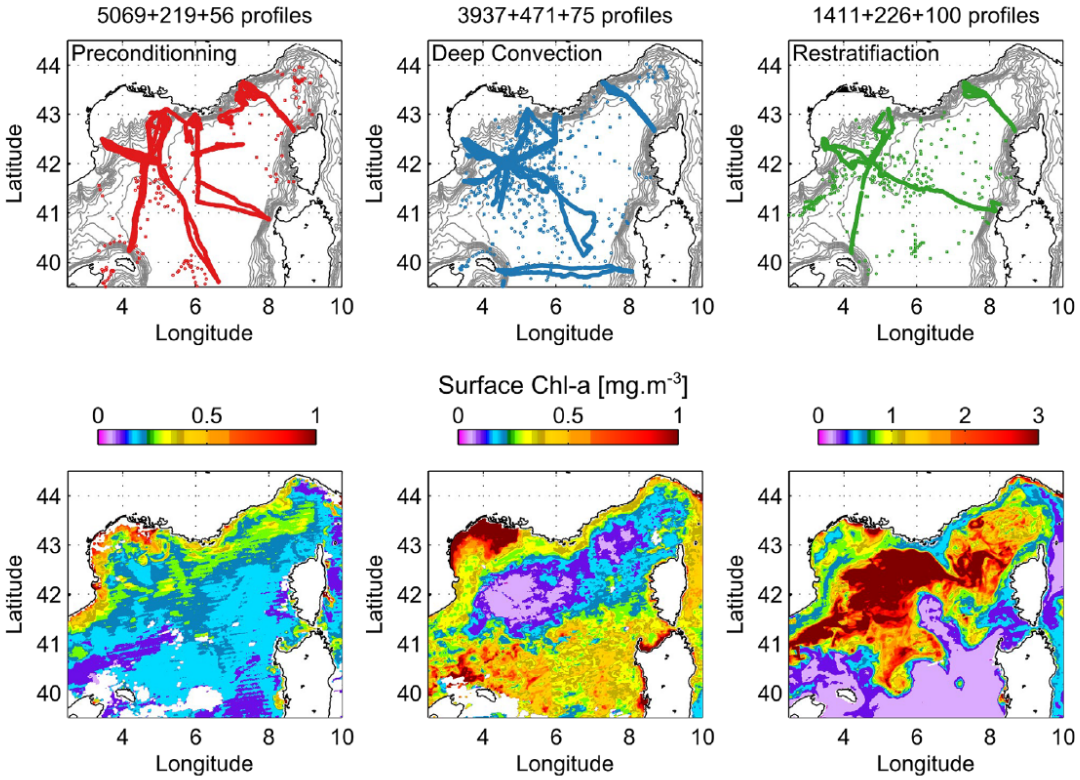

FIGURE 2.3: (top) Spatial coverage during the so-called preconditioning (1 September to 15 December 2012, left), violent mixing (15 December 2012 to 31 March 2013, middle) and restratification (1 April to 31 May 2013, right) phases of deep convection. The number of profiles, respectively collected by gliders, Argo profiling floats and Research vessels is indicated. (bottom) Surface chlorophyll-a concentration retrieved by satellite (L3 MODIS product) and averaged on (left) 1-2 November 2012, (middle) 13-21 February 2013, (right) 12-14 April 2013 that correspond to cloud-free periods during each phase. from Testor et al. (2017).

2.2 The convective plumes

One of the small scale features that could be observed is the convective plume. As can be seen in Figure 2.4, the vertical trajectory of the glider Campe was modified by vertical currents. Instead of its classical smooth saw-tooth trajectory, the glider underwent strong vertical velocities modifying its gliding pattern. The glider was able to cross the vertical stream in about 10 minutes, and the data collected along the way suggest that these downwelling waters where consistently colder and saltier than the mean surrounding waters.

[2]For more details on the experiment and a more thorough discussion on all the results briefly summed up hereafter, please refer to Testor et al. (2017).

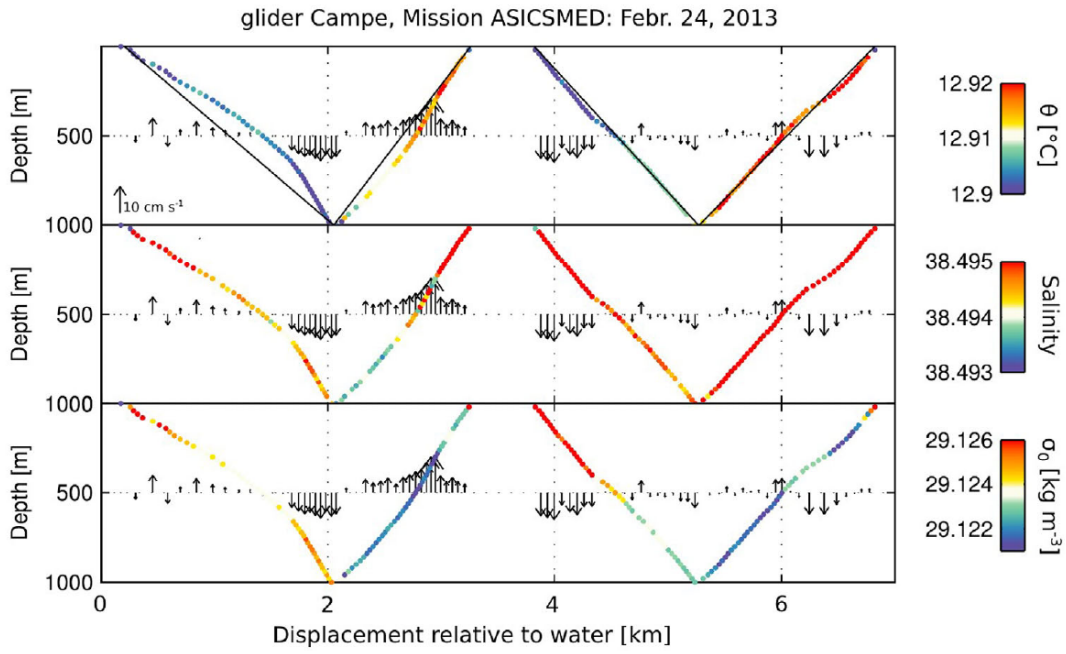

FIGURE 2.4: Vertical trajectory of a glider progressing through the Mixed Patch during violent mixing events colour-coded with potential temperature (top), salinity (middle), and potential density (bottom). Estimates of oceanic vertical velocities based on a glider flight model are displayed with black arrows.

2.2.1 Characterization of Convective Plumes Associated With Oceanic Deep Convection in the Northwestern Mediterranean From High-Resolution In Situ Data Collected by Gliders

Observing these first guess anomalous trajectories and strong downwelling waters encouraged a more thorough study of the so-called convective plumes, presented in the form of the following article published in *Journal of Geophysical Research: Oceans*.

AGU PUBLICATIONS

JGR

Journal of Geophysical Research: Oceans

RESEARCH ARTICLE
10.1002/2016JC012633

Special Section:
Dense Water Formations in the North Western Mediterranean: From the Physical Forcings to the Biogeochemical Consequences

Characterization of Convective Plumes Associated With Oceanic Deep Convection in the Northwestern Mediterranean From High-Resolution In Situ Data Collected by Gliders

Félix Margirier[1], Anthony Bosse[1,2], Pierre Testor[1], Blandine L'Hévéder[1], Laurent Mortier[1,3], and David Smeed[4]

[1]Sorbonne Universités (UPMC, Univ Paris06)-CNRS-IRD-MNHN, Laboratoire LOCEAN, Paris, France, [2]Geophysical Institute, University of Bergen, Bergen, Norway, [3]ENSTA ParisTech, Palaiseau, France, [4]National Oceanography Centre, Southampton, UK

Key Points:
- From a glider flight model, we extract for the first time the statistical physical and biogeochemical characteristics of convective plumes
- Intense vertical velocities are observed (up to 18 cm s^{-1}) and the plumes are found to cover about one third of the deep convection area
- Vertical velocities scaled by atmospheric fluxes inducing downward buoyancy fluxes with a vertical diffusion coefficient of 10 m^2 s^{-1}

Correspondence to:
F. Margirier,
felix.margirier@locean-ipsl.upmc.fr

Citation:
Margirier, F., Bosse, A., Testor, P., L'Hévéder, B., Mortier, L., & Smeed, D. (2017). Characterization of convective plumes associated with oceanic deep convection in the northwestern Mediterranean from high-resolution in situ data collected by gliders. *Journal of Geophysical Research: Oceans*, *122*. https://doi.org/10.1002/2016JC012633

Received 15 DEC 2016
Accepted 28 SEP 2017
Accepted article online 6 OCT 2017

Abstract Numerous gliders have been deployed in the Gulf of Lions (northwestern Mediterranean Sea) and in particular during episodes of open-ocean deep convection in the winter 2012–2013. The data collected represents an unprecedented density of in situ observations providing a first in situ statistical and 3-D characterization of the important mixing agents of the deep convection phenomenon, the so-called plumes. A methodology based on a glider-static flight model was applied to infer the oceanic vertical velocity signal from the glider navigation data. We demonstrate that during the active phase of mixing, the gliders underwent significant oceanic vertical velocities up to 18 cm s^{-1}. Focusing on the data collected by two gliders during the 2012–2013 winter, 120 small-scale convective downward plumes were detected with a mean radius of 350 m and separated by about 2 km. We estimate that the plumes cover 27% of the convection area. Gliders detected downward velocities with a magnitude larger than that of the upward ones (−6 versus +2 cm s^{-1} on average). Along-track recordings of temperature and salinity as well as biogeochemical properties (dissolved oxygen, fluorescence, and turbidity) allow a statistical characterization of the water masses' properties in the plumes' core with respect to the "background": the average downward signal is of colder (-1.8×10^{-3} °C), slightly saltier ($+4.9 \times 10^{-4}$ psu) and thus denser waters ($+7.5 \times 10^{-4}$ kg m^{-3}). The plunging waters are also on average more fluorescent ($+2.3 \times 10^{-2}$ μg L^{-1}). The plumes are associated with a vertical diffusion coefficient of 7.0 m^2 s^{-1} and their vertical velocity variance scales with the ratio of the buoyancy loss over the Coriolis parameter to the power 0.86.

1. Introduction

The deep convection phenomenon occurs in winter in the northwestern Mediterranean Sea and renews the deep waters by ventilating them. The volume of the newly formed deep waters depends both on the oceanic preconditioning and on air-sea fluxes inducing buoyancy losses at the surface. The Gulf of Lions is regularly subject to subsequent atmospheric forcings under the intense cold winds Tramontane and Mistral. In winter, those winds induce strong evaporation and an intense cooling of surface waters (∼−1,000 W m^{-2}; Leaman & Schott, 1991) and are responsible for buoyancy losses and vertical deep mixing. On the other hand, the horizontal circulation in the northwestern Mediterranean Sea controls heat and mass transfers and thus is a key to the ocean preconditioning of the deep convection events occurring in the Gulf of Lions, modulating in time and space the capacity of atmospheric forcing to trigger deep mixing (Grignon et al., 2010; Mertens & Schott, 1998).

Documented for the first time by the pioneer MEDOC Group in 1970 (MEDOC Group, 1970) and centered around 42°N, 5°E (on the Rhône deep sea fan), the processes involved in deep convection can be cut down into three phases (Marshall & Schott, 1999) that may overlap.

1.1. Hydrological Preconditioning

The convection event depends on the preconditioning which is variable over years as it depends on the hydrographic structure of the water column. The cyclonic circulation in the northwestern Mediterranean induces a doming of the isopycnals exposing sparsely stratified waters to the atmospheric forcing in the center of the gyre. The deep waters are thus nearer to the surface and easier to grasp for a local

Journal of Geophysical Research: Oceans 10.1002/2016JC012633

cooling/evaporation. Furthermore, the surface Atlantic Waters (AW) mix with warm and more particularly salty Levantine Intermediate Waters (LIW) lying below in the process, which can increase the efficiency of the mixing.

1.2. Vertical Mixing

The intense atmospheric forcing cools the surface waters and destabilizes the water column, especially in the preconditioned areas where plumes form when the mixing reaches great depths. According to the theory, their typical size is of 1 km in diameter over the whole mixed layer and the vertical velocities in those plumes can reach up to 10 cm s^{-1} (Leaman & Schott, 1991; Visbeck et al., 1996). This vision is only partial though, the mixed patch being variable both in size and depth from year to year and previously observed only from ADCP's on moorings at certain depths and only sampling plumes crossing the mooring lines. All the scales are at stake (Marshall & Schott, 1999, Figure 4) with plumes, eddies, and the gyre circulation interacting.

Both numerical and turning table experiments conducted by Maxworthy and Narimousas (1994)—see review by Marshall and Schott (1999)—indicate that the baroclinic instability exports new waters out of the mixed patch which can contribute to a slowing of the mixing as such. However, MEDOC Group (1970) suggested that this baroclinic instability could have a feedback on the ocean-atmosphere surface fluxes by bringing waters to the surface and maintaining the mixing. This is verified by numerical simulations which show that the combination of the atmospheric forcing and the baroclinic instability is responsible for the vertical mixing and is more powerful combined than taken separately (Legg & McWilliams, 2001; Straneo & Kawase, 1999). This demonstrates the dual role of the baroclinic instability and Visbeck et al. (1996) suggest a mixed-layer depth resulting from an equilibrium between the baroclinic instability and the forcing.

1.3. Lateral Exchanges and Spreading

After the intense forcing episodes, lateral energy transfers take over and eddies form. They spread due to the effects of stratification and rotation. Schott et al. (1996) observed fluctuations in temperature with a mooring placed along the Spanish coast, which could imply an incorporation of these waters to the northern current flowing along the continental slope north and west of the convection area. They estimated that 50% of the newly formed waters could escape with the current. Madec et al. (1991) numerical simulations hypothesized this mechanism while Testor & Gascard (2006) estimated that 50% of the newly formed waters spread in the basin in coherent (lifespan over 1.5 years) lenticular (thickness h $\sim$ 1 km) submesoscale eddies (5–10 km in radius).

During winter 2012–2013, open-ocean deep convection occurred in the Gulf of Lions (northwestern Mediterranean Sea) and has been thoroughly documented thanks in particular to the simultaneous deployment of several gliders, of Argo profiling floats, dedicated ship cruises, and a mooring located within the mixed patch (Testor et al., 2017). Because of the difficulty to conduct a cruise in winter due to strong weather events (Eriksen & Rhines, 2008), gliders are of crucial importance to observe oceanic processes such as deep convection. The surface of the mixed patch has been estimated to be 15,500 km^2, corresponding to a formation of 1.1 Sv of deep waters in 2012 (Durrieu de Madron et al., 2013) and 2 Sv in 2013 when up to five gliders were at sea simultaneously covering the area in a synoptic way (Bosse, 2015).

We compute water vertical velocities from a glider flight model to assess the vertical velocities associated with intense deep convection episodes in the Gulf of Lions in the winter 2012–2013 in section 2. Section 3 presents the derived method to detect convective plumes and to give a description of their properties relative to surrounding waters. We finally assess the plume coverage of the convective region and confirm the effect of rotation on the plume characteristics in section 4.

2. Materials and Methods

2.1. Description of the Data Set and Methodology

2.1.1. Data

The gliders data collected during the 2012–2013 winter provides an unprecedented density of in situ observations during an event of open-ocean deep convection. Gliders move along saw-tooth trajectories between the surface and a maximum depth of 1,000 m, covering a distance of 2–4 km in a time period of 2–4 h between two surfacings. They record temperature and salinity as well as biogeochemical properties

AGU Journal of Geophysical Research: Oceans 10.1002/2016JC012633

(dissolved oxygen, chlorophyll-a fluorescence, turbidity-optodes Anderaa, and Wet-Lab ecopuck FLNTU) along their trajectory. During the active phase of mixing of the deep convection, the gliders have undergone significant oceanic vertical upward and downward velocities, stronger than 10 cm s^{-1}, that could be seen by just looking at the pressure time series of the gliders. With a vertical speed of 10–25 cm s^{-1} relative to the water, gliders present trajectories that were significantly perturbed by the oceanic vertical velocities associated with the plumes. The gliders were equipped with an unpumped CTD probe (SBE-41) that generally needs to be corrected with an offset as a first order correction for each single deployment. The SBE-41 CTD sensor has an absolute accuracy of 0.002°C and 0.003 psu, and relative accuracies of 0.0001°C and 0.0007 psu. As in Bosse et al. (2016) and in Testor et al. (2017), we compared gliders data with nearby calibrated CTD casts from R/Vs (<15 km and <3 days), and with the calibrated mooring lines LION and DYFAMED (<2.5 km and <18 h, about the inertial period in this region). The cross-platform hydrographical consistency was checked in the deeper layers sampled by the gliders (700–1,000 m) because the T/S variability is relatively small at those depths. The deduced T and S offsets are of 0.001°C and of −0.003 psu for the deployment Campe/ASICSMED and of 0.001°C and of 0.01 psu for the deployment Milou/ASICSMED. This study focuses on statistical relative differences and the results are thus not affected by the applied offsets. In addition, the thermal lag issue of the unpumped CTD probe that can affect salinity measurements in strong thermoclines (order of 1–10°C over less than 10 m) has been corrected following Garau et al. (2011). Those are second-order corrections because there is no strong thermocline in the homogeneous convection area where the plumes are observed.

2.1.2. Glider-Static Flight Model

To go further and get quantitative water vertical velocities, a methodology based on a glider quasi-static flight model is applied to infer the oceanic vertical velocity signal from the glider navigation data, following the methods in Merckelbach et al. (2010) and Frajka-Williams et al. (2011). The glider is modeled in a quasi-steady flight and in the absence of vertical displacements. Thus, the vertical velocity of the water can be extracted from the gliders vertical movement, giving an estimate of the convective velocities.

The different forces exerted on the glider, represented in Figure 1, follow the ensuing equations (the definitions of the different variables are given in Table 1),

$$F_B = g\rho(V_g(1-\epsilon P+\alpha_T(T-T_0))+\triangle V_g), \tag{1}$$

$$F_g = m_g g, \tag{2}$$

$$F_L = \frac{1}{2}\rho S U^2 a\alpha, \tag{3}$$

$$F_d = \frac{1}{2}\rho S U^2 (C_{D_0}+C_{D_1}\alpha^2). \tag{4}$$

The projections of the glider-static equilibrium on the vertical and horizontal thus give,

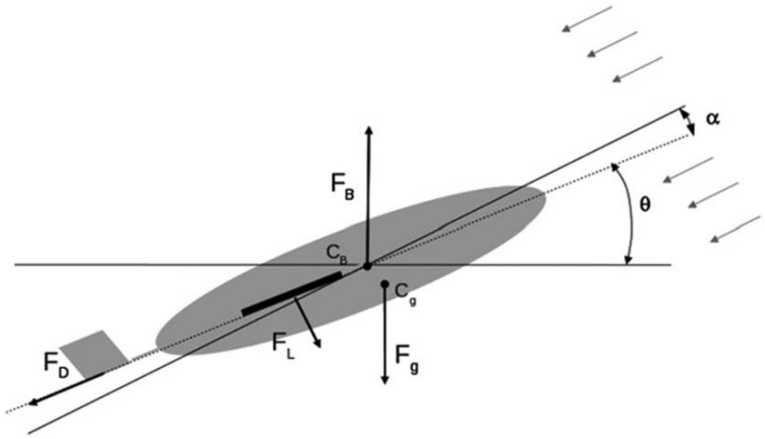

Figure 1. Schematic view of a glider flight on a vertical plane: Buoyancy force F_B, gravity F_g, lift F_L, and drag F_D; the sum of attack angle α and pitch θ makes the glide angle γ (from L'Hévéder et al., 2013).

Journal of Geophysical Research: Oceans 10.1002/2016JC012633

Table 1
Parameters of the Glider Flight, Their Origins and Their Typical Value During an Ascent or a Descent

Parameter	Description	Origin	Typical value	Unit
F_B	Buoyancy force	Computed		N
F_g	Gravitational force	Computed		N
F_L	Lift force	Computed		N
F_d	Drag force	Computed		N
U	Glider velocity	Computed	0.4	$m\ s^{-1}$
u_{glider}	Glider horizontal velocity	Computed		$m\ s^{-1}$
w_{glider}	Glider vertical velocity	Computed		$m\ s^{-1}$
w_{water}	Water vertical velocity	Computed		$m\ s^{-1}$
α	Attack angle	Computed	$\pm$2–3	°
γ	Glide angle	Computed	$\pm$25	°
θ	Pitch angle	Measured by glider sensors	$\pm$22	°
P	Water pressure	Measured by glider sensors		Pa
T	Water temperature	Measured by glider sensors		°C
ρ	Water density	Measured by glider sensors		$kg\ m^{-3}$
C_{D_0}	Parasite drag	Optimized	0.1	rad^{-2}
ϵ	Hull compressibility	Optimized	5.7×10^{-10}	Pa^{-1}
V_g	Glider volume	Optimized	55.5	L
T_0	Reference water temperature	Constant	13.1	°C
g	Acceleration of gravity	Constant	9.81	$m\ s^{-2}$
m_g	Glider mass	Characteristic of the glider	57	kg
$\triangle V_g$	Pumped volume	Characteristic of the glider	0.25	L
S	Wing surface area	Characteristic of the glider	0.1	m^2
C_{D_1}	Induced drag	Characteristic of the glider	2.88	rad^{-2}
a	Lift coefficient	Characteristic of the glider	6.1	rad^{-1}
α_T	Thermal expansion coefficient	Characteristic of the glider	7.05×10^{-5}	K^{-1}

$$/z : F_B - cos(\gamma)F_L - sin(\gamma)F_d - F_g = 0, \tag{5}$$

$$/x : cos(\gamma)F_d - sin(\gamma)F_L = 0. \tag{6}$$

The water's vertical velocity is estimated as the difference between the velocity derived from the rate of change of pressure and that predicted by the glider flight model.

$$w_{water} = \frac{dz_P}{dt} - w_{glider}. \tag{7}$$

In a quasi-static equilibrium, injecting equations (3) and (4) in the projection (equation (6)) of the equilibrium and considering that $\alpha + \theta = \gamma$ gives the following expression for the angle of attack α:

$$\alpha = \frac{C_{D_0} + C_{D_1}\alpha^2}{atan(\theta + \alpha)}. \tag{8}$$

In order to compute the water vertical displacements with precision, some parameters are optimized (see Table 1) with the following cost function:

$$J(C_{D_0}, \epsilon, V_g) = \sum \left(\frac{dz_P}{dt} - w_{glider} \right)^2. \tag{9}$$

Vertical movements of the water are minimized (the model makes the hypothesis there are none) over a 24 h period (long enough to consider that the mean vertical velocities are null). We are thus able to compute α from equation (8) and thus U (substituting equations (1)–(4) into equation (6)). We then obtain the glider's velocity components,

$$u_{glider} = Ucos(\theta + \alpha), \tag{10}$$

$$w_{glider} = Usin(\theta + \alpha). \tag{11}$$

And we then finally retrieve w_{water} from equation (7).

AGU Journal of Geophysical Research: Oceans 10.1002/2016JC012633

2.2. Validation of the Resulting Water Velocity

Figure 2 portrays the evolution of the resulting vertical water velocity in the absence and in the presence of a convection episode. The optimization algorithm converges and the parameters obtained by this method vary slightly: 10% of their values for C_{D_0} and ϵ, and the variation of the glider volume (10 cc) is negligible compared to its volume V_g (55,000 cc). Furthermore, the robustness of the method is highlighted by the fact that the extracted vertical velocities are not affected by the glider vertical movement (plunging or ascending). This is verified in Figure 2a: at 08:00 the glider, undergoing large water vertical velocities (larger than 5 cm s^{-1}), switches from a downcast to an upward motion and the water vertical velocity remains coherent during the change.

To assess the quality of our results, we compared the vertical water velocities computed with the glider data to the ones measured at the LION mooring line situated in the middle of the mixed patch at 42°02′N, 4°41′E and a bottom depth at 2,350 m (Houpert et al., 2016; Testor et al., 2016)—current meters moored at 150, 250, 500, and 1,000 m depths are used as the one at 2,315 m allows no comparison with the glider data. Figure 3 provides a comparison of those water vertical velocities. The glider data reproduce very well the distribution of vertical displacements both during convective episodes and in their absence. The 30-min sampling rate of the LION mooring's current meters does not allow more than two or three points inside a plume but does enable a statistical comparison with the gliders' data. Noticing that the velocities are never greater than 3–4 cm s^{-1} in the absence of convection, we thus used it to define a threshold for the detection of convective episodes: a convective episode is detected when 10% of the velocities are greater than 4 cm s^{-1} over a 24 h period. This enables an automatic detection of convective episodes, which are then cut down into convective plumes defined by both those velocities and a lateral extension over 100 m. We

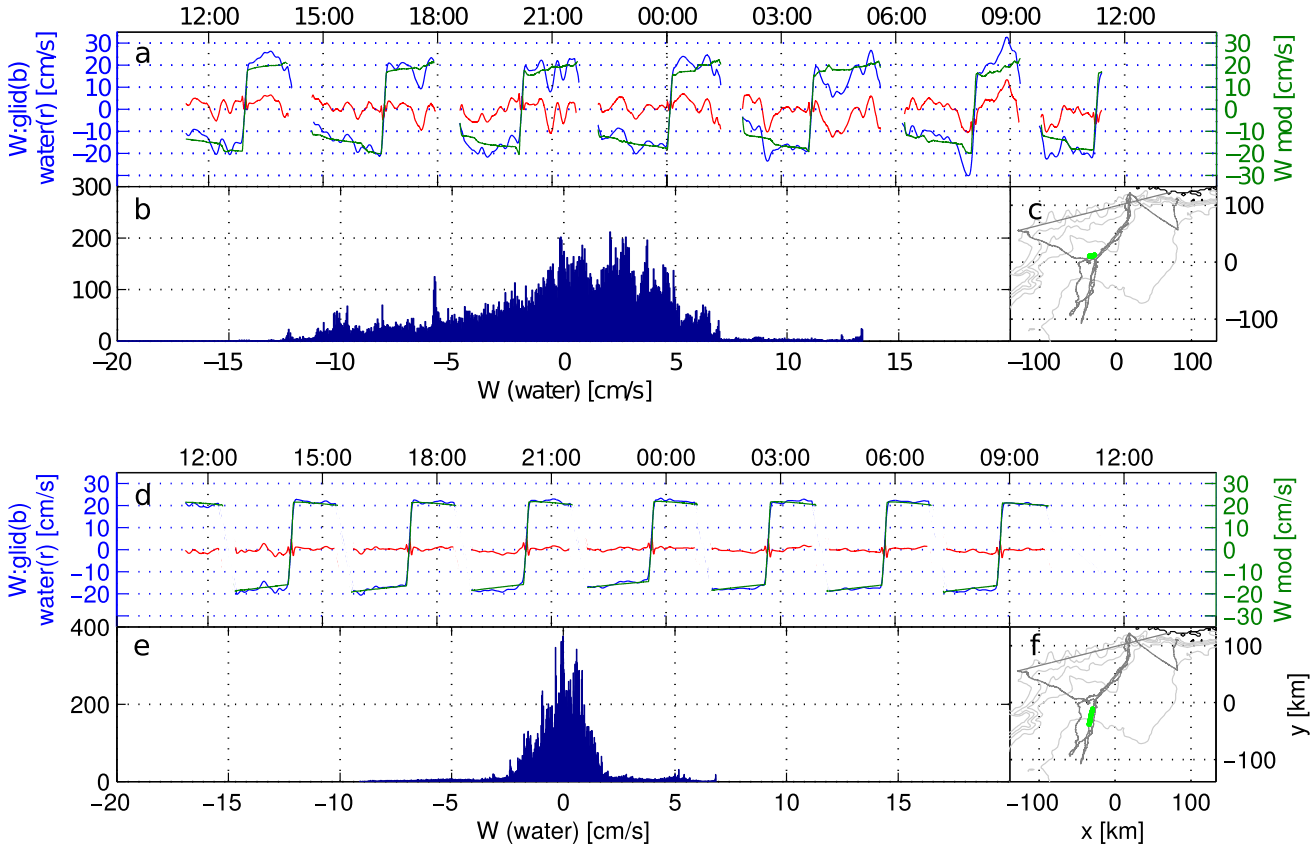

Figure 2. Flight parameters and resulting water vertical velocity in the absence of convection the 30 January 2013 (bottom) and during convection the 23 February 2013 (top). (a) Glider vertical velocity w_{glider} (blue), pressure gradient induced velocity $\frac{dZ_p}{dt}$ (green), and water vertical velocity w_{water} (red). (b) Distribution of water vertical velocities. (c) Glider trajectory, in green the portion represented above. (d) Glider vertical velocity w_{glider} (blue), pressure gradient induced velocity $\frac{dZ_p}{dt}$ (green), and water vertical velocity w_{water} (red). (e) Distribution of water vertical velocities. (f) Glider trajectory, in green the portion represented above.

Journal of Geophysical Research: Oceans 10.1002/2016JC012633

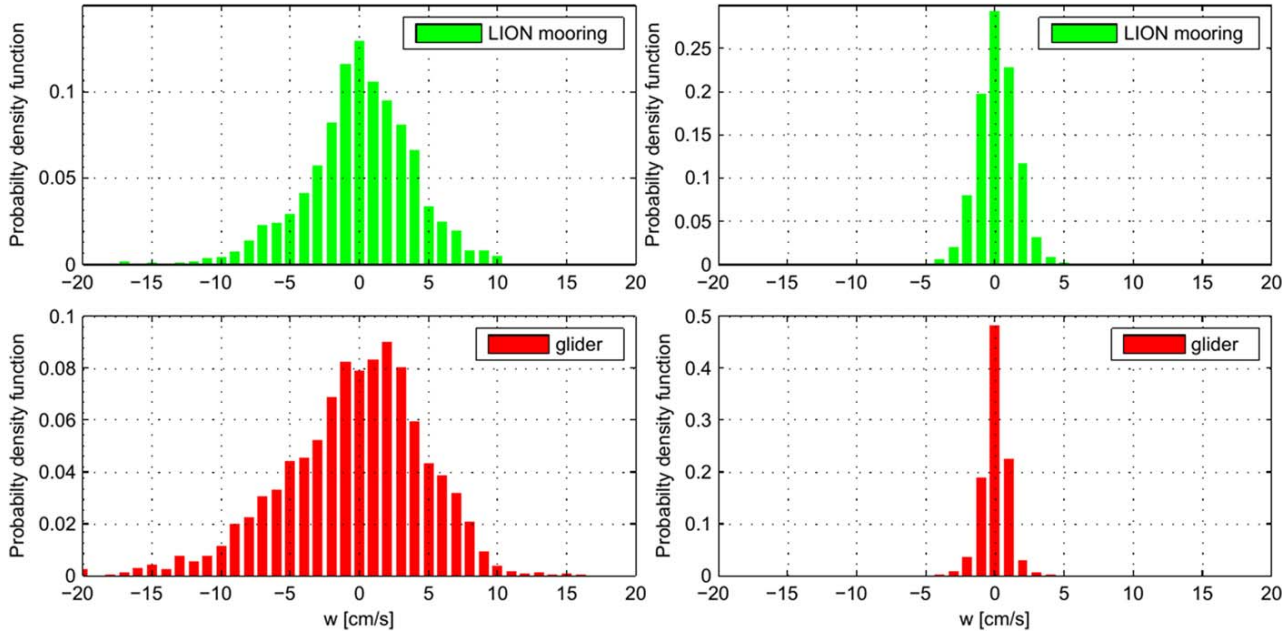

Figure 3. Velocities distribution over the first 1,000 m on the LION mooring (up) and measured by the glider (bottom) from 1 February 2013 to 15 March 2013. (left) During periods of high buoyancy loss (net heat fluxes <-500 W m^{-2}); (right) during low buoyancy loss (net heat fluxes >-100 W m^{-2}) episodes.

thus exclude the plumes for which only the border is sampled by imposing a minimum distance of 100 m during which the glider is exposed to those significant downwelling velocities. This enables the detection of 120 plumes over the two deployments Campe/ASICSMED and Milou/ASICSMED which were at sea during the intense convective winter of 2012–2013.

3. Characterization of Convective Plumes

The properties measured by glider Campe are represented in Figure 5. The glider performed north-south transects across the Gulf of Lions as can be seen in Figure 4 where the tracks of gliders Campe/ASICSMED and Milou/ASICSMED are shown. In Figure 5, one can notice the intense fronts of the northern current and the North Balearic front surrounding the mixed patch. During those transects, glider trajectories are not straight lines as we usually expect because of the strong vertical velocities associated with plumes deviating it. Figure 5 highlights various small-scale ($<$1 km) features associated with temperature, salinity, and density variations and questions the idea of a homogeneous mixed patch.

We also note that the waters are already homogeneous during the gliders' first passage in the Gulf of Lions (27 January to 3 February), indicating a previous mixing episode. No significant vertical velocities are detected during the first transect. The heat fluxes (retrieved from ALDERA reanalysis and interpolated along the glider track) are weak, inducing no buoyancy losses and thus no plumes at that time.

Later on, we detect two main episodes of convection (8–11 February and 24–27 February) where vertical velocities are large and the water is homogeneous over depths. Significant heat losses (consistently over $-1{,}000$ W m^{-2}) at the surface of the sea are followed by strong vertical velocities and active mixing. It is also noted that the waters get denser, colder, and richer in oxygen over time due to the mixing process.

If the glider was under vertical inertial movements, it would be associated with the Brunt-Väïsälä frequency $N \sim \frac{2*\Pi}{3600}$ (time scale of 1 h) but the stratification is a lot smaller in the mixed patch and N yields a period of 4–8 h. The plume persistence time scale is estimated to scale in f^{-1} by Marshall and Schott (1999), giving 17 h. Sea state varies on a scale of 4 h as a result of the variability of the atmospheric forcing, so considering the glider crosses a plume in 1–2 h, we can thus extract a typical convective plume (see Figure 6) to get its properties. Inside the plume core, the downwelling waters are colder and saltier, thus denser. The downwelling velocities are also greater than the upwelling ones around our structure. Some signatures also appear

AGU Journal of Geophysical Research: Oceans 10.1002/2016JC012633

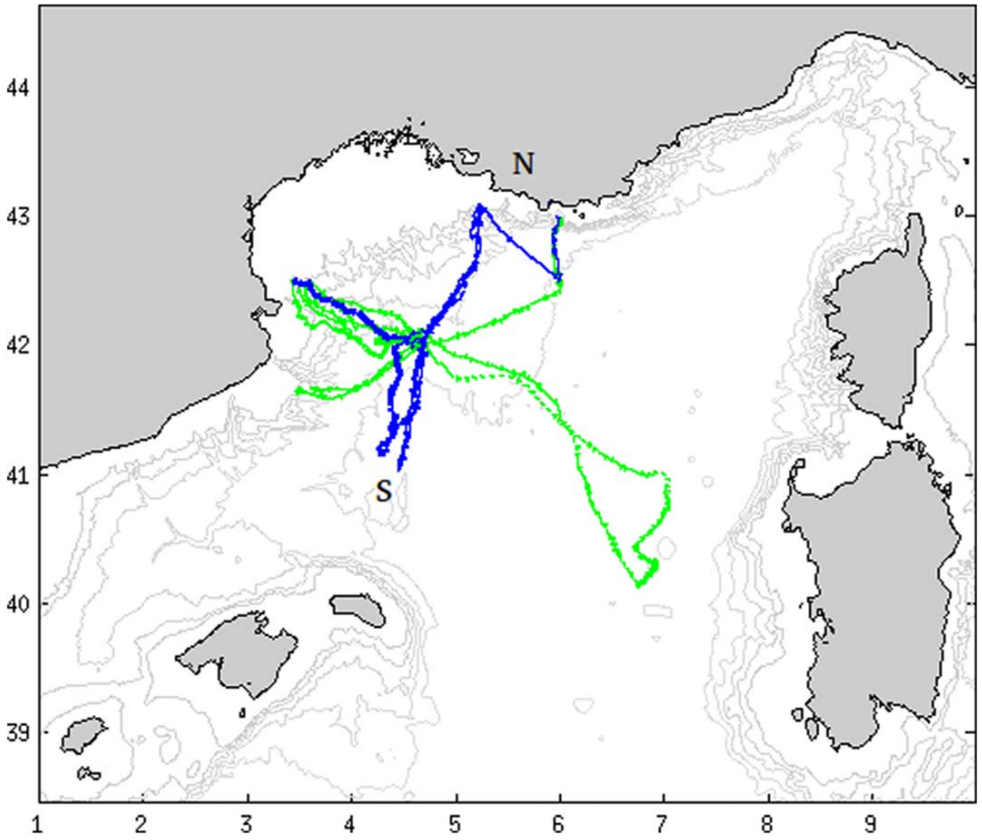

Figure 4. Milou/ASICSMED (green) and Campe/ASICSMED (blue) glider tracks. N (for North) and S (for South) are geographical markers for the transect used in Figure 5.

for the biogeochemical parameters, but not as clearly (oxygen is plotted relative to a trend estimated on a downcast/upcast).

In order to confirm those tendencies and generalize, we normalize the 120 detected plumes. To do this, we associate each plume to its radius (half of the distance where velocities are negative) and plot the set of data at a relative distance to the center of the structure (folding the plume around its center). The normalized folded plumes are superimposed in Figure 7. The running mean of those normalized plumes is performed on the points within the standard deviation after the exclusion of outliers (5th and 95th percentiles considering a Gaussian distribution). Negative velocities (-6 cm s^{-1}) are three times larger than positive ones (around $+2$ cm s^{-1}). The physical and biogeochemical properties of the plumes are plotted compared to their value at R = 1 where the vertical velocities are null. Their signatures are then retrieved statistically as the difference between the mean value far from the plume at $R = 2.5$ compared to that in the center of the plumes at $R = 0$. The temperature, salinity, density, and fluorescence panels in Figure 7 present a plateau in the core of the plume ($R < 0.4$) suggesting a coherent structure. The gray shading being the running standard deviation, the running standard error on the mean is then retrieved dividing by the square root of the number of points in the running bins and is very small due to the large number of points in each bin (minimum 1,363 points per bin). Statistically, the downwelling waters appear colder ($-1.81\pm0.04\times10^{-3}$ °C), slightly saltier ($+4.9\pm0.3\times10^{-4}$ psu) and thus denser ($+7.5\pm0.3\times10^{-4}$ kg m^{-3}). The results for the temperature are one order of magnitude greater than the accuracy of the sensor for the temperature (1×10^{-4} °C) and for the salinity, the results are of the order of magnitude of the sensor resolution (7×10^{-4} psu), the results being statistically significant due to the large number of plumes observed. They are also on average moderately more fluorescent (phytoplankton being dragged down, $+2.30\pm0.03 \times10^{-2}$ μg L^{-1}). Although no signal can be directly retrieved from the oxygen and turbidity panels, it is worth noting that individual plumes have small signatures in turbidity of different signs which may

Journal of Geophysical Research: Oceans 10.1002/2016JC012633

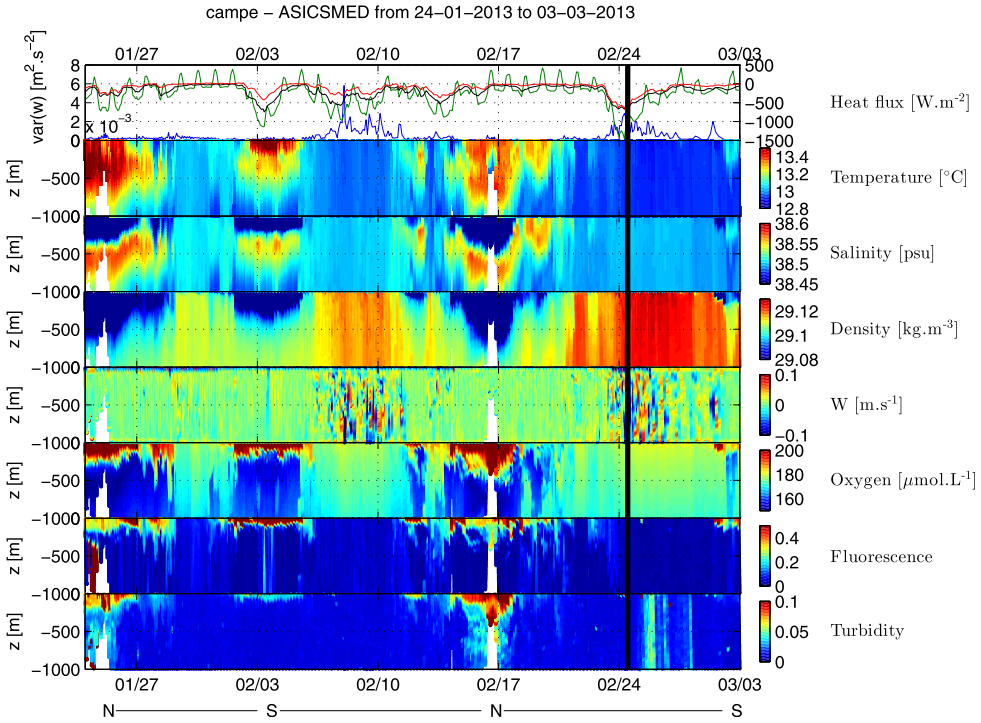

Figure 5. Glider transect Campe/ASICSMED. For the top figure, the variance of the vertical velocities during a yo (a downcast and an upcast) is represented in blue and the sensible, latent, and net heat fluxes are, respectively, in red, black, and green. The black vertical line corresponds to the plume represented in Figure 6. Two convective episodes of approximately three days are seen following important buoyancy losses due to the heat fluxes: 8–11 and 24–27 February. N and S letters represent the northern and southern outreaches of the glider (see Figure 4).

compensate overall, some show more turbid and oxygenated plunging waters while others have the opposite downwelling signature (not shown here). In general, the relatively small differences detected between the core of the plumes and their environment reflect the fact that the gliders evolve in an already well mixed area.

We assess the plumes' vertical structure by binning the collected data by the depth where the glider crossed the maximum vertical velocity of the plume. By doing so, we sort the plumes by depth of maximum velocity and are thus able to suggest a vertical structure of convective plumes. As the mixed layer reached the bottom during the mixing episodes (Houpert et al., 2016), the deceleration when reaching the bottom cannot be well represented here as the gliders did not fly deeper than 1,000 m. We observe that the vertical velocities in the plumes are somewhat larger when the plumes are detected deeper and that they seem to get wider as they descend, similarly to atmospheric convection.

4. Discussion

4.1. Spatial Coverage

In order to complete the study of plumes, we have to take into account that the glider crosses the plumes neither necessarily in its center nor horizontally. The vertical extension of a plume crossing has been found to vary from 200 m up to the whole extent of a descent/ascent: 1,000 m. The horizontal mean radius of the detected plumes is of 312 m. This is in good agreement with Marshall and Schott (1999) who predicted a typical lateral extension of 500 m. We consider a simple isotropic cylindrical model for the plumes and with the hypothesis that the glider can cross a plume any given way. Taking into account the 100 m threshold established previously for the detection, we find an effective plume radius of 350 m and a mean distance of 1.85 km in between plumes along a glider track. This is in good agreement with previous estimates made by Merckelbach and Smeed (2006) and Smeed et al. (2007) (R ∼300 m and 2 km between plumes) and

AGU Journal of Geophysical Research: Oceans 10.1002/2016JC012633

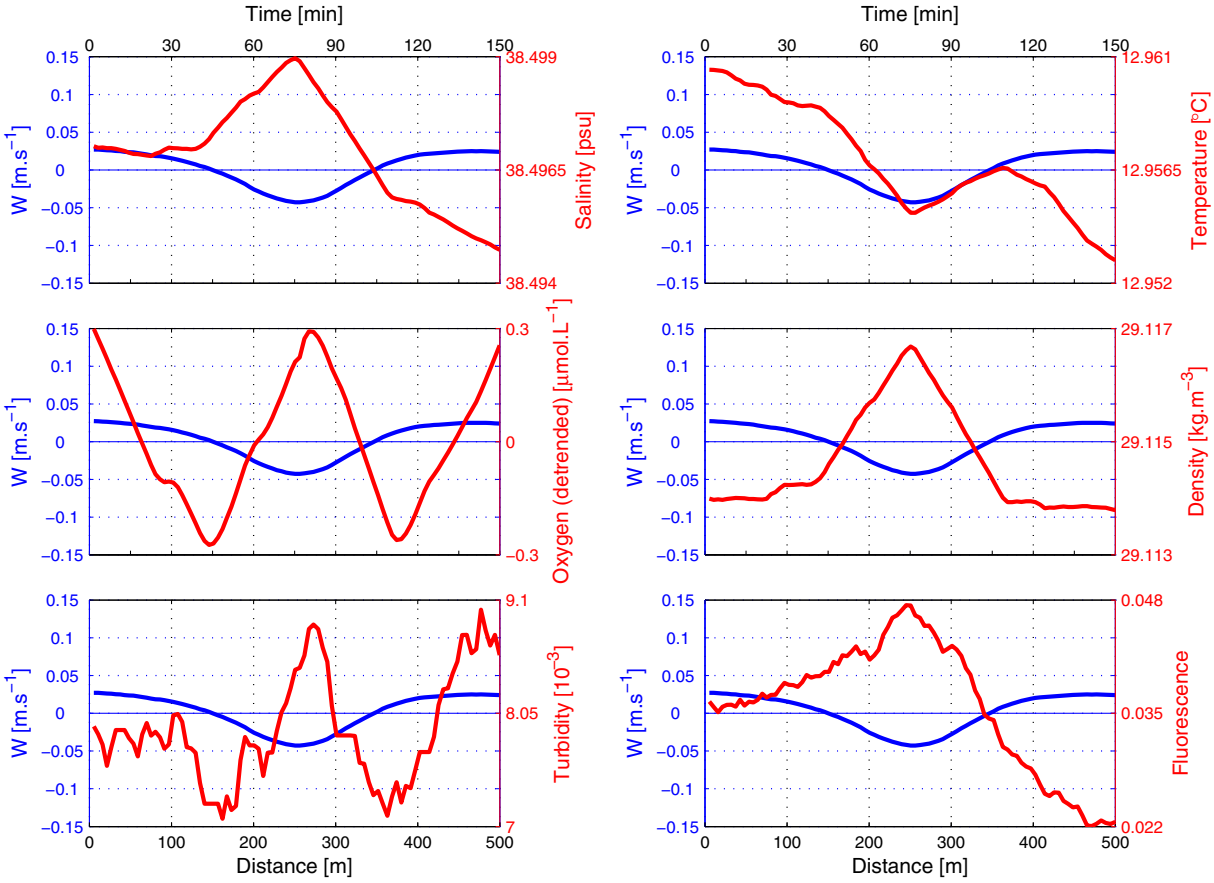

Figure 6. A typical convective plume (marked in time by a black vertical in Figure 5). Top left to bottom right: Salinity, temperature, oxygen (detrended); density, turbidity, and fluorescence (in red); water vertical velocity (in blue).

Paluszkiewicz et al. (1994, R ~300–500 m). Computing the mean distance between plumes along the glider track, we find that plumes cover 40% of the trajectory and considering an isotropic distribution of the plumes on a triangular horizontal grid with those distance characteristics gives a 27% coverage of the convective patch by negative velocities, while the rest is covered by positive and generally small velocities as suggested by Send and Marshall (1995). This simple coverage scheme and the associated velocity coverage of the area gives a 91% correspondence between the upwelling and downwelling waters, also allowing for lateral spreading at depth. The knowledge of the small structures in the convective patch could allow a better parametrization of this key phenomenon renewing deep waters in models. Ocean general circulation models see convection as a subgrid phenomenon and the physics of mixing are parametrized in order to render the distribution of heat and the mixing. Some LES models such as Paluszkiewicz et al. (1994) or the MITgcm used in Johannessen et al. (2013) attempted this finer parametrization which can now be completed with the current dataset. Our results can suggest paths toward better parametrization of convection in models.

4.2. Scalings

The theory developed in Maxworthy and Narimousa (1994) and Marshall and Schott (1999) predicts that the distribution of velocities is symmetrical when there is no impact of rotation and suggests a scaling for the vertical velocities depending on the surface buoyancy losses. The vertical mixing is not influenced by rotation when the convective layer depth limit $h^*=(B/f^3)^{1/2}$ is greater than the convective depth (B being the buoyancy loss, f the Coriolis parameter). Otherwise, Marshall and Schott (1999) predicted that the mixing would not be influenced by Earth's rotation and a symmetrical distribution of velocities in $(Bh)^{1/3}$. In the northwestern Mediterranean, $B=0.2\times10^{-6}$ to 0.5×10^{-6} m^2 s^{-3} which gives $h^*=450$ to 700 m and an associated $w=(Bh^*)^{1/2}=4$ to 7 cm s^{-1}. In the Gulf of Lions, the convection reached the bottom (2,300 m)

Journal of Geophysical Research: Oceans 10.1002/2016JC012633

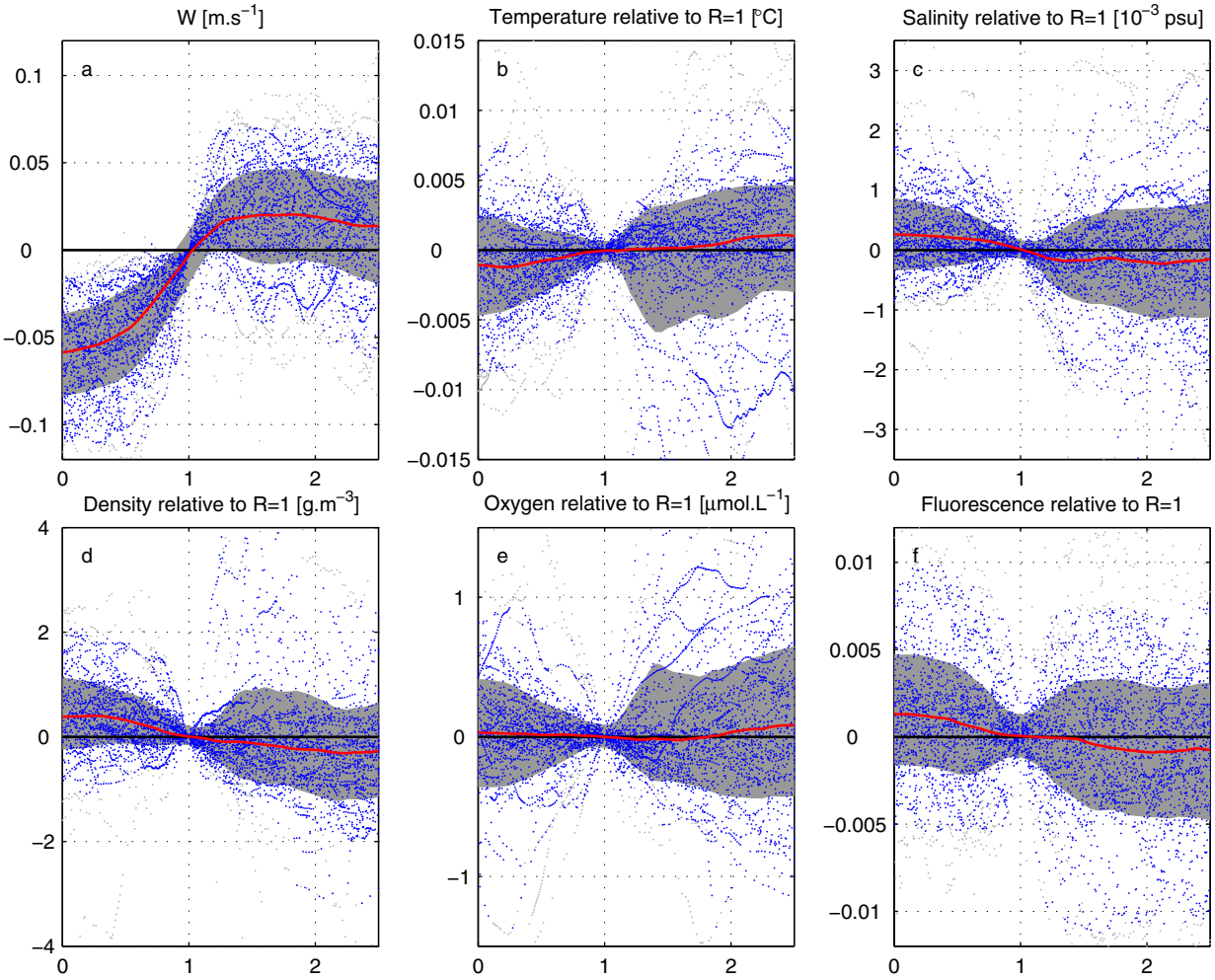

Figure 7. Plume tendencies as detected from two gliders (Campe/ASICSMED and Milou/ASICSMED) during the 2012–2013 winter. The point at R = 1 where the vertical velocities are zero is taken as the reference. The core of the plumes is at R = 0, the environing waters are considered at R = 2.5. The 5% higher and lower values (in gray) are considered outliers. The running standard deviation is in a grey shading and the running mean of the points is within the standard deviation is in red. (a) Water vertical velocity. (b) Temperature relative to R = 1. (c) Salinity relative to R = 1. (d) Density relative to R = 1. (e) Oxygen relative to R = 1. (f) Fluorescence relative to R = 1.

during our episode and we observed velocities up to 18 cm s^{-1}, confirming the influence of rotation on the observed plumes and the asymmetrical velocity distribution in Figure 3. Knowing that the observed convective plumes are under the influence of rotation, we test the scaling suggested by Marshall and Schott (1999). The scaling for the vertical velocities under the influence of rotation is estimated to be in $w=(B_0/f)^{1/2}$. Using the mean value $B_0 = -2.9\times10^{-7}$ m^2 s^{-3} above plumes, we get a vertical velocity of $w = 5.45$ cm s^{-1} in good agreement with what is observed in the plumes.

To complete the study, we suggest a scaling for the variance of w against the buoyancy loss inferred from the heat fluxes. The standard formula for the buoyancy loss gives $B_0 = g\ \frac{\alpha}{C_p}\ \frac{h_{net}}{\rho}$, α being the thermal expansion coefficient of the water, C_p the water heat capacity, h_{net} the net heat flux, and ρ the water density. Using the inferred B_0 and computing the velocity relative to fluxes during the intense episodes (net heat fluxes <-400 W m^{-2}), we consistently obtain a relation in $variance(w)=(B_0/f)^e$ where $e=0.86\pm0.01$ with an RMSE of 0.9992.

4.3. Vertical Diffusion Coefficient

Individual plumes induce intense vertical mixing and we can statistically estimate a vertical diffusion coefficient Kz associated with their overall effect on the water column. We examined in particular two intense

AGU Journal of Geophysical Research: Oceans 10.1002/2016JC012633

convection episodes (7–9 February and 23–25 February), the second one being represented in Figure 8. Both are characterized by large fluxes and the mixed layer reaching the bottom.

Knowing the size of the plumes, we estimate buoyancy fluctuations b' relative to a 1 h running mean. This is justified by the fact that 1 h represents about 1 km of horizontal glider displacement which is 1.5–2 times the diameter of a plume. The plumes are responsible for a vertical buoyancy flux determined by the correlation of w' and b'. By construction, $<w> = 0$ and thus $w = w'$. Figure 8 shows a $<w'b'> > 0$ tendency demonstrating a statistical buoyancy flux from the surface to the ocean interior. The intense cooling at the surface fits with the $B_0 = 2.9 \times 10^{-7}$ m^2 s^{-3} inferred from the net heat fluxes and is consistent with the increasing of buoyancy flux due to the plumes near the surface. The buoyancy loss then diminishes, its intensity approaching 10^{-7} m^2 s^{-3}. Now looking at the vertical distribution of buoyancy, we observe a mean decrease of buoyancy close to the surface after averaging the buoyancy of the 30 considered profiles. This results from a tendency of densification of the surface layer. The buoyancy distribution was computed relative to the surface, as temporal and spatial variability of the water column can induce lateral gradients of buoyancy. Parametrizing the statistical mean buoyancy flux during the mixing period by a diffusivity flux yields $<w'b'> = -K_z \frac{d<b>}{dz}$ (axis z pointing to the surface). We could thus infer a vertical diffusion coefficient K_z in layers of 50 m (see Figure 8f). After removing outliers caused by too weak or reverse buoyancy gradients between two consecutive layers, we found on average a mean diffusion coefficient of 5.0 ± 3.7 and 7.0 ± 4.3 m^2 s^{-1} for the two mixing events.

This is consistent with the vertical diffusion estimates made by a recent study by Durrieu de Madron et al. (2017, Figure 14) finding 10–50 m^2 s^{-1} to get vertically homogeneous profiles over 28 h for sediment plumes. The mean diffusion coefficient we found is also in good agreement with Klinger et al. (1996) numerical experiments on convective plume dynamics suggesting 10 m^2 s^{-1} for vigorous deep convective events.

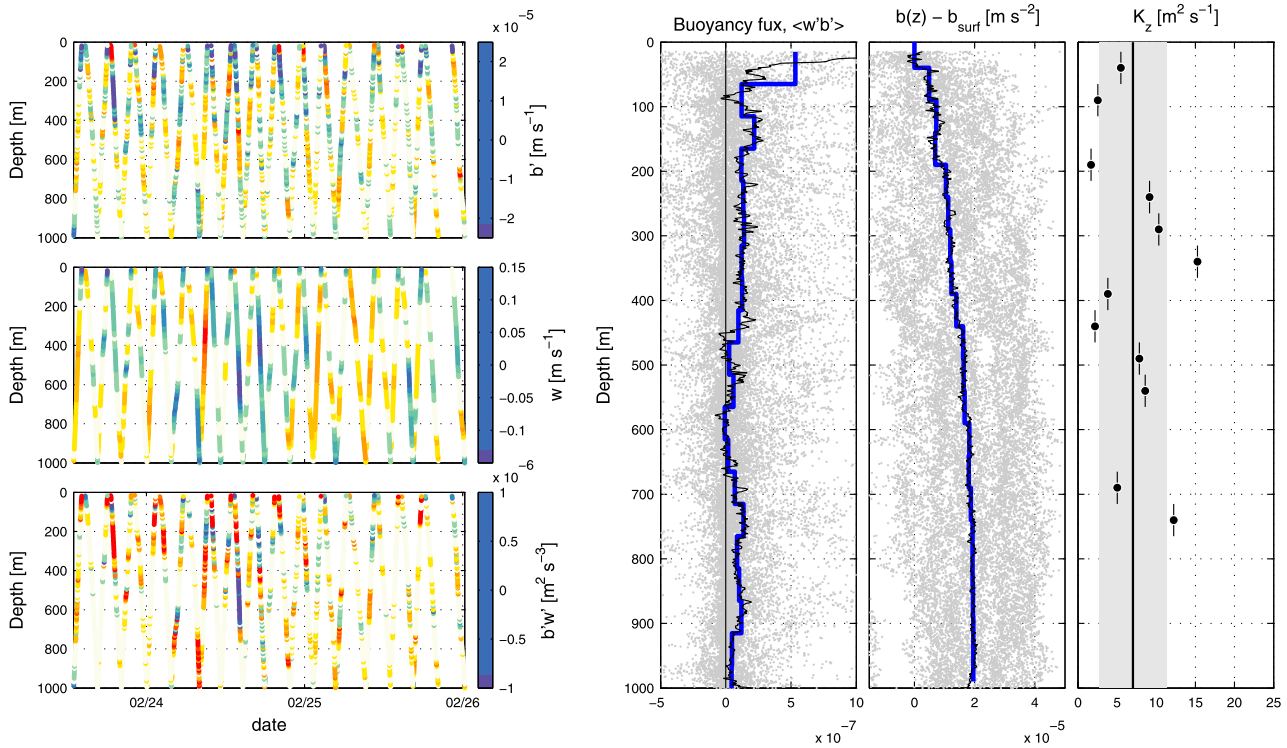

Figure 8. Glider flight conditions and buoyancy losses during a convective period of three days (23–25 February). The left figure shows the along-track buoyancy fluctuations, water vertical velocities, and buoyancy losses. The right figure shows the mean buoyancy fluxes in the water column and its 50 m binned values; the buoyancy relative to the surface and the associated vertical diffusion coefficient. Near-surface data of the top 15 m have been excluded to get rid of spurious data that could have been caused by the rough sea state or cooling of the glider by cooling of the instrument at the surface.

Journal of Geophysical Research: Oceans 10.1002/2016JC012633

5. Conclusions and Perspectives

Building on the methods presented in Merckelbach et al. (2010) and Frajka-Williams et al. (2011), our study aims at a deeper understanding of the role of convective plumes in the mixing of physical and biogeochemical tracers during deep open-ocean convection events. It provides for the first time a comprehensive characterization of convective plumes on a statistical basis showing an asymmetry between up and down movements with stronger downward velocities. The downward velocities are of higher magnitude than the upward ones (-6 versus $+2$ cm s^{-1} on average). We highlight the relation between these vertical movements and the physical and biogeochemical water properties. Statistically, the plunging waters are colder (-1.8×10^{-3} °C), moderately saltier ($+4.9 \times 10^{-4}$ psu) and thus denser ($+7.5 \times 10^{-4}$ kg m^{-3}) than the surrounding upward ones. The downward waters are also on average a little more fluorescent ($+2.3 \times 10^{-2}$ μg L^{-1}) as phytoplankton is being dragged down. For the first time, the horizontal scales associated with these circulation features are computed from in situ data. The plumes are distant from each other by 2 km on average and have a mean radius of 350 m for their downward component. The newly found properties of the convective plumes as well as their vertical structure is assessed and a description of the convective area is suggested. The plumes get wider and more intense as they get deeper and they cover 27% of the convective area.

The scaling suggested in Marshall and Schott (1999) has been found to be coherent with the observation of the Gulf of Lions plumes under the effect of rotation. A further distribution of the vertical velocity variance is given in $(B_0/f)^{0.86}$. This description could allow for a better parametrization of deep convection in global ocean circulation models as a vertical diffusion coefficient of 7 m^2 s^{-1} has been found to describe the buoyancy losses in the plumes. In atmospheric models, Plant and Craig (2008) suggest a stochastic description of plumes scheme for deep convection, suitable for use in both climate and NWP models. They use a probability distribution function to find plumes which could be inferred from our results as well as their characteristics.

In terms of observations, gliders are not yet able to sample deeper than 1,000 m. The development of gliders able to dive deeper could enable a complete characterization of the plumes by the sampling of their whole vertical extension. The development of new onboard sensors could also allow a further characterization of the physical and biogeochemical properties of the plunging waters. Considering that Durrieu de Madron et al. (2017) use the same glider Campe to compute sediment resuspension in shallower regions, these developments could allow the observation of the plume structure at depth and their interaction with the bottom turbid boundary layer.

Acknowledgments
The hydrographical data were collected and made freely available by the Coriolis project and programs that contribute to it (http://www.coriolis.eu.org). We would like to acknowledge the staff of the National Pool of Gliders of DT-INSU for the sustained gliders deployments. Captains and crew of R/V Le Tethys II (INSU), Le Provence (Phares et Balises), L'Atalante (Ifremer), and Le Suroit (Ifremer), as well as scientists, engineers, and technicians who participated to the MOOSE-GE, HyMeX, DEWEX, and DOWEX different cruises are also warmly thanked. Support was provided by the French MISTRALS program (HyMeX and MERMeX components), the French ANR ASICSMED, the MOOSE long-term observatory (AllEnvi-INSU), and the EU projects FP7 GROOM (grant 284321), FP7 PERSEUS (grant 287600), FP7 JERICO (grant 262584), and the COST Action ES0904 Everyone's Gliding Observatories.

References

Bosse, A. (2015). *Circulation générale et couplage physique-biogéochimie à (sous-) mésoéchelle en Méditerranée Nord-occidentale à partir de données in situ* (Ph.D. thesis). Paris, France: Université Pierre et Marie Curie.

Bosse, A., Testor, P., Houpert, L., Damien, P., Prieur, L., Hayes, D., . . . Mortier, L. (2016). Scales and dynamics of submesoscale coherent vortices formed by deep convection in the northwestern Mediterranean Sea. *Journal of Geophysical Research: Oceans*, *121*, 7716–7742. https://doi.org/10.1002/2016JC012144

Durrieu de Madron, X., Houpert, L., Puig, P., Sanchez-Vidal, A., Testor, P., Bosse, A., . . . Raimbault, P. (2013). Interaction of dense shelf water cascading and open-sea convection in the northwestern Mediterranean during winter 2012. *Geophysical Research Letters*, *40*, 1379–1385.

Durrieu de Madron, X., Ramondenc, S., Berline, L., Houpert, L., Bosse, A., Martini, S., . . . the ANTARES Collaboration. (2017). Deep sediment resuspension and thick nepheloid layer generation by open-ocean convection. *Journal of Geophysical Research: Oceans*, *122*, 2291–2318.

Eriksen, C. C., & Rhines, P. (2008). Convective to gyre-scale dynamics: Seaglider campaigns in the Labrador Sea 2003–2005. In R. R. Dickson, J. Meincke, & P. Rhines (Eds.), *Arctic-subarctic ocean fluxes* (pp. 613–628). Dordecht: Springer. https://doi.org/10.1007/978-1-4020-6774-7_26

Frajka-Williams, E., Eriksen, C. C., Rhines, P. B., & Harcourt, R. R. (2011). Determining vertical water velocities from Seaglider. *Journal of Atmospheric and Oceanic Technology*, *28*, 1641–1656.

Garau, B., Ruiz, S., Zhang, W. G., Pascual, A., Heslop, E. E., Kerfoot, J., & Tintoré, J. (2011). Thermal lag correction on Slocum CTD glider data. *Journal of Atmospheric and Oceanic Technology*, *28*(9), 1065–1071.

Grignon, L., Smeed, D. A., Bryden, H. L., & Schroeder, K. (2010). Importance of the variability of hydrographic preconditioning for deep convection in the Gulf of Lion, NW Mediterranean. *Ocean Science*, *6*(2), 573–586.

Houpert, L., Durrieu de Madron, X., Testor, P., Bosse, A., D'ortenzio, F., Bouin, M., . . . Raimbault, P. (2016). Observations of open-ocean deep convection in the northwestern Mediterranean Sea: Seasonal and interannual variability of mixing and deep water masses for the 2007–2013 period. *Journal of Geophysical Research: Oceans*, *121*, 8139–8171. https://doi.org/10.1002/2016JC011857

Johannessen, O. M., Lygre, K., & Eldevik, T. (2013). *Convective chimneys and plumes in the northern Greenland Sea* (pp. 251–272). Washington, DC: American Geophysical Union. https://doi.org/10.1029/158GM17

Klinger, B. A., Marshall, J., & Send, U. (1996). Representation of convective plumes by vertical adjustment. *Journal of Geophysical Research: Oceans*, *101*(C8), 18175–18182.

Leaman, K. D., & Schott, F. A. (1991). Hydrographic structure of the convection regime in the Gulf of Lions: Winter 1987. *Journal of Physical Oceanography*, *21*(4), 575–598.

Legg, S., & McWilliams, J. C. (2001). Convective modifications of a geostrophic eddy field. *Journal of Physical Oceanography*, *31*, 874–891.

Journal of Geophysical Research: Oceans 10.1002/2016JC012633

L'Hévéder, B., Mortier, L., Testor, P., & Lekien, F. (2013). A glider network design study for a synoptic view of the oceanic mesoscale variability. *Journal of Atmospheric and Oceanic Technology*, *30*, 1472–1493. https://doi.org/10.1175/JTECH-D-12-00053.1

Madec, G., Chartier, M., Delecluse, P., & Crépon, M. (1991). A three-dimensional numerical study of deep-water formation in the northwestern Mediterranean Sea. *Journal of Physical Oceanography*, *21*, 1349–1371.

Marshall, J., & Schott, F. (1999). Open-ocean convection: Observations, theory, and models. *Reviews of Geophysics*, *37*(1), 1–64.

Maxworthy, T., & Narimousa, S. (1994). Unsteady, turbulent convection into a homogeneous, rotating fluid, with oceanographic applications. *Journal of Physical Oceanography*, *24*(5), 865–887.

MEDOC Group. (1970). Observation of formation of deep water in the Mediterranean Sea, 1969. *Nature*, *225*, 1037–1040. https://doi.org/10.1038/2271037a0

Merckelbach, L., & Smeed, D. (2006). *Simulating gliders*. Paper presented at EGO Conference, Paris.

Merckelbach, L., Smeed, D., & Griffiths, G. (2010). Vertical water velocities from underwater gliders. *Journal of Atmospheric and Oceanic Technology*, *27*(3), 547–563.

Mertens, C., & Schott, F. (1998). Interannual variability of deep-water formation in the northwestern Mediterranean. *Journal of Physical Oceanography*, *28*(7), 1410–1424.

Paluszkiewicz, T., Garwood, R., & Denbo, D. (1994). Deep convective plumes in the ocean. *Oceanography*, *7*(2), 37–44.

Plant, R., & Craig, G. (2008). A stochastic parameterization for deep convection based on equilibrium statistics. *Journal of Atmospheric Sciences*, *65*, 87–105. https://doi.org/10.1175/2007JAS2263.1

Schott, F., Visbeck, M., Send, U., Fischer, J., Stramma, L., & Desaubies, Y. (1996). Observations of deep convection in the Gulf of Lions, northern Mediterranean, during the winter of 1991/92. *Journal of Physical Oceanography*, *26*, 505–524.

Send, U., & Marshall, J. (1995). Integral effects of deep convection. *Journal of Physical Oceanography*, *25*(5), 855–872.

Smeed, D., Merckelbach, L., Griffiths, G., Bryden, H., Grignon, L., Testor, P., & Legg, S. (2007*). Deep ocean convection: Observations from an adaptive network of underwater gliders (doconug)*.

Straneo, F., & Kawase, M. (1999). Comparisons of localized convection due to localized forcing and to preconditioning. *Journal of Physical Oceanography*, *29*(1996), 55–68.

Testor, P., Durrieu de Madron, X., Mortier, L., D'ortenzio, F., Legoff, H., Dausse, D., . . . Houpert, L. (2016). LION observatory data. SEANOE. https://doi.org/10.17882/44411

Testor, P., & Gascard, J.-C. C. (2006). Post-convection spreading phase in the northwestern Mediterranean Sea. *Deep Sea Research Part I: Oceanographic Research Papers*, *53*(5), 869–893.

Testor, P., Houpert, A. B., Margirier, L., D'ortenzio, F., Mortier, F., Legoff, L., . . . Ribotti, A. (2017). Multi-scale observations of deep convection in the northwestern Mediterranean Sea during winter 2012–2013 from a multi-platform approach. *Journal of Geophysical Research: Oceans*. https://doi.org/10.1002/2016JC012671.

Visbeck, M., Marshall, J., & Jones, H. (1996). Dynamics of isolated convective regions in the ocean. *Journal of Physical Oceanography*, *26*, 1721–1734. https://doi.org/10.1175/1520-0485(1996)026<1721:DOICRI>2.0.CO;2

2.2.2 Additional remarks on convective plumes

One of the key components lacking in the study is that of the vertical properties of the plumes. As shown in Figure 2.5, the glider crosses the plumes not only just in the top 1000 m of the water column but also over a vertical extension. From the observed plumes, it seems that there is an intensification at depth, as the deepest observed plumes are also the more potent. However, these observations are not statistically significant yet. With the development of deep gliders and more observations in the mixing area, a vertical characterisation of the plumes could be devised.

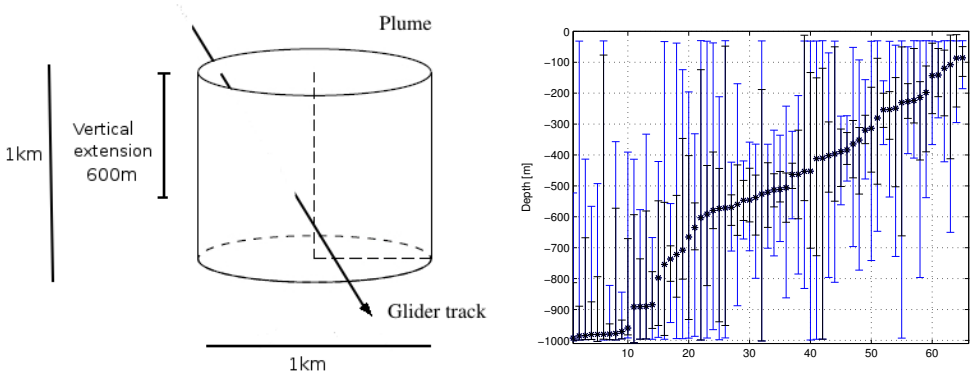

FIGURE 2.5: (left) Schematic representation of a glider crossing a convective plume. (right) Sorted depths at which the plumes were observed for the deployment Campe-ASICSMED: in blue the extension of the plume and surrounding waters considered in Figure 7 of the previous article, in black the portion of the plume of negative downwelling velocities.

This first in-situ statistical characterisation of convective plumes provides useful estimates to modellers. A specific parameterisation of convection has already been introduced in atmospherical models and this study provides the ideal framework to test a similar one in oceanic models. This study indeed not only describes the characteristics and spatial coverage of the mixing agents, but is also included in an extensive framework characterising the basin before, during and after this mixing phase. A possible approach could be similar to the meteorology atmospheric models using a convective fraction of a grid cell as a parameter. Some high resolution process models are also getting better at representing plumes and could help with the development of nests in the convective regions as well. As will be shown in Chapters 3 and 4, the models are not as good in representing the deep waters as they are in representing surface and intermediate ones, and such a parameterisation could provide an improvement.

2.3 Updating the Marshall & Schott description of deep convection

This section presents a brief summary of the main results from the joint special issue on deep convection (Dense water formations in the Northwestern Mediterranean: from the physical forcings to the biogeochemical consequences) published in *Journal of Geophysical Research: Oceans and Journal of Geophysical Research: Atmosphere*. For further information, refer to the recent preface article [Conan et al. (2018)] and to the review article to which I contributed [Testor et al., 2017][3]. This extensive study enabled a better understanding of the hydrodynamical processes at stake, thanks to the numerous observations and the numerical experiment conducted. Marshall and Schott (1999) pointed out that a major step forward would be made when the insights we have of deep convection and the interplays between the different scales would be better understood, enabling a 3 dimensional parameterisation of the occurring processes. 15 years later, this experiment is a good step forward in that direction, as we were successfully able to better describe the occurring processes (especially at finescales) both qualitatively and quantitatively. Moreover, the mixed patch was described on a 10 day basis, giving a chronology of the event like never before.

The main results can be summed up in six major categories:

- The dynamics of the atmosphere and air-sea fluxes. The mesoscale dynamics of the cold and dry winter winds over the Gulf of Lions were explored [Drobinski et al., 2016] and the winter integrated buoyancy loss was identified as the main component acting for dense water formation interannual variability [Somot et al., 2016].

- The interannual variability of dense water formation. Thanks to the intensification of the monitoring of the basin since 2007, Madron et al. (2017); Houpert et al. (2015); Houpert et al. (2016) have been able to reveal that each deep convection episode forms warmer and saltier waters overlapping in the basin depending on their respective densities. From 2009 to 2012, the WMDW formation rate was estimated to range between 0.91 and 1.25 Sv from observations, consistent with the 0.0 to 2.67 Sv estimates from satellite data [Herrmann et al., 2017].

- The deep water formation during winter 2013. Thanks to the very intense observation network, which was confirmed to be able to represent the basin in an OSSE [Waldman et al., 2016a], a formation rate for the winter 2013 was inferred through various methods: mixed patch volume [Herrmann et al., 2017], dissolved oxygen ventilation of the deep waters [Coppola et al., 2017], and the newly formed dense water volume [Testor et al., 2017]. The latter, most robust method, estimated a 2.0 ± 0.2 Sv formation rate, consistent with the approximations obtained from using the other methods. The observations enabled numerous model evaluations of their regional product [Estournel et al., 2016b; Lebeaupin Brossier et al., 2017; Damien et al., 2017; Waldman et al., 2017], where the obtained dense water formation rates ranged between 1.33 and 2.59 Sv. The models

[3]The first page of the article can be found in Appendix A.

with more finescale resolution were best performing, confirming the key role of the rim patch and submesoscale coherent vortices described in Testor et al. (2017).

- The effects of small scales and intrinsic ocean variability on dense water formation. A number of known processes were thoroughly observed and characterised for the first time: frontal instabilities [Giordani et al., 2017], **S**ubmesoscale **C**oherent **V**ortices (SCVs) [Bosse et al., 2016] and convective plumes [Margirier et al., 2017]. Modelling studies showed that the intrinsic variability can explain most of the deep convection's interannual variability [Waldman et al., 2018a] and that the displacement of the front bounding the convection zone is key to the oceanic preconditioning [Estournel et al., 2016a].

-The effect of deep water formation on biogeochemical budgets and primary production. Kessouri et al. (2018) further confirmed that deep convection drastically impacts the nutrient distribution both in the surface and at depths, and that it thus controls the trophic network. They further estimated that deep convective areas are 3 to 8 times more effective in exporting organic carbon at depth than stratified regions. Bosse et al. (2017) also showed the enhancing carbon intake and sequestration role played by SCVs. The convective depth controls the phytoplankton community in spring and the surface nutrient content for at least a year [Severin et al., 2017], especially when convection reaches the bottom layer where sediment resuspension occurs [Madron et al., 2017].

- The response of the zooplankton community to dense water formation. The deep convection has been characterised as a region exporting organic matter and enhancing the energy transfer to higher trophic levels [Severin et al., 2017; Kessouri et al., 2018]. The herbivorous species of zooplankton dominate in spring in the mixed patch area which is more densely populated than the peripheral zone. The community compositions were similar during the mixing and the bloom phases when copepods dominated [Donoso et al., 2017].

The new diagram for deep convection

Thanks to all the information listed above, we came up with the diagram presented in Figure 2.6 during the violent mixing phase. It completes the picture presented by Marshall and Schott (1999) in Figure 0.7. We know that the three phases overlap and interact, and this diagram precisely displays the role played by submesoscale in deep convection, be it for the preconditioning, the intense mixing or the restratification and spreading. The top diagram shows a first mixing event, plumes not yet reaching the bottom, cascading taking place near the coast and symmetric instabilities near the rim of the mixed patch. SCVs are formed, exporting newly formed waters at different intermediate depths (after earlier having helped with the preconditioning [Bosse et al., 2015][4]). Later and after further mixing, the MLD can reach the ocean floor and SCVs are also formed attached to the ocean floor, contributing to the spreading of newly formed WMDW.

The fact that this experiment was a success should encourage similar intense efforts to unravel other processes in various regions of the world. Its very scalable multiplatform approach makes it easier to reproduce in other contexts, and a similar promising

[4]If a plume reaches such a structure, the mixing will be enhanced.

experiment (the PERLE mission) is now being conducted in the Eastern Mediterranean to quantify the LIW formation rates as well as the processes at stake in this extremely warm and salty context.

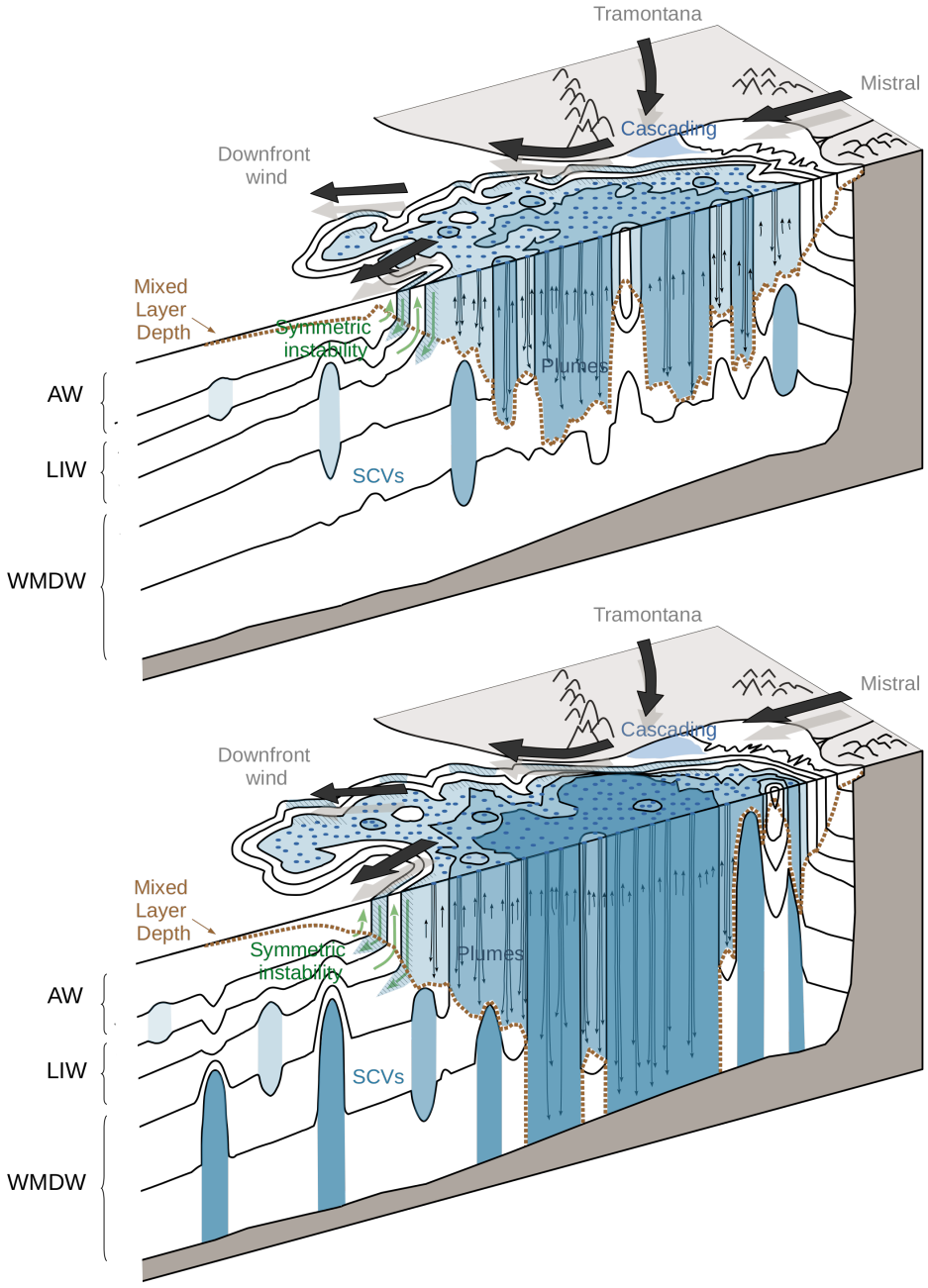

FIGURE 2.6: Schematic diagram of the evolution of the convection area during the violent mixing phase in a period of 1-2 weeks. Underlying stratification/outcrop is shown by selected isopycnals (continuous black lines). The volume of fluid just mixed by convection is shaded and colour coded according to potential density classes, from Testor et al. (2017).

Chapter 3

The Levantine Intermediate Waters in the Northwestern Mediterranean Sea

Contents

3.1 The LIW, from the Ligurian Sea to the Northwestern Mediterranean

A first look (see Figure 1.14) at the temperature and salinity profiles collected in the Northwestern Mediterranean Sea over the past 15 years during the MOOSE intensified sampling era shows that the intermediate and deep waters get warmer and saltier with time. This warming and salinification of the LIW has been documented in key regions along its circulation. Ozer et al. (2016) observed the long-term trends in the South-East Eastern basin at its formation point. As can be seen in Figure 3.1, the warming and salinification at mean 0.03°C .year^{-1} and 0.005 year^{-1} rates, respectively, has been observed over the past 30 years. Ozer et al. (2016) also documented the changes in nutrient contents, mean chlorophyll-a concentration and LIW mean core depth over this period from CTD measurements, which showed a variability in opposite phase with T and S.

After its formation, the LIW then mixes with surrounding waters and progressively gets its high salinity, high temperature signature eroded. In very active zones like the Sicily Channel, they are intensely mixed through turbulent processes [Iudicone, 2003; Vladoiu et al., 2018]. In calmer regions, mixing below the LIW may be induced by double diffusive salt fingers, notably in the Tyrrhenian Sea where salt fingers are near permanent [Durante et al., 2016]. Mixing above the LIW may be induced by double diffusive convection with the surface layers [Carniel et al., 2008].

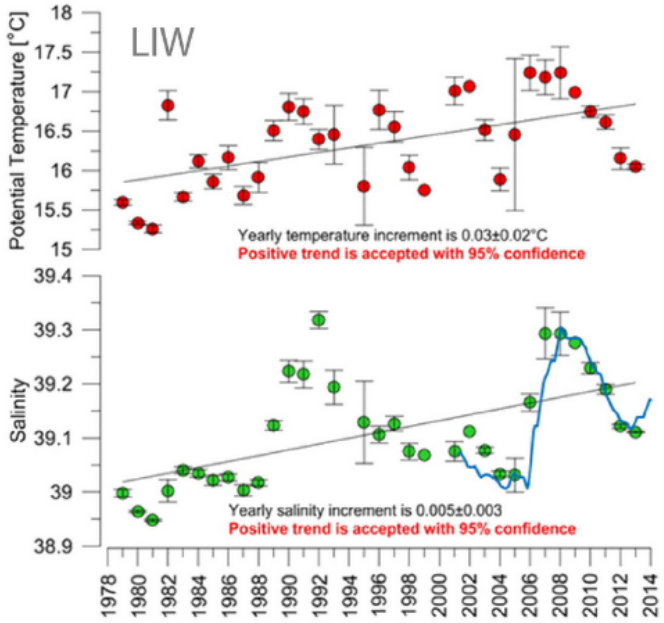

FIGURE 3.1: Inter-annual and long-term changes of temperature (top) and salinity (bottom) in the LIW, derived from 30 years of CTD profile measurements in the South-East Mediterranean Sea. The confidence interval is shown when the number of observations is > 3. The smoothed salinity time series of three deep Haifa Section stations is superimposed in blue, from Ozer et al. (2016).

Although the LIW core is diluted as it is advected, Schroeder et al. (2017) observed similar mean 0.024°C .year^{-1} and 0.006 year^{-1} rates from mooring line measurements and CTD casts over the past 20 years at the Sicily Channel choke point further along the circulation (see Figure 3.2). The changing rates seem conserved. Although measurements have shown this trend to also propagate to the Western Basin, no precise study has been made investigating these increases yet. The glider endurance lines in the Northwestern Mediterranean Sea enable the investigation of the intermediate water properties at high resolution along its circulation path from the Ligurian to the Balearic Sea.

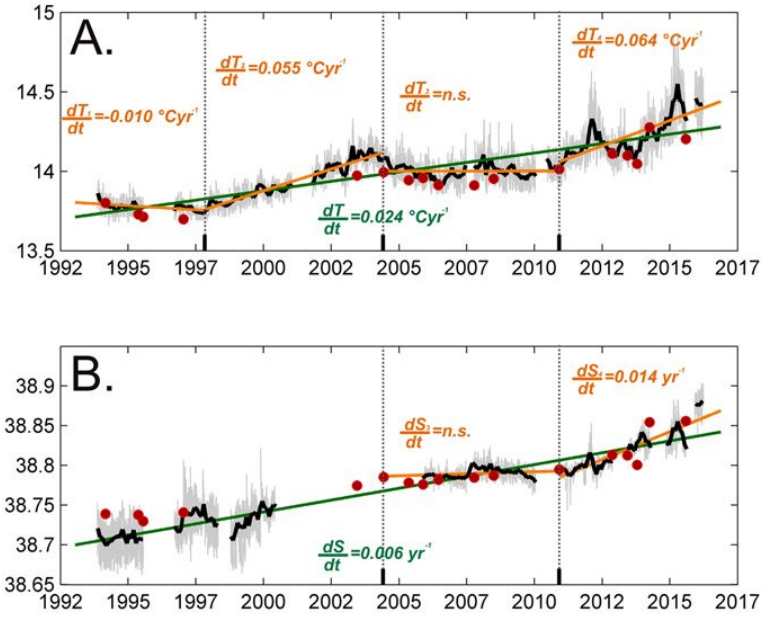

FIGURE 3.2: LIW time series (3-hourly in light grey) of (A) temperature and (B) practical salinity at 400 m depth in the Sicily Channel. Red dots indicate ship CTD measurements. The monthly mean time-series is shown in black. The green line represents the long-term trend line, while short-term trends found for different periods detected by means of the change point analysis are shown in orange. For each trend line the trend value is given, if significant, in the same colour as the corresponding line. The vertical dashed lines indicate change points, from Schroeder et al. (2017).

3.2 Warming and salinification of intermediate waters in the Northwestern Mediterranean Sea

The dataset described in Chapter 1 and the new knowledge of deep convection presented in Chapter 2 encouraged an in-depth study of the LIW properties and circulation times in the Northwestern Mediterranean, presented below in the form an article to be submitted shortly in *Nature: Scientific reports*. In the following, only the temperature will be shown as the salinity displays the same behaviour, salinity figures can be found in Appendix B.

Warming and salinification of intermediate waters in the Northwestern Mediterranean Sea

Félix Margirier[1,*], Pierre Testor[1], Emma Heslop[2], Katia Mallil[1], Anthony Bosse[3], Laurent Coppola[4], Fabrizio D'Ortenzio[4], Louis Prieur[4], Vincent Taillandier[4], Xavier Durrieu de Madron[5], Laurent Mortier[6], and Patrick Raimbault[7]

[1]CNRS-Sorbonne Universités (UPMC Univ. Pierre et Marie Curie, Paris 06)-CNRS-IRD-MNHN, UMR 7159, Laboratoire d'Océanographie et de Climatologie (LOCEAN), Institut Pierre Simon Laplace (IPSL), Observatoire Ecce Terra, 4 place Jussieu, F-75005 Paris, France.
[2]IOC UNESCO, Paris, France.
[3]Geophysical Institute, University of Bergen and Bjerknes Center for Climate Research, Bergen, Norway.
[4]Sorbonne Universités (UPMC Univ. Pierre et Marie Curie, Paris 06), UMR 7093, Laboratoire d'Océanographie de Villefranche (LOV), Observatoire Océanologique de Villefranche/mer, France.
[5]CNRS-Université de Perpignan, Centre de Formation et de Recherche sur les Environnements Méditerranéens (CEFREM), Perpignan, France.
[6]ENSTA–Paristech, Laboratoire d'Océanographie et de Climatologie (LOCEAN), Palaiseau, France.
[7]Aix-Marseille Université, Université de Toulon, CNRS, IRD, MIO UM 110, 13288, Marseille, France.
[*]felix.margirier@locean-ipsl.upmc.fr

ABSTRACT

The Mediterranean Sea, especially responsive to climate change, has been subjected to gradual temperature and salinity increases. Thanks to a new high spatial and temporal resolution dataset enabled in particular by the glider endurance lines in the Northwestern Mediterranean over the past 10 years, we compute time series of Levantine Intermediate Water (LIW) properties in the Northwestern Mediterranean Sea. The warming and salinification of the LIW reported in recent studies at its formation point are observed in the Ligurian Sea at similar rates of 0.06 °C.year^{-1} and 0.012 year^{-1}, possibly demonstrating such trends over decades. We show deep convection is another major local process that impacts the characteristics of the LIW in the Northwestern basin. The basin has seen a step increase of +0.3 °C and +0.08 in salinity in 2014, the first year without deep convection since 2008. The warming and salinification of the LIW has since then been invading the Northwestern basin in the absence of strong regulating deep convective events until 2017. The intermediate waters are also less ventilated and this likely has significant biogeochemical impacts.

Introduction

The Mediterranean Sea is a regional sea characterized by a basin-scale cyclonic circulation, active sites of intermediate and deep water formation and ubiquitous and energetic meso- and submesosale dynamics. The time scales associated with its density driven circulation are 10 times shorter than that of the global ocean, and its rapid and amplified responses to stress linked to climate change make the Mediterranean Sea a key region for climate change observation[1,2]

The Mediterranean Sea exchanges heat and salt with the global ocean through the Strait of Gibraltar. Fresh Atlantic Waters (AW) enter in the surface layer while saltier and colder (on average over a year) Mediterranean waters exit at depth. The fresh Atlantic Waters follow a cyclonic circulation along the continental slope, circulation during which they are subject to evaporation and mixing, in particular by a vigorous mesoscale activity, gradually becoming more saline. The Atlantic Waters are transformed in relatively colder and saltier intermediate and deep waters due to air-sea exchanges through strong winter heat loss events, and due to mixing with surrounding resident Mediterranean waters. The Mediterranean is one of the rare hot-spots for deep water formation in the global ocean. Deep water formation contributes to the overturning thermohaline circulation of the Mediterranean Sea, ventilating the deep waters and – as in the global ocean – exporting surface properties to the deep layers.

In the Northwestern Mediterranean Sea, deep water formation events occur and may be driven both by intense winter atmospheric events and by ocean preconditioning. The relatively fresh (and cold in winter) AW can mix with the underlying warm and salty Levantine Intermediate Waters (LIW) to produce new Western Mediterranean Deep Waters (WMDW) in a preconditioned area centered in the Gulf of Lion where deep isopycnals are closer to the surface. The LIW properties are thus key for the deep ventilation process[3].

Formed in the Eastern Mediterranean, the LIW follows a cyclonic path along the continental slope, beneath the surface

waters, to the Western Mediterranean. The intermediate waters pass through the Sicily Channel and into the Tyrrhenian basin, reaching the Northwestern Mediterranean either through the Corsica Channel or along the coasts of Corsica and Sardinia, about a decade after its formation. The LIW have been found to become saltier and warmer in recent years in the Eastern basin[4] and in the Sicily Channel[5].

Through an intensifying monitoring in the Western Mediterranean, an abrupt shift in the properties of LIW has been observed. In particular, both by the French "MOOSE" and the Spanish "Canales" glider endurance lines. Combining these core glider missions with additional datasets available in the region (ship CTD, moorings, profiling floats, XBTs) provides a dataset of 10 years of observations spread across the Northwestern Mediterranean region. This dataset was used to investigate the drivers and impact of the 2014 winter abrupt increases of 0.3 °C and 0.08 in temperature and salinity in the center of the basin, which appear to be propagating through the basin from the western side of Corsica to the Balearic Islands. Observing this abrupt change identified through the glider endurance lines encouraged a multi-platform approach, and the combination of the profile datasets with the mooring locations allows for a better understanding of the impact of deep convection events on the LIW and intermediate layers of the Western Mediterranean, leading to a discussion of the possibility of deep convection events occurrence in the framework of a warming Mediterranean.

Results

With this new high spatial and temporal resolution dataset in the Northwestern Mediterranean with the inputs of gliders since 2007, a new level of understanding of these trends is enabled. The data was sorted in regional boxes (Figure 1) along the cyclonic circulation in the Northwestern Mediterranean Sea, where the temperature and salinity time series typical of the LIW are computed. The LIW is characterized by a subsurface salinity and/or temperature maximum (Figure 2). A regime shift is observed in 2014, when warmer and saltier LIW invaded the Western Mediterranean intermediate waters in the absence of deep convection, which would have exported heat and salt to the deep waters (Figure 3, years 2009-2013 compared to recent years).

Influx from the Eastern basin

The LIW properties are propagated from the Eastern to the Western basin as it flows through the Sicily Channel[5]. It then enters the Ligurian Sea circulating along Sardinia and Corsica and from the Tyrrhenian Sea (Figure 1).

The high resolution monitoring of the Ligurian Sea allows for a geographical classification of the LIW circulation associated with the Northern Current vein into two boundary regions, 'Calvi' and 'Nice', and an 'offshore' region. Over the past ten years, the LIW properties in these different areas have consistently gradually increased by 0.06 °C.year^{-1} and 0.012 psu.year^{-1} (Figure 2), consistent with the input from the Eastern basin reported by Schroeder et al.[5] (0.06 °C.year^{-1} and 0.014 year^{-1}) in the Sicily Channel.

The 'Calvi' box shows little variability for LIW around this linear trend, and is typical of the LIW entering the northwestern Mediterranean Sea after their long journey from its formation site. The 'Nice' box follows about the same patterns but the LIW is here slightly less warm and salty, as a result of mixing with resident and offshore waters following its path along the continental slope. Cross-correlating the time series allows an estimation of the circulation time from 'Calvi' to 'Nice' of about 40 days (equivalent to 0.07 $m.s^{-1}$, $R^2 = .92$). The offshore waters exhibit similar trends except for a few dents, notably in 2012 and 2013 (black stars on Figure 2). These correspond to the mixing events during winter (see Figure 3), cropping the LIW, which was mixed offshore with the fresh (and cold in winter) AW laying above, thus eroding its core properties. This effect was not long-lasting, as the advected LIW reconquered the intermediate layers during the year as can be seen in Figures 2 and 3. A third dent in the offshore component can be observed in summer 2014, possibly due to variations in the input waters that show a variability of the same order.

Deep convection in the Gulf of Lions

As these anomalies propagate with the circulation (an estimated 20 days from 'Nice' to the 'Northern Current vein', equivalent to 0.14 $m.s^{-1}$, $R^2 = .78$), they are advected in the Gulf of Lions, a region subject to potential deep convection events. The deep convection events act as a sink for LIW, exporting in particular its heat and salt into the deep layers, where the WMDW has been found to warm and salinify[6–8]. This was the case during the period 2009-2013 (black stars in Figure 2), when deep convection happened every winter. In the winters of 2009-2013, the LIW was mixed with the fresh and cold overlaying AW, as well as with the fresh and cold WMDW underneath. Then, the LIW temperature and salinity increase from April to December, in both the offshore and boundary regions. This increase continues until the next convection episodes that bring back the LIW characteristics to levels observed the winter before, thus regulating the LIW properties that would be propagated along the circulation to the rest of the basin.

A jump is observed in 2014 in the subsurface signature of LIW waters both in temperature (+0.3 °C) and salinity (+0.08) as the winter mixing did not reach great depths (430 m observed at LION) and the LIW were less diluted compared to previous years. Since then, mild convection events until 2017 have modified the LIW properties offshore every winter. However, it

seems that the winter mixing was not strong enough to restore them to the values observed before, and temperature and salinity have steadily increased both in the coastal and offshore regions at the same rate as the input observed in 'Calvi'.

The LIW has not only been able to retain its temperature and salinity since 2013, but is also occupying a larger portion of the water column as 4 years without deep convection allowed it to preserve its core and invade the intermediate layers in the Gulf of Lions (Figure 3). The intermediate layers have shifted very rapidly to a warmer and more saline state, which has been increasing ever since in the quasi-absence of ventilation. The cumulative net heat fluxes revealed that the leap 2013/2014 winter was the weakest winter in terms of cumulated net heatflux over the observed time period (Figure 5). The 2012/2013 deep convection event was very intense, which is also reflected in the fluxes as the preconditioning was similar between these two transitioning years. In the absence of intense winters since, and with a slightly increased stratification (Figure **??**), the LIW was allowed to invade the Western Mediterranean basin. A strong winter will be needed to break the cycle as the deep stratification has sligthly increased (Figure **??**).

Propagation to the Balearic Sea and the Western Basin

The signal is advected to the Balearic Sea, where the 2014 Gulf of Lions jump is observed with a lag of 3 to 5 months depending on the region. It takes an estimated 80 days (equivalent to 0.094 $m.s^{-1}$, $R^2 = .87$) for the anomalies to propagate from the 'Northern Current vein' to the 'Ibiza Channel' (Figure 2), consistent with previous estimates. The signal then propagates to the 'Ibiza-Mallorca' region lagged by an additional 10 to 20 days (equivalent to 0.057 $m.s^{-1}$, $R^2 = .81$), and to the 'Menorca' region after 40 more days (equivalent to $0.086 m.s^{-1}$, $R^2 = .84$). The temperature and salinity drop observed in 2014 in the 'Ibiza-Mallorca' box (black cross in Figure 2, is likely due to the presence of an eddy in the Ibiza Channel, blocking the LIW recirculation pathway and injecting older and thus less warm and saline LIW into the considered region from the Southern Western Mediterranean Basin. After 2014, warmer and saltier LIW occupy the Balearic Sea and are propagated to the rest of the Western Mediterranean Basin (Figure 4). The absence of deep convection has enabled a consequent warming and salinification of the intermediate layers of the Balearic Sea over a very short time period, which is propagating Southwards.

Discussion

In the absence of deep convection, the LIW have been able to invade the Western Basin and the intermediate waters have been rapidly and intensely heated and salinified in the process. The heat and salt content at intermediate levels has leaped to a new state (Figure 4). From 2007 to 2013, when deep convection happened every year[7], the intermediate layer properties remained stable in temperature and salinity, but were also ventilated regularly. The core of the water volume in the Gulf of Lions was comprised of deep waters. Since 2014, the intermediate waters throughout the basin have warmed and salinified. They are also now poorer in oxygen, as the old LIW is characterized by an oxygen minimum. The phytoplankton dynamics are altered in the absence of ventilation[9] as the nutrients are less brought to the surface. The water volume repartition between the deep and intermediate waters is also changed, as the LIW continues invading a larger portion of the water column. The Northwestern Mediterranean preconditioning for deep convection has changed little since the last deep convection event, as the deep stratification has only slightly increased (Figure **??**). Deep convection is driven by a combination of preconditioning and heat losses[10], and as the intermediate salt content gets more significant, fluxes sufficient to crop the LIW could trigger a new deep convection event.

Climate projections do not agree on the occurrence of deep convection in future climate scenarios, however they all predict a warming and salting of the Mediterranean basin. The Western Basin intermediate waters are regulated by the deep convective years, which seem to have maintained the Western Mediterranean Basin in a quasi-steady state for several consecutive years. The LIW keeps warming and salinifying at its formation point, so the observed trend is expected to continue at least at the same rate, and as the LIW properties change, so do the Winter Intermediate Water (WIW)[11] and the WMDW formed by their mixing. The deep convective episodes have indeed been documented to massively transfer heat and salt to the deep waters from the supply provided by the intermediate waters[6,12,13]. In this marine protected area, such a quick and intense warming could likely have an important impact on the biogeochemical cycles and on the pelagic marine life[14] as well as on the benthic ecosystems[15]. As a warming and salinification of the intermediate and deep water masses is observed[16], the same trend is to be expected in the upcoming years for the Mediterranean outflow into the Atlantic Ocean.

Methods

Some 166083 profiles have been collected by gliders, profiling floats, CTDs, XBTs and MBTs in the Northwestern Mediterranean basin over the 2007-2018 period in the different regions of interest. The profiles were harmonized using the method described in Bosse et al.[17] to generate a coherent database. A regional approach was adopted to assess both the variability and the evolution of water masses along their course. The focus is set on the 8 regions presented in Figure 1 along the cyclonic circulation of the Northwestern Mediterranean Sea comprising offshore and alongshore components. In these regional boxes, a

water masses' view is adopted to evaluate the impact of climate change and the effect of deep convection on the evolution of the Levantine Intermediate Waters (LIW). The LIW core properties are extracted for each profile for which only one characteristic point is kept and plotted in the time series presented in Figure 2. These core properties points are the temperature and/or salinity maximum under the 29 $kg.m^{-3}$ isopycnal. In winter and when the whole water column is fully homogeneous after being mixed, the water column properties are kept as a definition of the LIW for the analysis, although it would not be LIW in the strict sense. The key component of our data resides in the very high spatial and temporal resolution of our database, mainly enabled by the gliders as only one point is retrieved per profile. This is allowed thanks to the merging of the French and Spanish efforts enabling a high temporal and spatial resolution analysis of the regime shift in intermediate waters. The mooring lines at the DYFAMED (43.41 N 7.89 E) and LION (42.04 N 4.68 E) locations were completed in the sub-surface as in Houpert et al.[7] with the LION (42.06 N 4.64 E) and AZUR (43.38 N 7.83 E) Météo France surface buoys and and sub-surface mooring lines. The interpolation presented in Figure 3 relies on a two layer analysis : objective analyses were performed for the surface (0-700 m) and deep (700 m-bottom) layers separately, using 20 days/50 m and 3 months/200 m respectively. All profiles within a 15 km radius (approxiamatively equivalent to the deformation radius in the North-Western Mediterranean) as well as the mooring line data were used to perform the said objective analyses.

References

1. Giorgi, F. & Lionello, P. Climate change projections for the mediterranean region. *Glob. Planet. Chang.* **63**, 90 – 104 (2008). DOI https://doi.org/10.1016/j.gloplacha.2007.09.005. Mediterranean climate: trends, variability and change.
2. Bethoux, J. & Gentili, B. Functioning of the mediterranean sea: past and present changes related to freshwater input and climate changes. *J. Mar. Syst.* **20**, 33–47 (1999).
3. Grignon, L., Smeed, D., L. Bryden, H. & Schroeder, K. Importance of the variability of hydrographic preconditioning for deep convection in the gulf of lion, nw mediterranean. *Ocean. Sci. Discuss.* **7**, 51–90 (2010).
4. Ozer, T., Gertman, I., Kress, N., Silverman, J. & Herut, B. Interannual thermohaline (1979–2014) and nutrient (2002–2014) dynamics in the levantine surface and intermediate water masses, se mediterranean sea. *Glob. Planet. Chang.* (2016).
5. Schroeder, K. *et al.* Rapid response to climate change in a marginal sea. *Sci. Reports* **7** (2017).
6. Testor, P. *et al.* Multiscale observations of deep convection in the northwestern mediterranean sea during winter 2012–2013 using multiple platforms. *J. Geophys. Res. Ocean.* **123**, 1745–1776 (2018). DOI 10.1002/2016JC012671.
7. Houpert, L. *et al.* Observations of open-ocean deep convection in the northwestern mediterranean sea: Seasonal and interannual variability of mixing and deep water masses for the 2007-2013 period. *J. Geophys. Res. Ocean.* (2016).
8. Rohling, E. J. & Bryden, H. L. Man-induced salinity and temperature increases in western mediterranean deep water. *J. Geophys. Res.* **97**, 11191–11198 (1992).
9. Kessouri, F. *et al.* Vertical mixing effects on phytoplankton dynamics and organic carbon export in the western mediterranean sea. *J. Geophys. Res. Ocean.* (2018).
10. Marshall, J. & Schott, F. Open-ocean convection: Observations, theory, and models. *Rev. Geophys.* **37**, 1–64 (1999). DOI 10.1029/98RG02739.
11. Vargas-Yáñez, M. *et al.* Extreme western intermediate water formation in winter 2010. *J. Mar. Syst.* **105-108**, 52–59 (2012).
12. Somot, S. *et al.* Characterizing, modelling and understanding the climate variability of the deep water formation in the north-western mediterranean sea. *Clim. Dyn.* (2016).
13. Schroeder, K., P. Gasparini, G., Tangherlini, M. & Astraldi, M. Deep and intermediate water in the western mediterranean under the influence of the eastern mediterranean transient. *GEOPHYSICAL RESEARCH LETTERS* **33** (2006).
14. Coma, R. *et al.* Global warming-enhanced stratification and mass mortality events in the mediterranean. *Proc. Natl. Acad. Sci. United States Am.* **106**, 6176–81 (2009).
15. Danovaro, R. Climate change impacts on the biota and on vulnerable habitats of the deep mediterranean sea. *Rendiconti Lincei. Scienze Fisiche e Nat.* (2018). DOI 10.1007/s12210-018-0725-4.
16. Borghini, M., Bryden, H., Schroeder, K., Sparnocchia, S. & Vetrano, A. The mediterranean is becoming saltier. *Ocean. Sci.* **10**, 693–700 (2014). DOI 10.5194/os-10-693-2014.
17. Bosse, A. *et al.* Scales and dynamics of submesoscale coherent vortices formed by deep convection in the northwestern mediterranean sea. *J. Geophys. Res. Ocean.* (2016).

Acknowledgements

Hydrographical data were collected, and made freely available by the Coriolis project (http://www.coriolis.eu.org) and programmes that contribute. We would like to acknowledge the staff of the French National Pool of Gliders (DT-INSU/CNRS-CETSM/Ifremer) for the sustained gliders deployments carried out in the framework of MOOSE, as well as the intensive deployments during this 2012-2013 DEWEX experiment and to warmly thank Captains and crews of R/V *Le Tethys II* (CNRS/INSU, France), R/V *Le Provence* (Phares et Balises, France), and R/V *Le Suroît* (Ifremer, France) and R/V *Urania* (CNR, Italy), as well as all scientists, engineers, technicians and students who participated to the MOOSE-GE, HyMeX/SOP1 and SOP2, DEWEX, and DOWEX different cruises and autonomous platforms deployments. Support was provided by the French "Chantier Méditrranée" MISTRALS program (HyMeX and MERMeX components), the ANR ASICSMED project (ANR 12-BS06-0003), the MOOSE long-term observatory (SOERE/AllEnvi-SNO/INSU), the spanish institute SOCIB, the Bio-Argo project (CNES-TOSCA) and the ANR NAOS project (ANR J11R107F), as well as the NATO STO-CMRE NOMR12 experiment. Support was also provided by the EU projects FP7 GROOM (Grant Agreement No. 284321), FP7 PERSEUS (Grant Agreement No. 287600), FP7 JERICO (Grant Agreement No. 262584) and the COST Action ES0904 "EGO" (Everyone's Gliding Observatories).

Author contributions statement

F.M. wrote the main manuscript text, F.M., A.B. and E.H. prepared figures F.M., A.B., E.H. and P.T. conceived and conducted the experiments, All authors analyzed the results and reviewed the manuscript.

Additional information

Competing financial interests: The authors declare no competing financial interests.

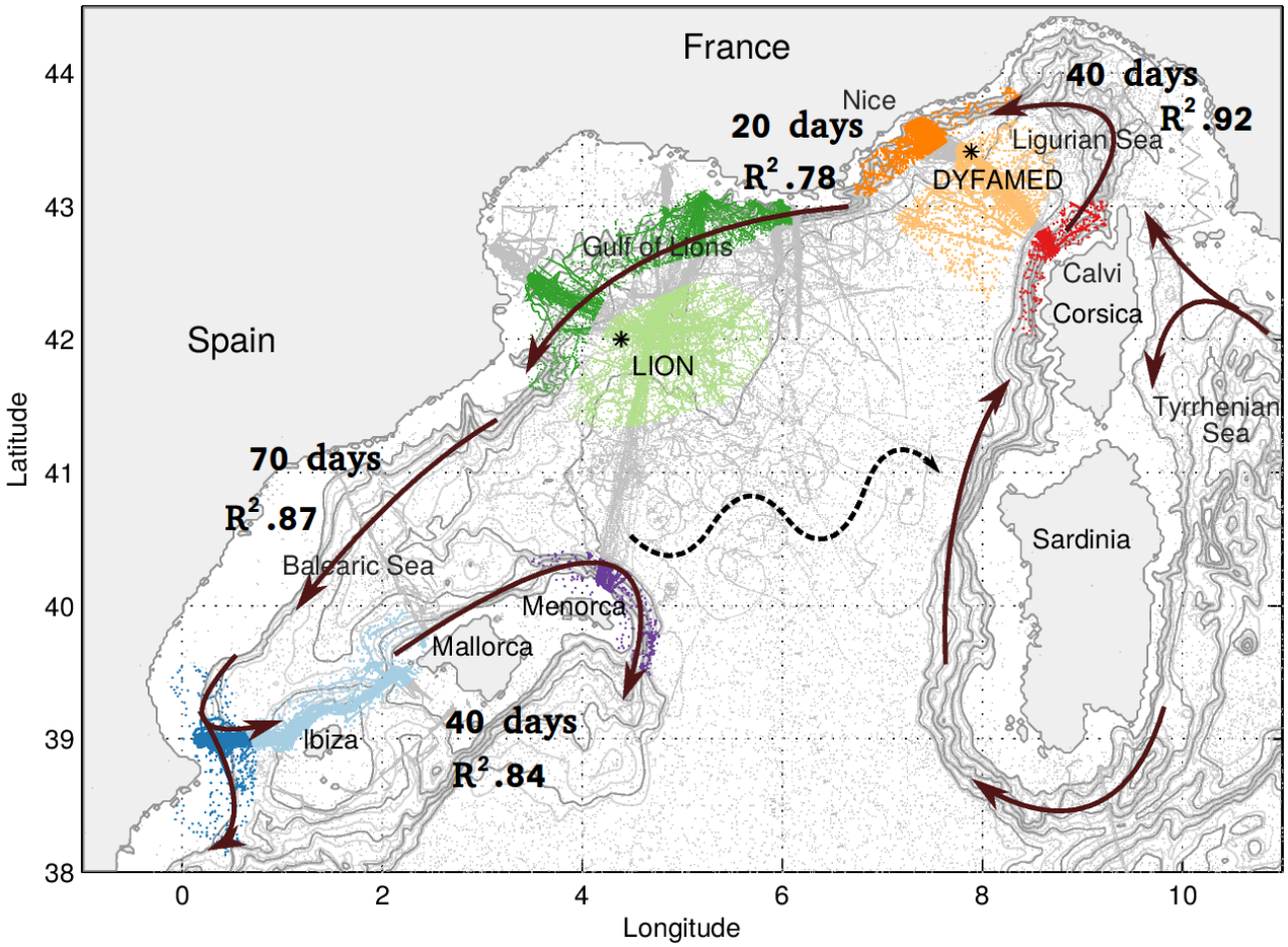

Figure 1. The regional boxes chosen in our study. The color-code is respected in later figures. Orange for the Ligurian Sea, green for the Gulf of Lions and blue for the Balearic Sea. Each region is composed of coastal and off-shore components. The scattered points represent all the single profiles collected. The two mooring locations are indicated by the black stars. The main LIW circulation path is indicated in the brown arrows and the North Balearic front in black.

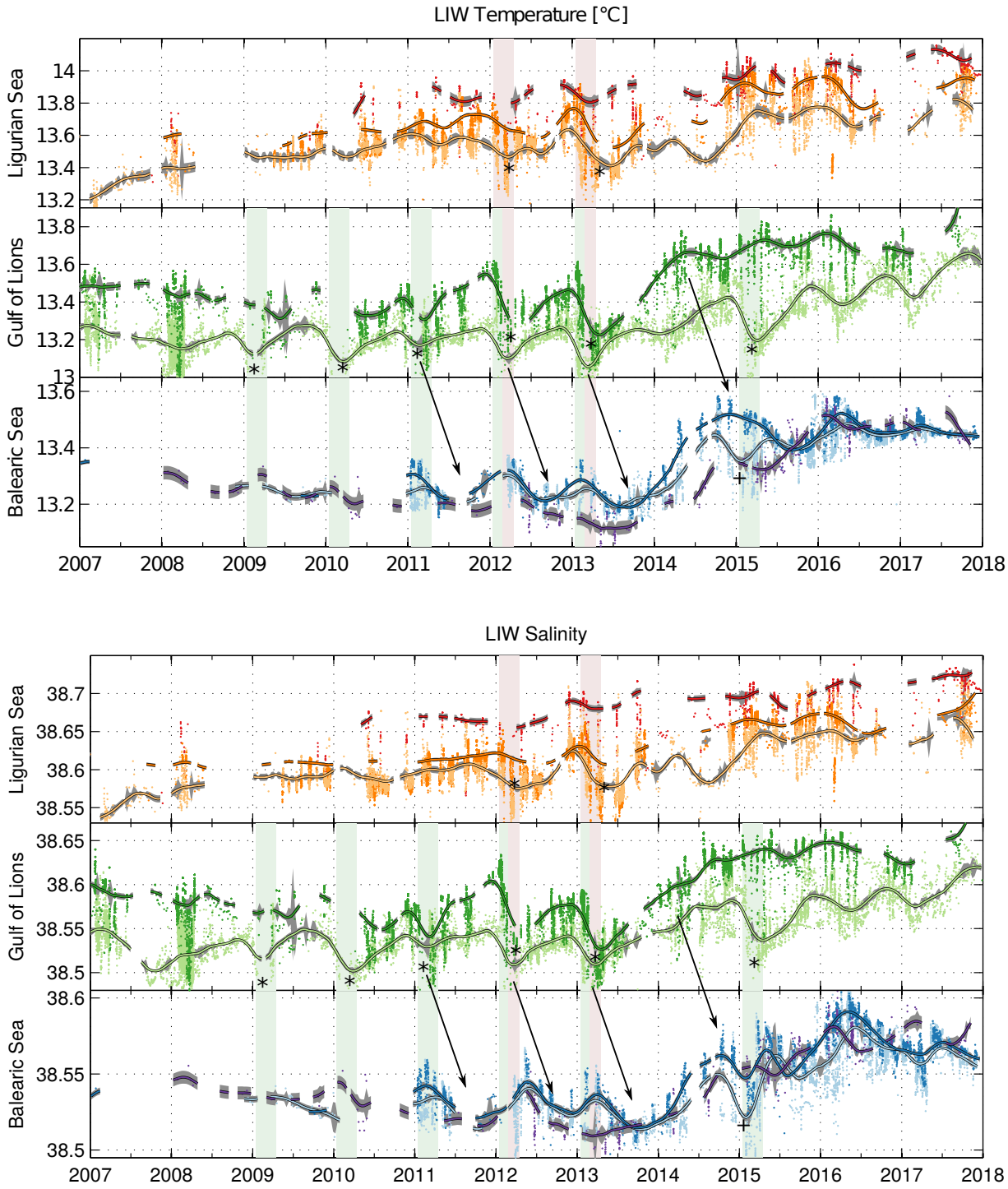

Figure 2. Temperature and salinity 2007-2018 time series in the Ligurian basin, Gulf of Lions and Balearic Sea. The color-code is that of Figure 1: Calvi in red, offshore in light orange, Nice in dark orange ; the Northern Current vein in dark green and offshore in light green ; along the Spanish coast in dark blue, Ibiza-Mallorca in light blue and purple for Menorca. The deep convective winters in the Ligurian Sea and in the Gulf of Lions are presented with purple and green vertical patches, respectively. The black contoured curves represent the running mean over a 90 day period and the grey patches around them represent the running sample standard deviation in the considered region (the very large number of points explains its low value). All the extracted points in each region are plotted in the respective color.

7/10

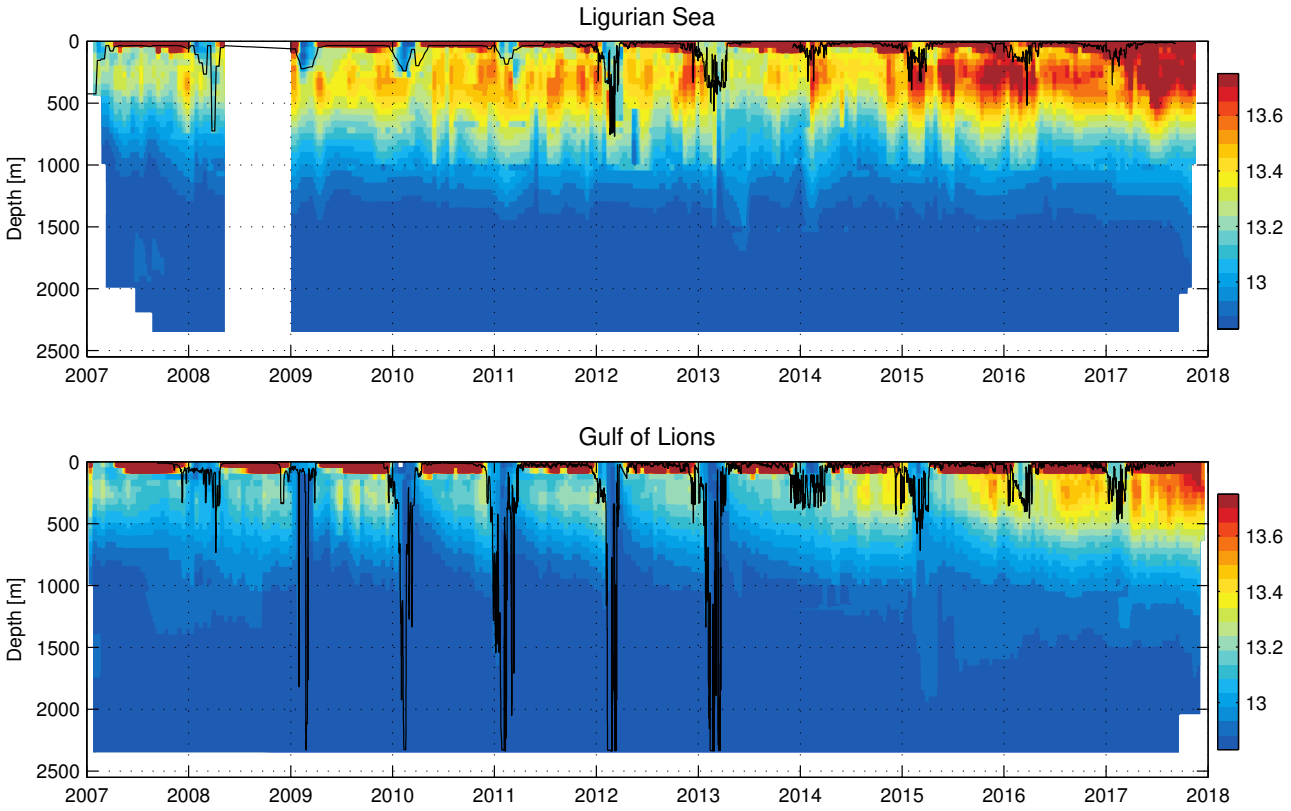

Figure 3. Temperature Hovmöller diagrams at the (top) DYFAMED (43.41 N 7.89 E) and (bottom) LION (42.04 N 4.68 E) mooring locations for the Ligurian Sea and the Gulf of Lions respectively (the salinity structure is similar). All the profiles within a 15 km radius of the mooring location are used, as well as the mooring line measurements for this interpolation. The black contour represent the mixed layer depth, computed as in Houpert et al.[7]. Since 2013 and the absence of deep convection, the LIW has invaded a larger portion of the water column.

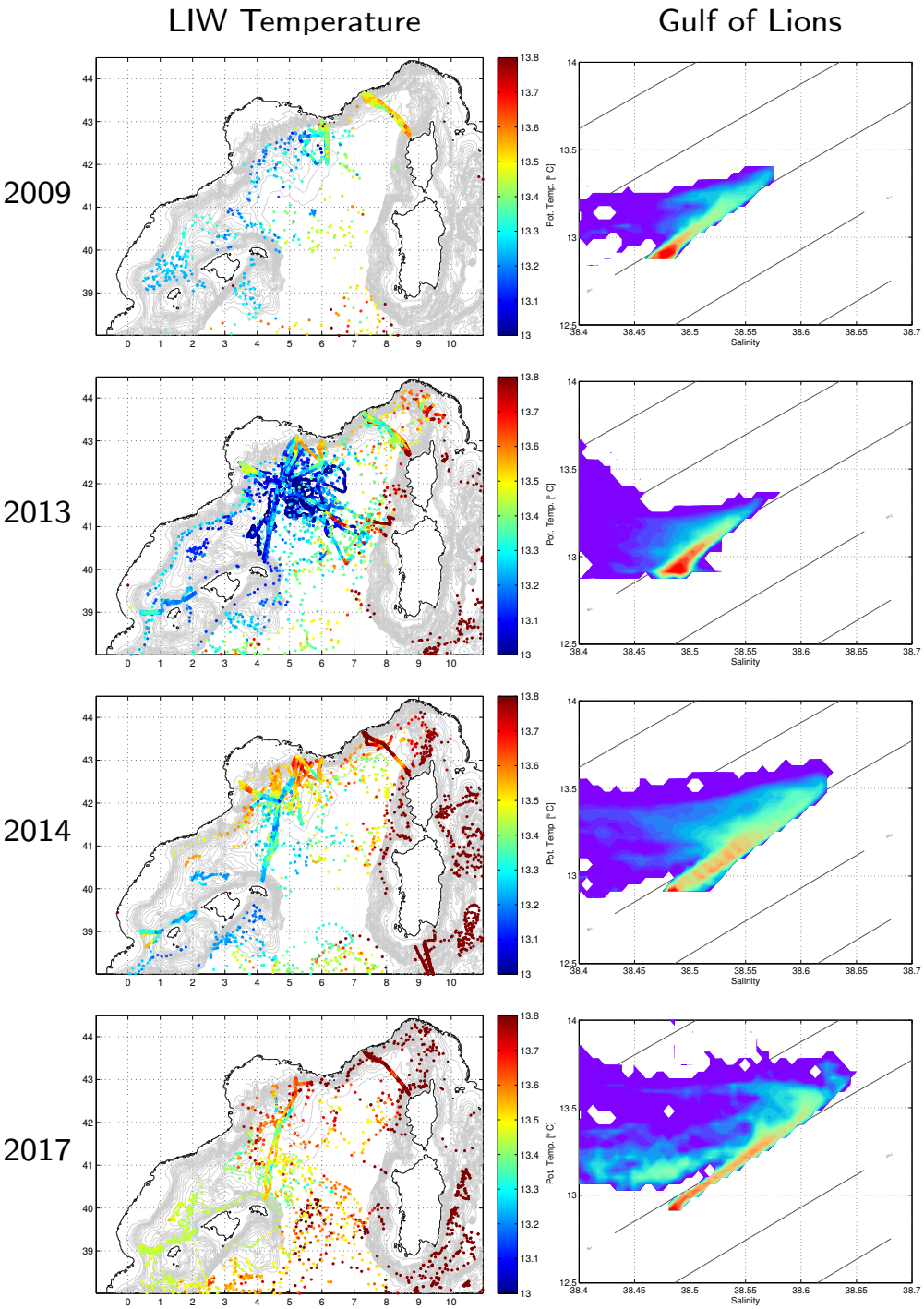

Figure 4. (left column) Temperature of the LIW in the Northwestern Mediterranean Sea over the two regimes between 2007-2013 and 2014-2017. LIW temperature and salinity (not shown) remain constant prior to the 2014 absence of convection, the warming and salinification are then observed throughout the basin. (right column) Analogue water properties in a volumetric Temperature and Salinity diagram in the Gulf of Lions box in Figure 1. All the yearly profiles are taken into account as a red colour accounts for a high density of points and thus volume of water, and purple accounts for a low one. The years with deep convection (2007-2013) present a high volume of waters with the same properties (WMDW), while in the following years the conserved LIW takes a larger portion of the water column, as the waters are distributed on the mixing line between the WMDW and the LIW.

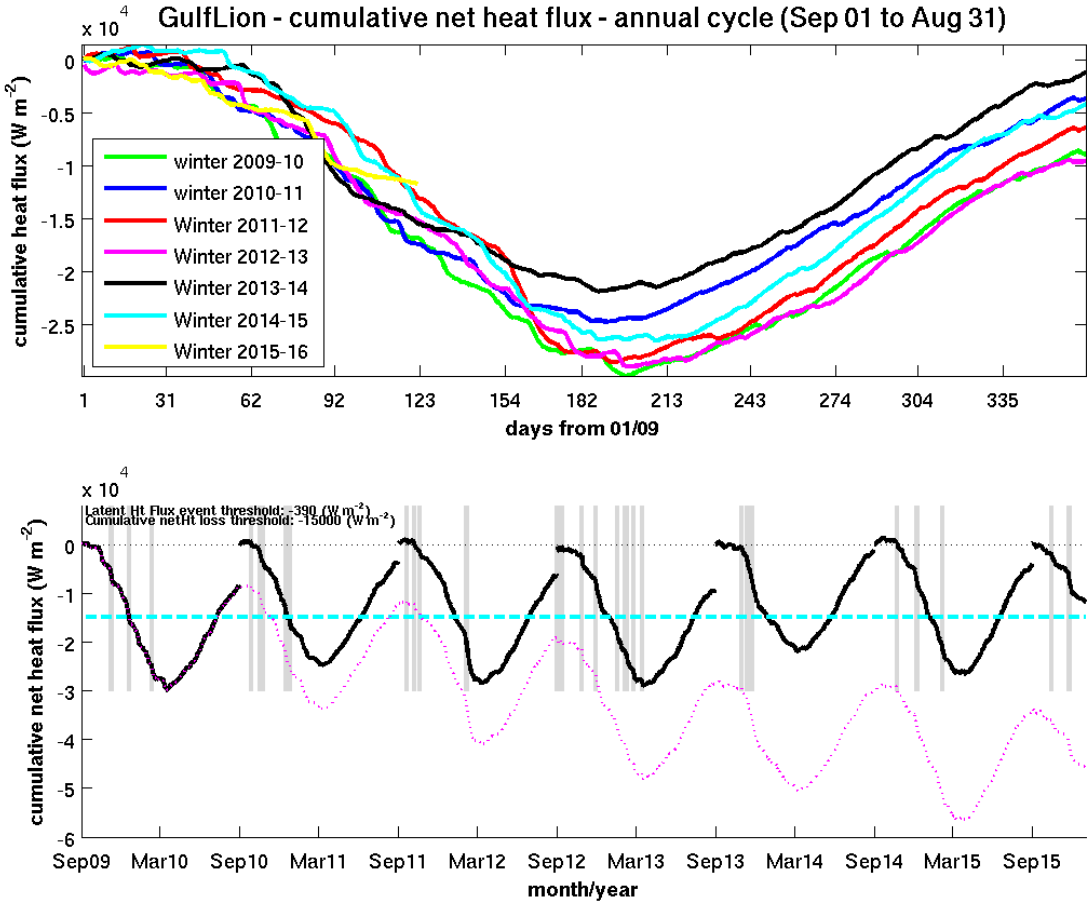

Figure 5. Cumulative net heatfluxes in the Gulf of Lions from September 1st to August 31st. (top) Year to year cumulative heatfluxes in the Gulf of Lions from a model reanalysis. (bottom) The whole time series, presenting the overall losses on the 6 year time period. Events of magnitude higher than 400 W.m^2 are presented in the form of grey vertical bars.

3.3 Additional remarks

The publication of this article is pending updated atmospheric fluxes in the Gulf of Lions. With the updated fluxes, and in the context of a slightly decreased preconditioning, it should be possible to quantify the atmospheric fluxes needed to trigger convection to the ocean floor. The transition between the two states of the basin occurred in winter 2013/2014[1], which was the weakest of all presented in terms of cumulated net heatflux. Additionally, the fluxes chronology should provide a means to show the importance of strong forcing events throughout the year, as the winter 2010/2011 was not that strong in terms of cumulated net heatflux, but the forcing at the beginning of the winter was significant and deep convection did occur. Similarly, the 2011/2012 event was not starting off strong but saw a long intense cooling, enabling the convection to reach the bottom.

The new state of the basin and the questions arising from it in terms of the deep convection future possibility of occurrence are addressed in Chapter 4.

3.4 Model comparison and OSSE

The LIW time series presented in Section 3.2 provides a new tool to evaluate model performance. In order to assess the ability of the NEMO Med12 reanalysis (described in Section 1.1.7) to reproduce the variabiliy of LIW properties, we submitted it to the same treatment as the observations. Model outputs were considered like data profiles and the core properties were extracted in the same way, taking the maximum temperature and/or salinity under the 29 $kg.m^{-3}$ isopycnal. The same regions as in Section 3.2 were considered for the model outputs.

Unfortunately, the model atmospheric forcings only spans from 1973 to 2014 and the time period does not coincide perfectly with that of the observations (2007-2018). However, similarly to what has been going on since the winter 2013/2014, the winters 2006/2007 and 2007/2008 were non convective after four consecutive deep convective years when the convection reached the bottom. So although the time frame is not exactly the same, similar processes are available for study.

Although the model has a known warm and salty bias, it is able to capture the long-term trends in the LIW. In the Ligurian Sea, the mean warming and salinification rates are respectively of 0.05°C $.year^{-1}$ and 0.007 $year^{-1}$, of the same order of magnitude as the observed rates. The model also successfully captures the coastal gradients and reproduces well the variability. The model's ability to represent deep convection is confirmed in the Gulf of Lions, where the model accurately shows the interannual variability in the intermediate waters. The LIW is indeed dented in a similar way to that illustrated in the observations when deep convection occurs and they are mixed. The stable temperature and salinity observed when successive convective years occur is also well represented, and, during the 2006/2007 transitional winter, a jump is observed in both temperature

[1] An event that can be noted several times in historical time series too, but never as thoroughly observed and documented.

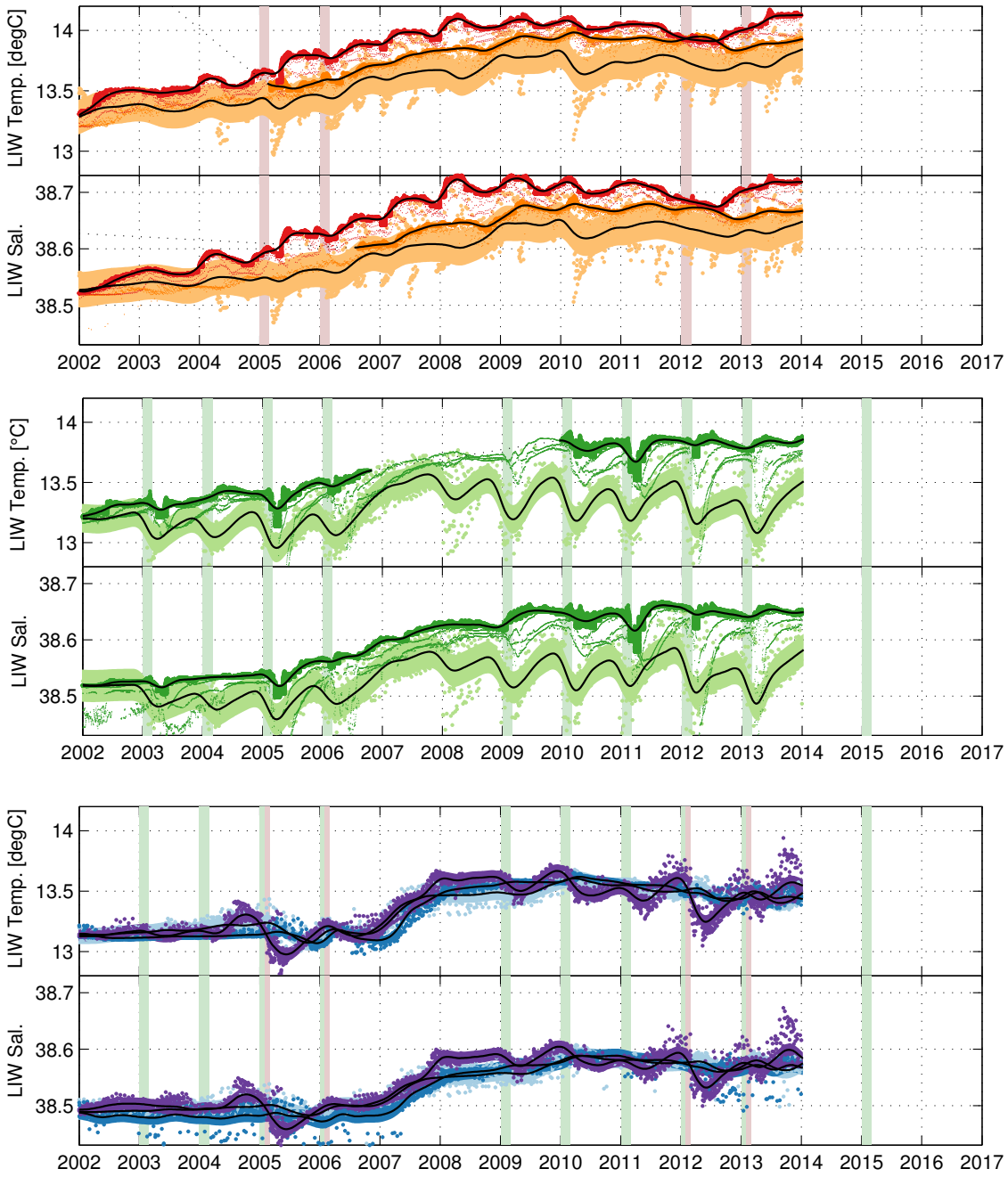

FIGURE 3.3: Model LIW temperature and salinity time series in the three regions: (top) In the Ligurian Sea, (middle) In the Gulf of Lions, (bottom) In the Balearic Sea. The colour-code is the same as that of Figure 1 in Section 3.2.

and salinity like the observed one in 2013/2014. The circulation time between the different boxes is in good agreement with the estimates from the observations (see Section 3.2). Moving along the circulation to the Balearic Sea, an issue rises. Due to the presence of a near permanent 'Catalan' eddy off the coast of Barcelona in the model[2], the Balearic Sea circulation is not represented correctly. As can be seen in the time series of Figure 3.3,

[2]Eddy sometimes also observed at sea, but far from being permanent. It is less permanent in higher resolution versions of the model.

the 2006/2007 jump is observed first in the Menorca region before the Ibiza and Mallorca ones, contrary to the observations. The eddy is recirculating waters directly to Menorca, bypassing its trajectory in the Balearic Sea.

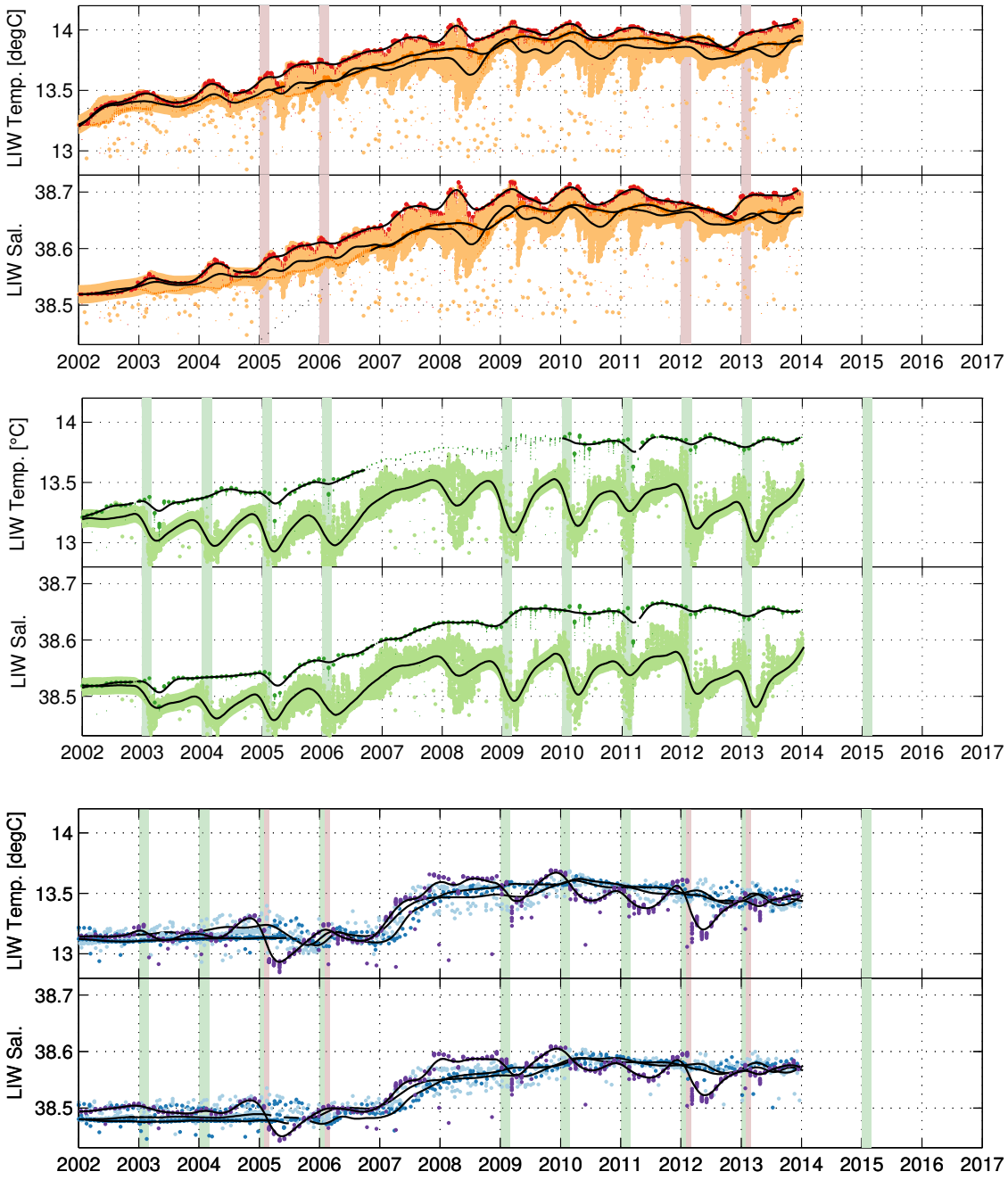

FIGURE 3.4: Simulated model sub-sampling by SIGLID LIW temperature and salinity time series in the three regions: (top) In the Ligurian Sea, (middle) In the Gulf of Lions, (bottom) In the Balearic Sea. The colour-code is the same as that of Figure 1 in Section 3.2.

The method presented in Section 3.2 to plot the time series relies on the extraction of one point corresponding to the core of the LIW per profile. As such, and now that we have established the model's ability to reproduce the time series of LIW in agreement

with the observations, one of the main questions arising is whether or not the method is legitimate in observing the basin properties. In order to estimate the observations' ability to represent what the basin is undergoing and to track the observational strategy's score, we sub-sampled the model outputs. This OSSE approach using synthetic observations in the model enables not only an evaluation of the model performance but also in turn an evaluation of the sampling strategy and an evaluation of future ones. In our case and for the study of the LIW, because only one point per profile is extracted and beacuse the core of the observational dataset is the glider endurance lines, only gliders were simulated along the observational endurance lines using a glider simulator developed by L'Hévéder et al. (2013). This provides a tool allowing to launch simulated gliders in the model. More than sub-sampling the model or using a hypothetical ideal glider trajectory within the model, the simulated instrument glides through the model waters and is exposed to the model velocities. This ensures that a region that could not be sampled by a glider for velocity frontier reasons (a front that is too strong for instance) would not be accessible. It also ensures a reasonable sampling rate compared to that of observations. Three gliders were launched in the three different regions: the first one in the Ligurian Sea, the second one in the Gulf of Lions and the third one in the Balearic Sea, reproducing the observational transects. The results are presented in Figure 3.4.

Comparing Figures 3.3 and 3.4 reveals that the sub-sampling of the model is able to reproduce the model outputs. In the offshore Ligurian and Gulf of Lions boxes, the difference between the outputs is smaller than 0.005 both in temperature and salinity. In the other coastal boxes, naturally more rarely sampled by the simulated gliders, the agreement is of 0.01, within the confidence interval of the observations. Having shown the model's ability to reproduce the observed time series and having in-turn proven the sub-sampling's ability to reproduce what is going on in the model, we can say that the model is satisfactory (with the exception of the Balearic Sea eddy) and that the sampling strategy is legitimate in its representation and monitoring of the basin. A welcome transect would be a Menorca–Sardinia glider endurance line to close the region and enable more accurate budgets like the ones computed for the 2012/2013 winter (see Chapter 2).

Chapter 4

The role of deep convection in regulating the Western Mediterranean Basin

Contents

4.1 A new state of the Western Mediterranean

4.1.1 Deep convection occurrences

Deep convection is intermittent and the volume of WMDW formed from year to year also varies [Houpert et al., 2016]. As proven in the previous chapter, its absence since winter 2012/2013 has drastically changed the state of the basin, as the warmer and saltier input of LIW has been allowed to invade the intermediate layers of the basin. The intermediate layer core is not only saltier and warmer, but the LIW also occupy a larger portion of the water column and represent a larger volume compared to previous years in these regions. Deep convection mostly depends on two components: the preconditioning and the atmospheric forcing. The object of this section is to investigate whether this absence of deep convection has changed the preconditioning and whether it will compromise the possibility for future deep convective events. The possibility of consecutive deep convection events triggering each other will also be discussed, as the records do not show isolated deep convective years, and as the basin seems to jump from a convective state (2003/2006 then 2009/2013) into a non-convective one (2007/2008 then 2013/2017).

4.1.2 Stratification

Basin-wide stratification

A recent modelling study by Waldman et al. (2018) suggests that atmospheric fluxes play a larger role in deep convection occurrence than the oceanic preconditioning. They argue that the preconditioning is always present due to the gyre circulation doming the isopycnals, although varying in intensity depending on the year. In order to verify this hypothesis, the vertical stability of the water column was assessed using the *Brünt − Väisälä* frequency:

$$N^2 = -\frac{g}{\rho}\frac{\partial \rho}{\partial z} \tag{4.1}$$

where g is the gravity acceleration, ρ the potential density and z the depth of the water parcel. The parcel is only stable when $N^2 > 0$ and the larger the N^2 the more energy is needed to mix the water column [E. Gill, 1982]. A stratification index was then computed by integrating N^2 over the water column, accounting for the buoyancy content of the water column, a more relevant variable to compare to the atmospheric forcing.

Figure 4.1 presents typical stratification index maps at 1500 m[1] depth during the two periods from 2010 to 2013 and 2014 to 2016. These scatter plots suggest that the preconditioning in the basin has indeed changed, if only in generating a smaller region of low stratification index. The regime change operated in winter 2013/2014 seems to have reduced the gyre core of weakly stratified waters. The high stratification index seen in 2016 suggests that intense atmospheric forcing would be needed for a convective event that would be localised around the LION mooring location, where stratification appears weakest. Also, thermohaline staircase-like structures indicative of double diffusive salt fingers (such as those commonly observed below the LIW in the Tyrrhenian Sea [Durante et al., 2016]), have been increasingly observed throughout the entire Western Mediterranean Basin in recent years. The presence of more salt finger structures could be due to the stronger gradients induced by the presence of non-mixed LIW, which generates larger temperature and salinity gradients between the intermediate and deep layers of the Northwestern Mediterranean . The Moose-ge2017 cruise notably observed the basin-wide presence of such structures with double diffusive staircases with 80 m wide steps on average.

Stratification at the LION mooring location

In order to verify this increase in stratification, the index was computed at the LION mooring location as a Hovmöller time series. The stratification index in the core of the convective region is presented in Figures 4 and 5 of the article in Section 3.2. In Figure 4, the stratification index is computed over the whole water column, whereas Figure 5 disregards the first 200 m, overlooking the seasonal cycle. Figure 5 shows that the deep preconditioning of the water column has slightly decreased since 2013 and in the absence

[1] When convection reaches below the LIW, it usually reaches near the bottom.

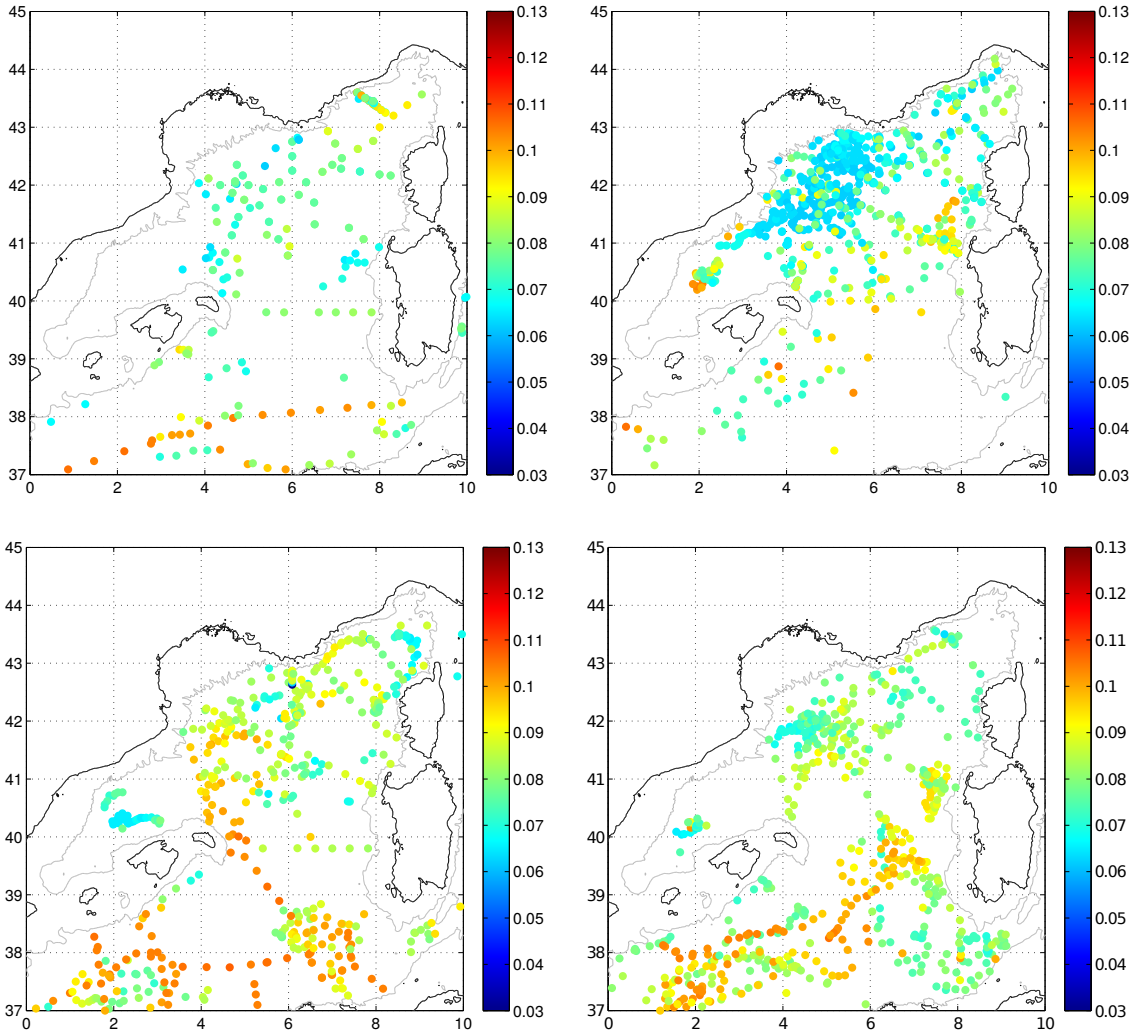

FIGURE 4.1: Basinwide stratification index during the preconditioning phase at 1500 m depth during the two 2010-2013 (top) and 2014-2017 periods (bottom). All profiles deeper than 1500 m are considered. Other years can be found in Appendix B.

of deep convection. The available heat content presented in these same figures shows the energy needed to mix the water column to the chosen depth, which has also slightly increased, further suggesting the need for a stronger atmospheric forcing to trigger a new convective winter.

In order to verify the impact of the invasion of the intermediate layer by the very salty LIW on the stability of the water column, the relative contribution of temperature and salinity to the stratification can be expressed as:

$$N^2 = N_T^2 + N_S^2 \tag{4.2}$$

$$N_T^2 = -g\alpha \frac{\partial T}{\partial z} \tag{4.3}$$

$$N_S^2 = g\beta \frac{\partial S}{\partial z} \tag{4.4}$$

where α and β are the thermal expansion coefficient and the saline contraction coefficient, respectively:

$$\alpha = -\frac{1}{\rho}\frac{\partial \rho}{\partial T} \tag{4.5}$$

$$\beta = \frac{1}{\rho}\frac{\partial \rho}{\partial S} \tag{4.6}$$

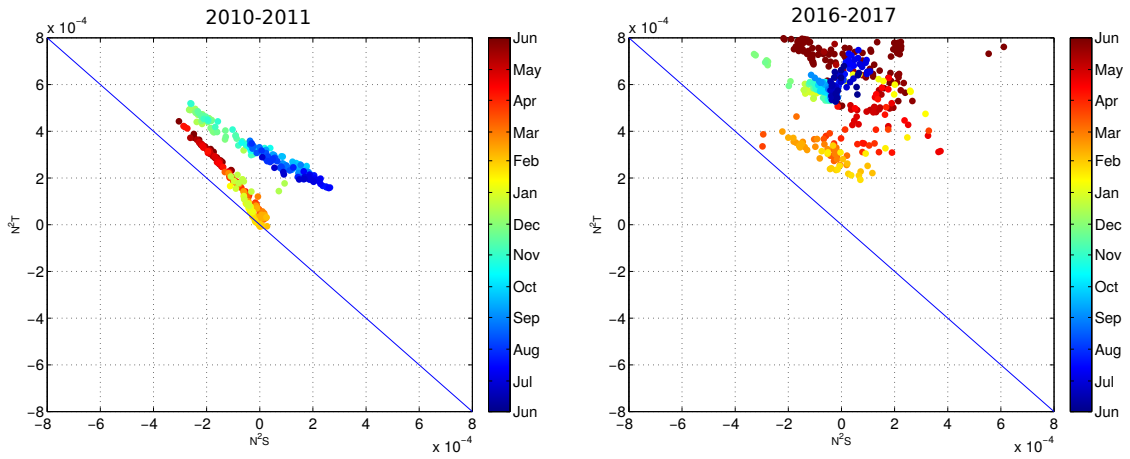

FIGURE 4.2: Turner diagram of water column stability in temperature (N^2T) and salinity (N^2S) in the Gulf of Lions. Under the blue line, the water column is gravitationally unstable. Three stable scenarios are possible: if N^2T and N^2S are both positive the temperature and salinity both contribute in stabilising the water column, if N^2T is positive and N^2S negative the stabilising temperature gradient is accompanied by destabilising salinity gradient and vice-versa. The months are represented in the colourbar, from June 2010 to June 2011 on the left panel, and from June 2016 to June 2017 on the right panel. Other years can be found in Appendix B.

Figure 4.2 depicts the water column stability in terms of the temperature and salinity relative contributions, throughout two typical years in the two states of the basin mentioned previously. From June 2010 to June 2011, typical of a state with consecutive deep convective years, a seasonal cycle for the stratification clearly appears. Starting in June 2010, the salinity stratification gradually decreases as the LIW re-invades the intermediate layers, injecting destabilising salt at intermediate depths. This LIW input also has a slight temperature stabilising effect, but not quite as important as the salt destabilising factor. In January, under the intense atmospheric cooling and evaporation, the water column is brutally mixed and jumps to the (0,0) coordinate corresponding to a well mixed water column. Then, similarly to what was seen in 2010, the LIW input as well as the surface warming come into play and restabilise the water column. In 2016/2017, typical of a state with consecutive non-deep convective years, the water column stability seems to be temperature dominated, as the salt input at intermediate levels is always present and thus not as important a factor. The stratification is also higher and the mixing induced that winter does not destabilise the water column enough to mix it, as is confirmed by the convection only reaching 300-400 m depth that year.

Stratification versus atmospheric fluxes

To further investigate the role of atmospheric forcing compared to that of the preconditioning, the atmospheric cumulative net heatfluxes (retrieved from the ERA Interim-Med reanalysis) are represented in Figure 4.3. The 2013-2014 transition winter between the two regimes is one of the weakest ones observed and that explains why there was no deep convection that year. On the contrary, the following 2014-2015 winter had more intense atmospheric fluxes but no deep convection. The ocean preconditioning thus has to play an important role as well.

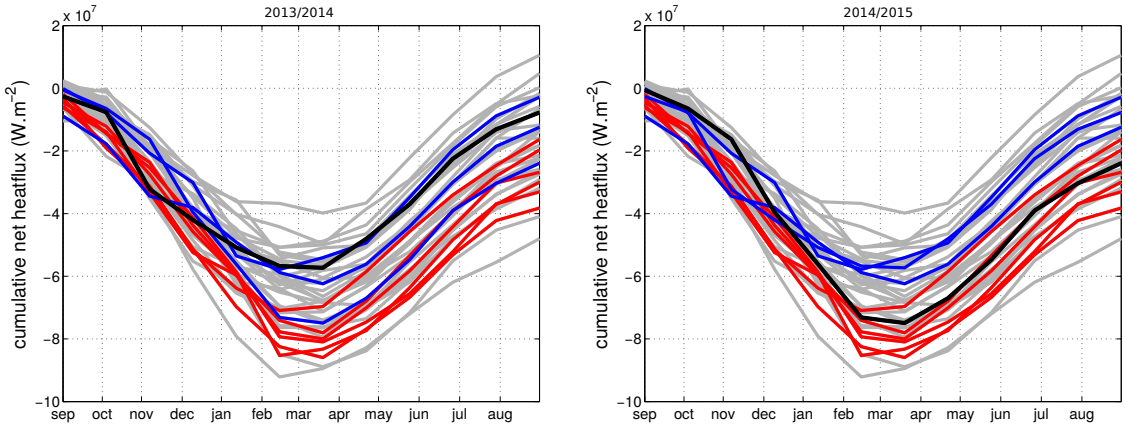

FIGURE 4.3: Cumulative net heatfluxes in the Gulf of Lions. The historical fluxes are in grey. Over the 2007-2017 observed period, the deep convective year are in red, the non deep convective ones in blue. The weak 2013/2014 transition winter fluxes are on the left, the 2014/2015 on the right panel.

Figure 4.4 superimposes the stratification index at 2000 m depth with the cumulative net heatfluxes over the observed period. Although no significant change is observed in terms of the total stratification index between the two regimes, the stratification under the LIW layer does increase. This suggests that the LIW which was able to invade the basin after the weak mixing of 2013-2014 has increased the deep stratification, making it more difficult to convect to the ocean floor. Although the cumulative net heatfluxes do not account for very intense and very brief atmospheric forcing, the timing of the forcing has to be such that it is still intense when the MLD reaches the LIW layer.

Looking at the broader historical context in Figure 4.5, the weaker years in term of atmospheric forcing are as expected non-convective ones and the stronger ones are convective. However, a twilight zone lies between them where fluxes alone cannot capture the whole story. The stratification index below the LIW layer seeems to be the relevant index characterising the ocean preconditioning, and the convective character of the preceding year is thus key, as it naturally preconditions the gyre for the following winter.

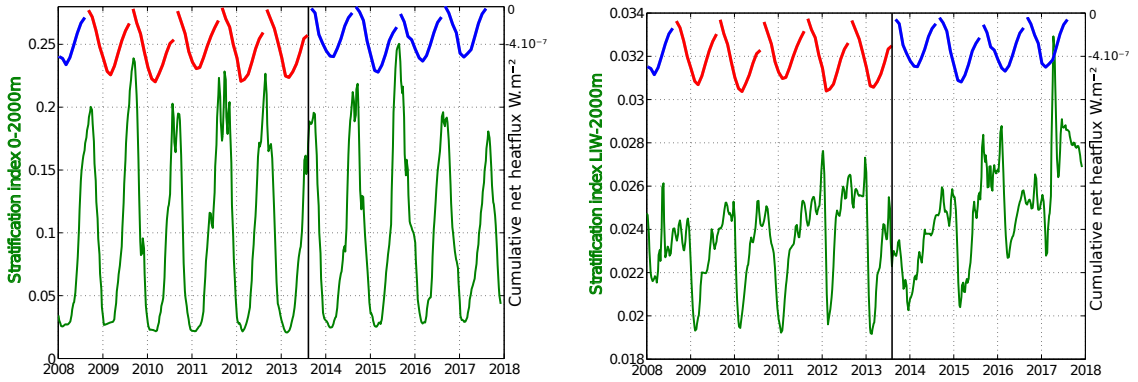

FIGURE 4.4: Stratification index and cumulative net heatfluxes in the Gulf of Lions

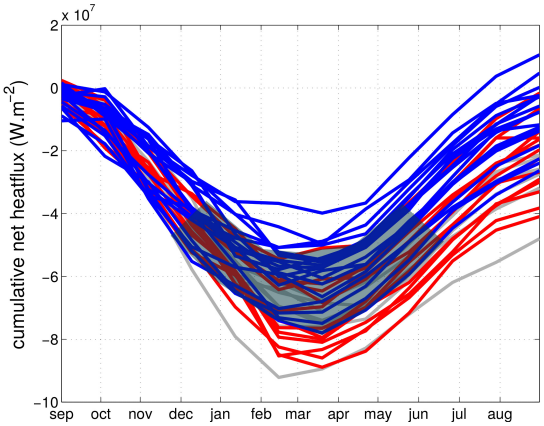

FIGURE 4.5: Historical cumulative net heatfluxes in the Gulf of Lions (starting in 1979). The deep convective year are in red, the non deep convective ones in blue. The grey patch highlights a "twilight zone" where fluxes do not determine alone the convective character of a winter.

4.2 A future without deep convection ?

After 4 consecutive winters without deep convection, and as climate models predict less open-ocean deep convection in their scenarios, the question of the occurrence possibility of deep convection arises. The LIW is not the only water mass affected and driving deep convection, and this is further discussed in this section.

4.2.1 AW, WIW and WMDW

With a similar technique to that presented in the previous chapter to compute time series of LIW, the AW properties were computed for each profile as the mean temperature and salinity over the 28.95 kg.m^{-3} isopycnal (Figure 4.6). The mean was taken instead of a maximum or minimum as for the LIW as the core of the AW is not well defined and the mean represents better the yearly signal. Modulated by the seasonal cycle, both the AW temperature (although not significant) and salinity (significantly) have slightly increased

in winter in this surface layer[2], also preparing the potential formation of warmer and saltier deep waters formed through mixing with the LIW. It is worth noting that both these warming and salinifying trends observed in the AW and LIW are not associated with a significant density change. If the surface waters warm more quickly than their salt content increases, a surface layer could be formed that would be tougher to breach through atmospheric forcing.

[2]The NEMO Med12 model is also able to satisfyingly reproduce these time series.

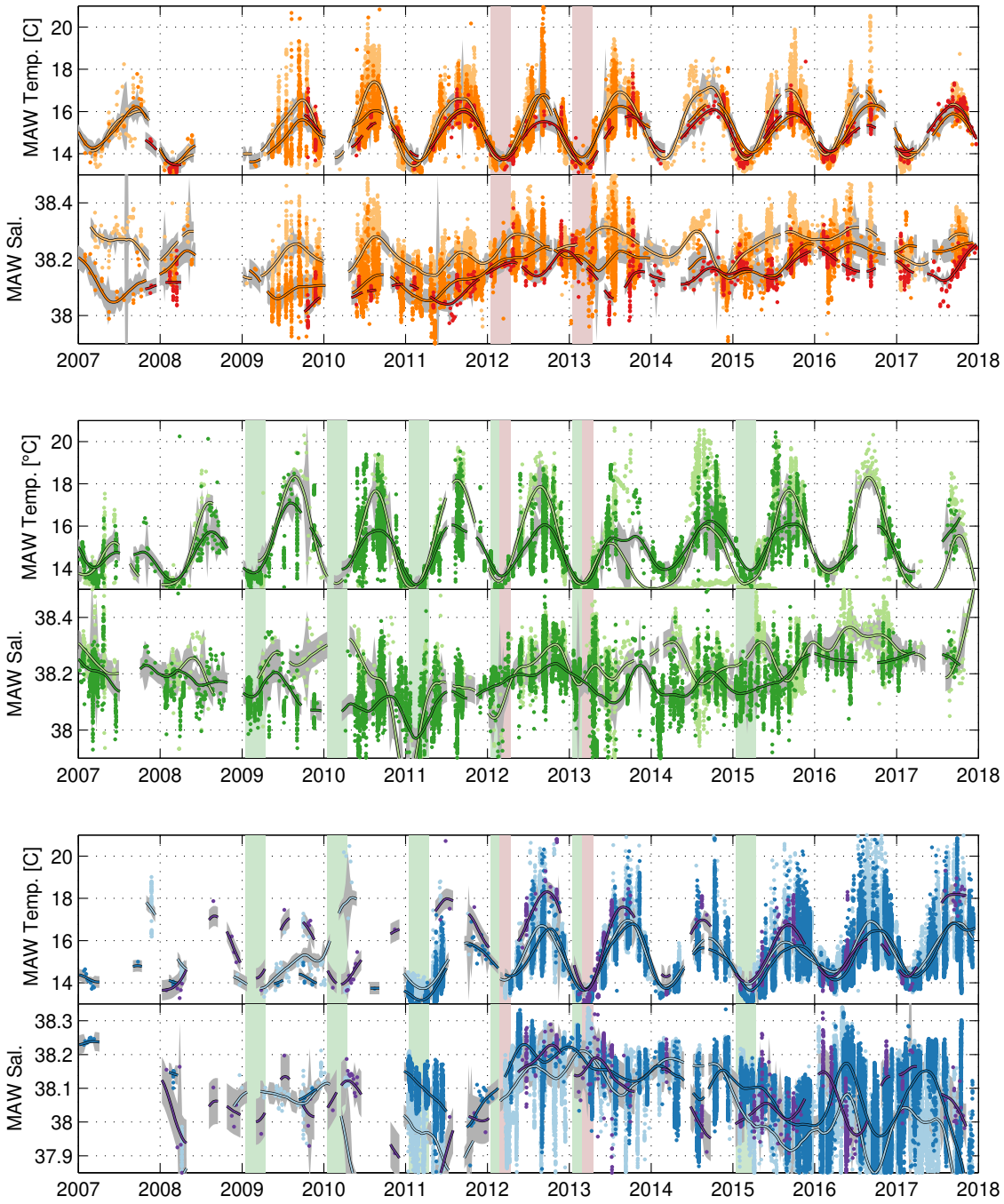

FIGURE 4.6: AW water properties throughout the basin for the 2007/2018 period. The colour -code is that of Figure 1 in the article in Section 3.2: red in the Ligurian Sea, green in the Gulf of Lions and blue in the Balearic Sea.

These warmer and saltier **m**odified **A**tlantic **W**ater (mAW) have still been mixed since winter 2012/2013, but instead of forming deep waters, WIW were formed. The volumetric θ/S diagram presented in Figure 4.7 shows how the absence of deep convection forms a much larger volume of WIW than during convective years (some WIW can also be formed at the rim of the mixed patch through baroclinic instabilities). In 2013, after a deep convective year, most of the water volume found in the Balearic Sea is in the

deep waters. On the contrary, in 2017, the water volume is more partitioned between the WMDW and the LIW. In 2017, a bulge of WIW appears with a much larger volume than in 2013. Although some WIW is formed every year, when there is no deep convection, more WIW is produced as the whole mixed patch contributes, compared to the rim of it or selected periods during deep convective years [Juza et al., 2018].

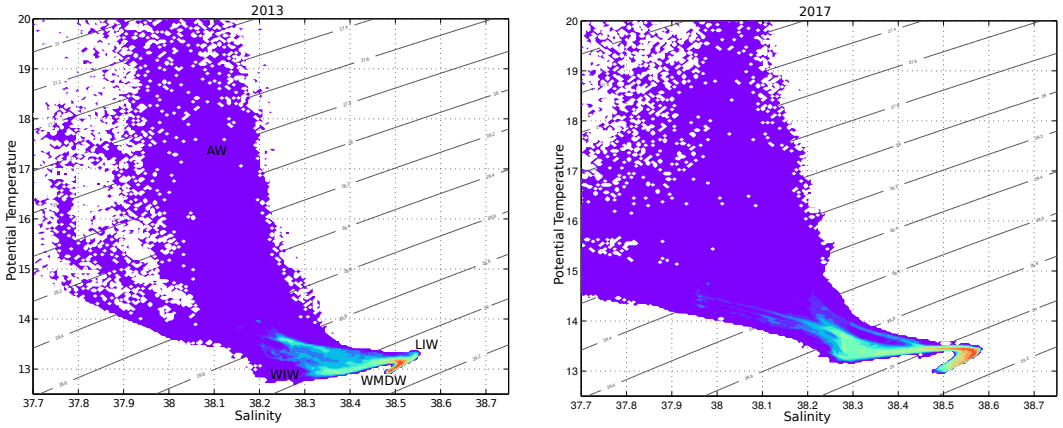

FIGURE 4.7: Yearly volumetric θ/S diagrams in the Balearic Sea (Mallorca region) in 2013 after an intense deep convective year (left) and in 2017, a year which barely saw convection to 450 m (right). Isopycnals are plotted in grey. The red colour vouches for a high concentration of points and thus a high volume of water at said characteristics, purple for a low concentration of points. Other years can be found in Appendix B.

To further document this least described Mediterranean water mass [Pinot et al., 1999], Louis Dupin conducted an internship on the WIW at the IEO-Centro Oceanogràfico de Baleares in summer 2016, and I supervised his work during the month he spent on the Moose-ge2016 cruise. His main conclusions were that the WIW presence in the Balearic Sea is strongly dependant on the intensity of the previous winter in the Gulf of Lions, and that it is mostly present in spring and summer before being advected away from the region. He also detected a warming and salinifying trend in the WIW properties previously reported by Heslop et al. (2012).

In order to better characterise these trends, Katia Mallil and I supervised a group of students on-board the Moose-ge2018 cruise (Sarah Gani, Yves Ponçon and Quentin Jutard) to devise a WIW detection tool. Compared to a classical view characterising waters within a temperature and salinity range as WIW, an algorithm was devised to detect a local temperature minimum between the 28.75 kg.m^{-3} and 29.05 kg.m^{-3} isopycnals and extract the core WIW properties (Figure 4.8). Thanks to this automated detection, the WIW was found to be more present in recent years compared to the 2009/2013 deep convective years, during which close to no WIW was detected, confirming the results seen in Figure 4.7.

Figure 4.9 presents yearly θ/S diagrams in the Gulf of Lions from 2000 to 2017. Not only can the invasion of the LIW be seen with the intensification of its properties, but the WMDW is also evident. The evolution described in Houpert et al. (2016) with yearly jumps associated with deep convective episodes appears. Since 2013 and in the absence

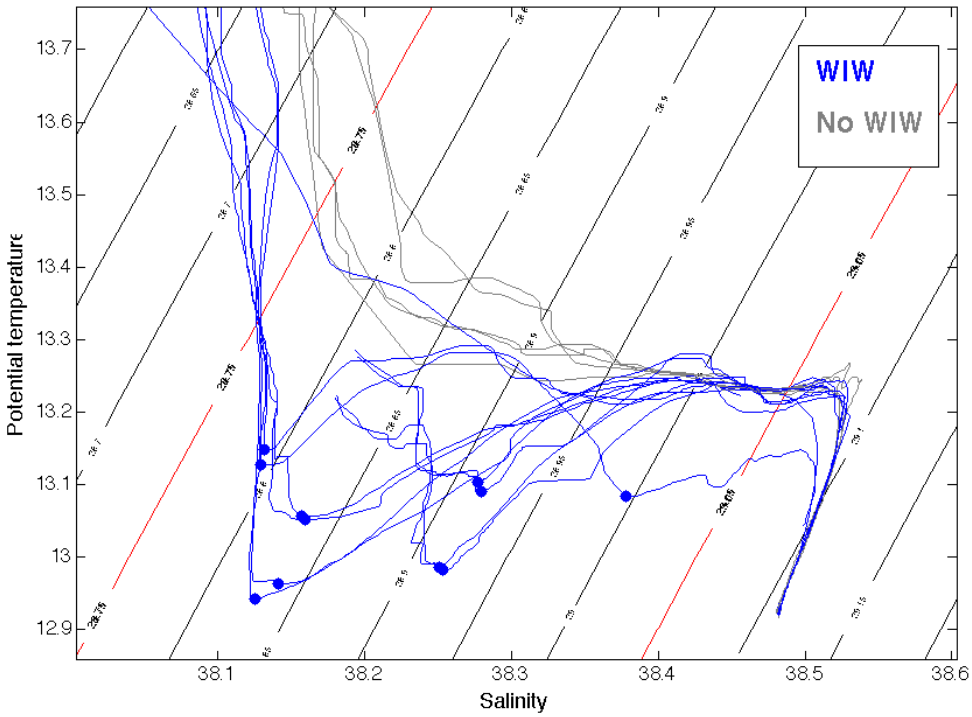

FIGURE 4.8: WIW detection algorithm performance in the Balearic Sea.

of deep convection, the deep waters have also mixed and were less salty in 2017 than when they were formed in 2013. This can also be observed in the WMDW time series presented in Figure 4.10, where jumps in the temperature and salinity of the newly-formed deep water appear. The deep waters, like the other water masses, are getting warmer and saltier as they store the heat and salt exported at depth by the deep convection events. Were there a next deep convective episode, the deep waters formed should be warmer and saltier than ever, as the intermediate waters have been accumulating heat and salt over the past 4 years without deep convection, and would have continued to do so without the occurrence of a deep convective winter in 2017/2018 (see Section 4.2.2).

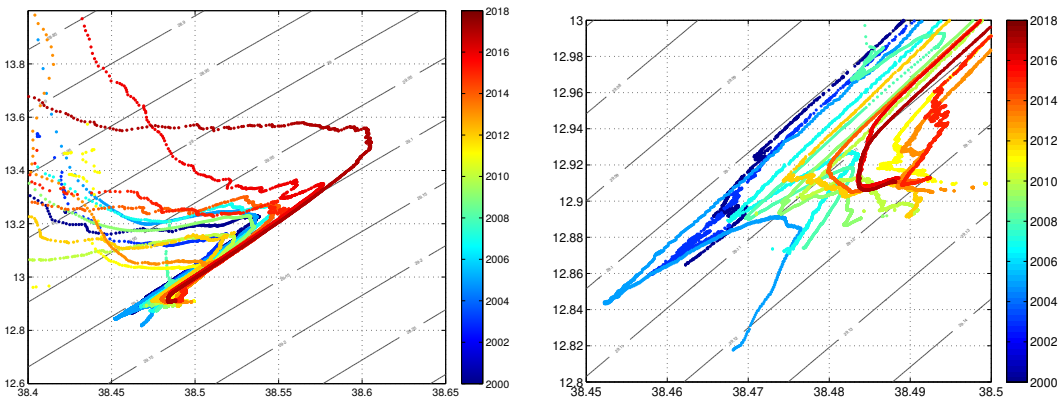

FIGURE 4.9: Yearly mean θ/S diagrams in the Gulf of Lions from 2000 to 2017. (left) Zoom on the Intermediate and deep waters, (right) Zoom on the deep waters. Isopycnals are plotted in grey.

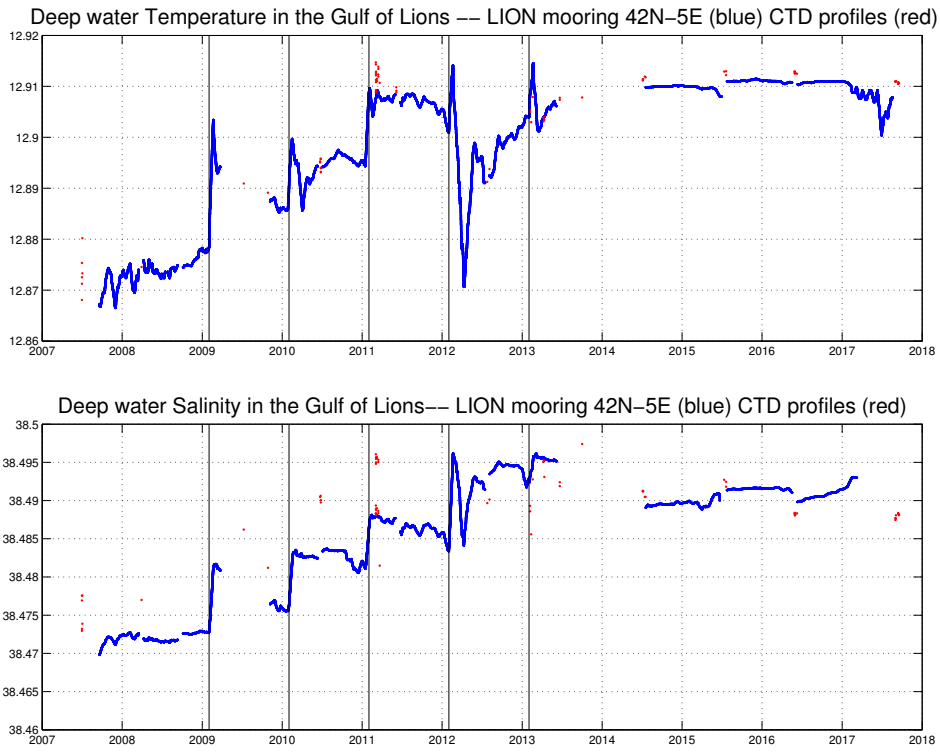

FIGURE 4.10: Deep water potential temperature and salinity at the LION mooring location. Mooring data in blue, CTD casts in red. The black vertical lines indicate deep convective years.

4.2.2 Deep convection event during winter 2017/2018

A prediction of warmer and saltier deep waters than ever is verifiable as the 2017/2018 winter has been a deep convective one. This winter has indeed been very harsh over the Northern Mediterranean and deep water formation was expected. It was first detected by the glider Tintin on the MooseT02-18 transect presented in Figure 4.11: The water column appears fully homogeneous from the surface down to 1000 m in the Gulf of Lions at

the beginning of February 2018. The inferred raw temperature and salinity values were of 13.1°C and 38.51. Later on, an Argo float detected that the convection had reached 1900 m, measuring raw temperatures and salinities of 13.0°C and 38.5. Preliminary results from the May Moose-ge2018 cruise presented in Figure 4.12 show that the newly formed waters stabilised around 1850 m and were characterised by 12.98°C and 38.5, significantly warmer and saltier than any deep waters previously observed. However, the horizontal extension of the new deep waters was limited, as the Moose-ge2018 cruise only detected the presence of the new deep waters near the LION mooring location. Further investigation could enable a better quantification of the limited volume of new waters formed. Furthermore, the glider transect presents some ventilated intermediate waters after January 21, suggesting the localised formation of intermediate waters prior to the deep convective event.

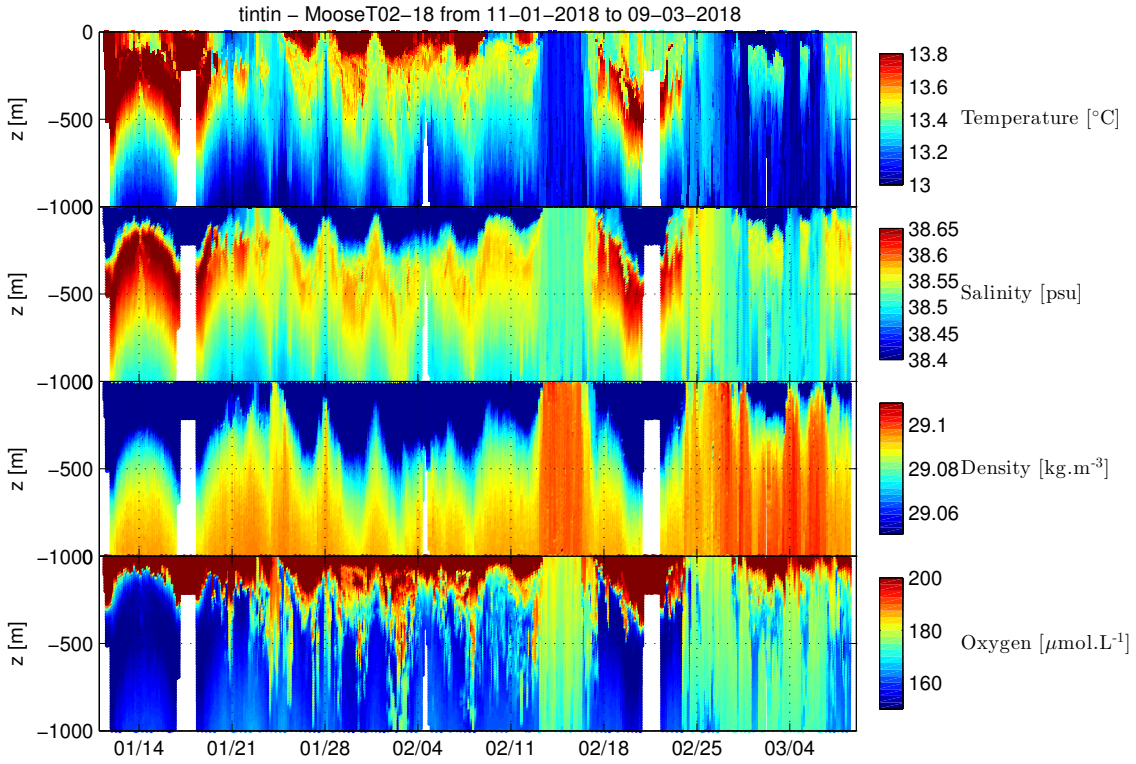

FIGURE 4.11: Tintin/MooseT02-18 glider deployment properties from 11/01/2018 to 09/03/2018. The glider recorded, from top to bottom panels: potential temperature, salinity, density and oxygen.

Moreover, convection was also observed in the Ligurian Sea, both with gliders and Argo profiling floats. The MLD was found to reach 800 m, the deepest since winters 2004/2005 and 2005/2006 which convected to the bottom. In doing so, the intermediate waters, usually comprised of old LIW poor in nutrients and oxygen, were intensely ventilated as can be seen in preliminary results (Figure 4.13). As convection occurs every year at least down to the LIW layer in the Gulf of Lions, it seems that the Ligurian Sea was more impacted by this strong winter in ventilating its intermediate waters. The Ligurian Sea has undergone a significant change, with this mixing of LIW inducing temperature

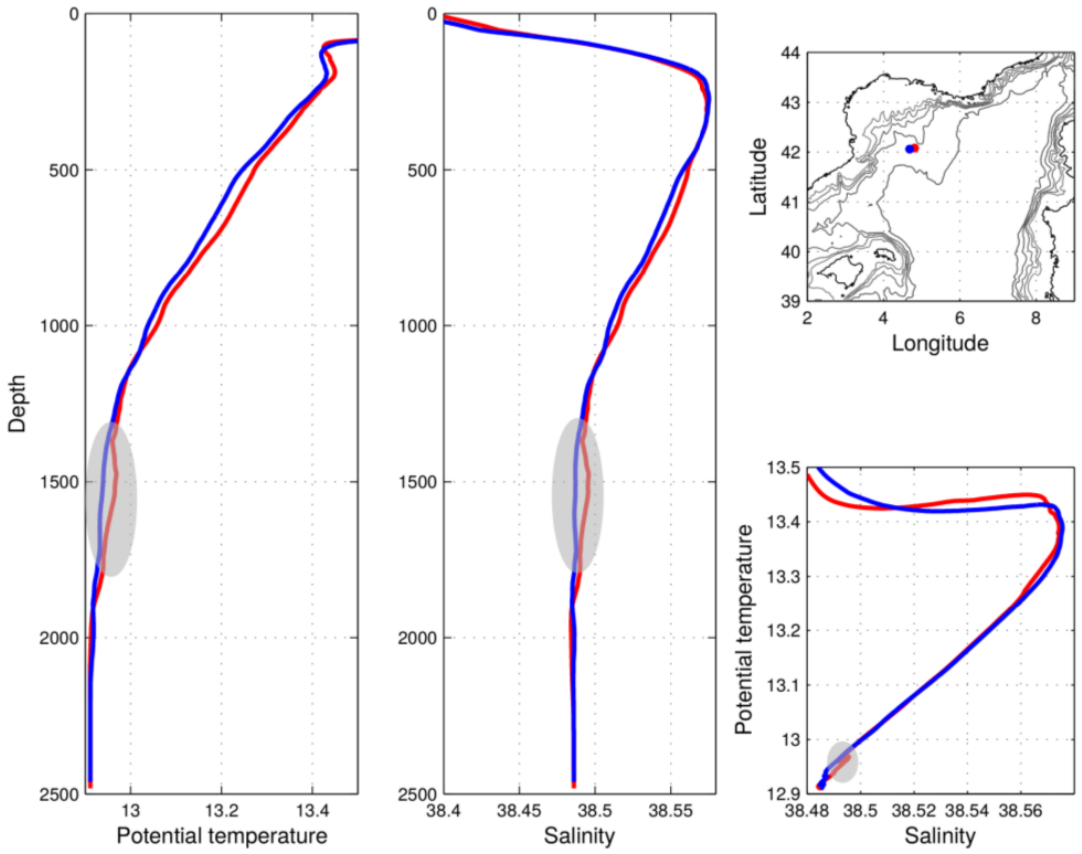

FIGURE 4.12: Potential temperature (left) and salinity (middle) profiles and potential temperature/salinity diagram (right) collected during the Moose-ge2018 cruise (leg 1, station 040 and 041). The newly formed deep waters are circled in the grey patch.

and salinity decreases as well as an O_2 increase. This is likely to have biogeochemical implications, which are to be monitored in the upcoming year.

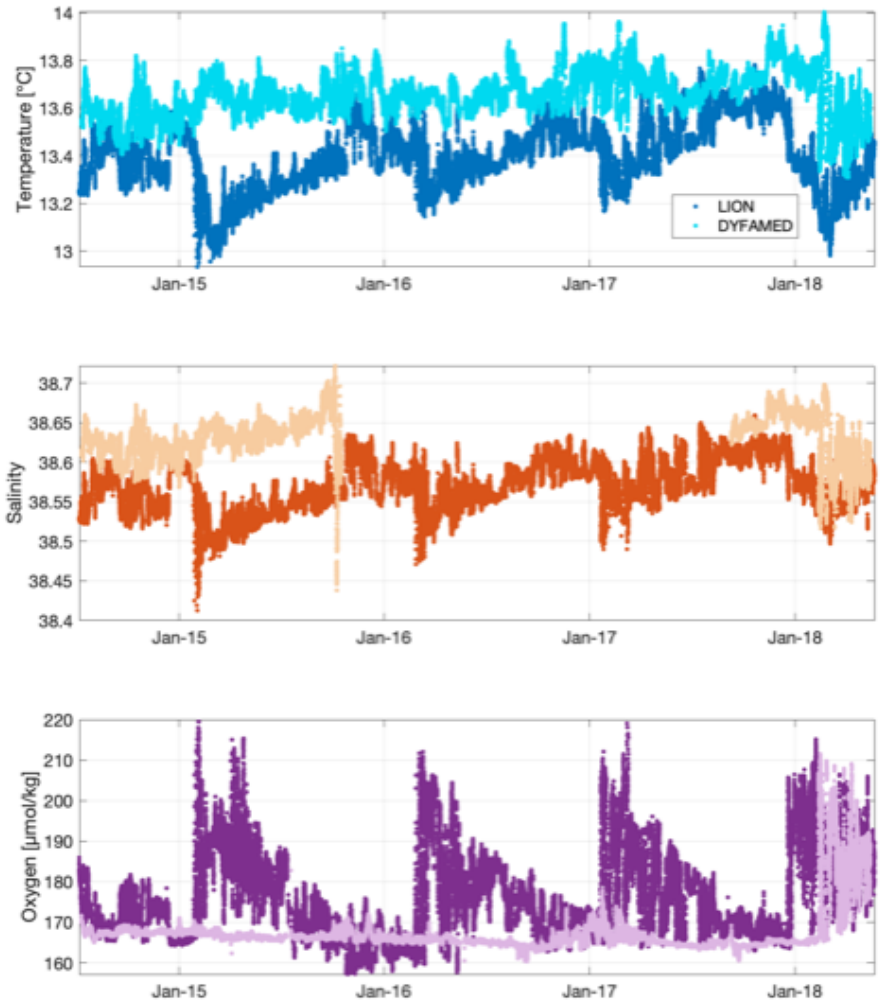

FIGURE 4.13: Preliminary potential temperature (top), salinity (middle) and oxygen (bottom) measurements from the LION and DYFAMED moorings in the LIW layer (30 min sampling rate). The data from the DYFAMED mooring line have been calibrated with the monthly CTD casts for 0_2. The data at LION is raw but probably only needs an offset in 0_2. The salinity sensor at DYFAMED was discarded for 2 years due to malfunctioning. Courtesy of Laurent Coppola.

Moreover, looking at the atmospheric fluxes for winter 2017/2018 displayed in Figure 4.14, it appears that winter 2017/2018 was an intense one. It indeed lies just outside the "twilight zone" described in section 4.1.2 and the heatfluxes have been strong enough to reverse the situation and trigger deep convection despite the increased stratification below the LIW layer.

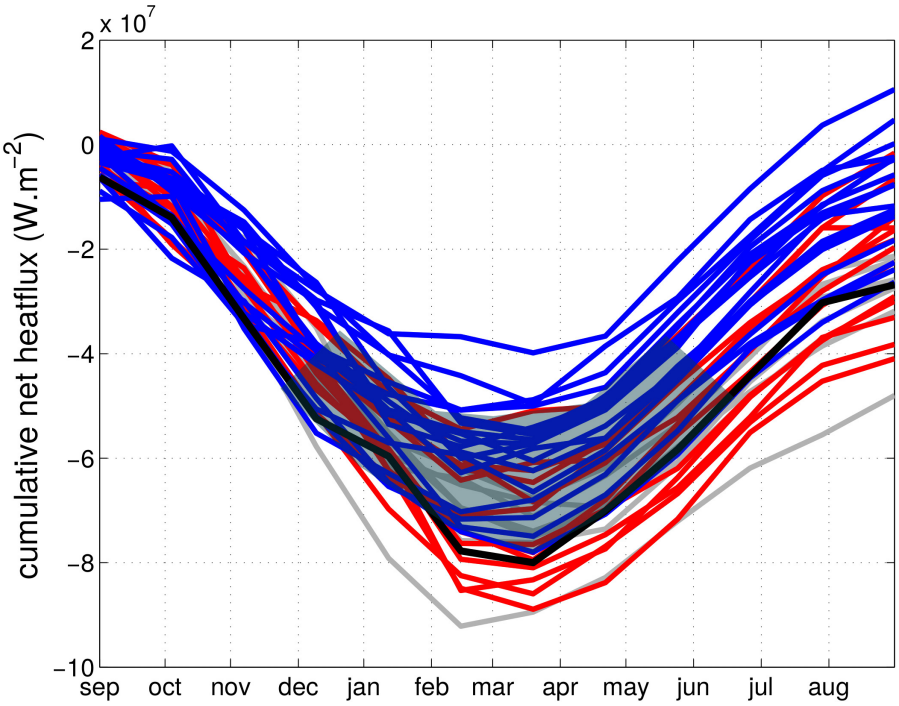

FIGURE 4.14: Cumulative net heatflux in the Gulf of Lions for the year 2018 (in black). In blue are the non-deep convective winters, in red the convective ones. The grey shading represents the "twilight zone".

4.2.3 Anticipating deep convection events

Climate models predict a reduction in the number of deep convection events in the future, and the fact that a slight stratification increase was observed may tilt in this direction. However, these same models also predict more intense extreme events, and an extreme winter could well mean the formation of a very large volume of deep water. No clear atmospheric teleconnection has been found to correspond with the winter intensity over the Gulf of Lions yet, as neither the Arctic Oscillation nor North-Atlantic Oscillation seem to match [Hurrell et al., 2001].

Despite the lack of planning tools to predict the occurrence of deep convection, the properties of newly formed deep waters can be inferred from the known water column properties. Figure 4.15 presents a tool to predict the mixed water properties. Thanks to the intense monitoring available in the Gulf of Lions, the temperature and salinity properties of the water column are accessible at a high temporal resolution. The temperature and salinity sections in Figure 4.15 illustrate the invasion of LIW at intermediate depth, and the planned water mass properties reflect that presence. The computation of the planned water mass properties was made with a one-dimensional mixing and oceanic heat storage model developed by Lilly et al. (2003). The water column is vertically mixed and the surface fluxes are assumed to change the vertically averaged temperature and salinity in a constant ratio. Thanks to the 10 years of data available, the model fluxes parameterisation was adjusted for the Gulf of Lions. The bottom sections in Figure 4.15

present the predicted integrated temperature and salinity of a mixed homogeneous water column reaching a particular depth. The properties of the waters formed by the 2018 deep convection event were accurately computed (3 months in advance, calibrated with the advection computed from the time series), as the diagram predicts deep waters with a temperature of 12.995°C and a salinity of 38.505 at 1900 m depth. This tool can provide a valuable estimation of new deep water properties for impact studies on the benthic flora and fauna, which are especially sensitive to brutal environmental changes [Rastelli et al., 2018].

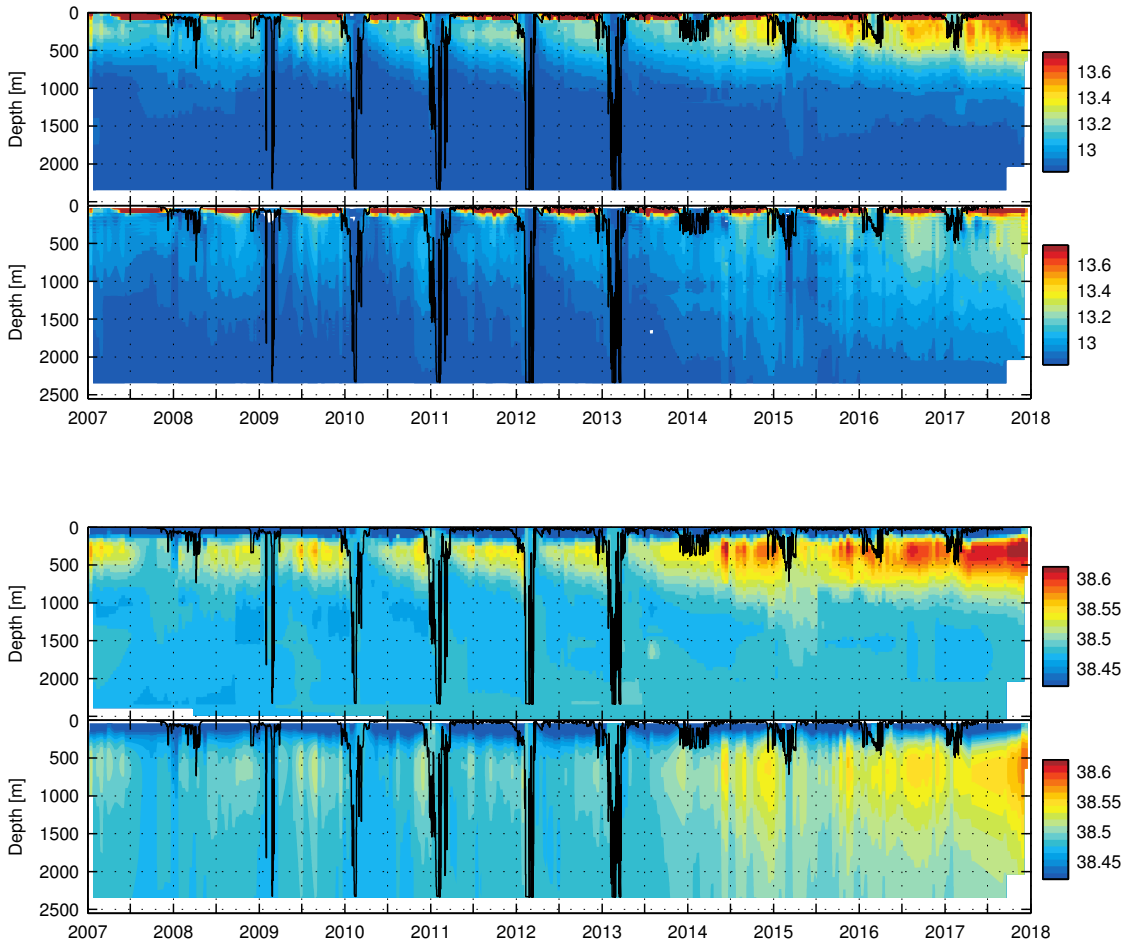

FIGURE 4.15: Temperature and salinity Hovmöller diagrams at the LION (42.04 N 4.68 E) mooring location in Gulf of Lions. All the profiles within a 15km radius of the mooring location are used, as well as the mooring line measurements for this interpolation. The black contour represents the mixed layer depth, computed as in Houpert et al. (2016). For both temperature and salinity, the top diagram represents the observed water column properties, while the bottom one corresponds to the temperature or salinity value of a mixed water column at each depth: if the mixing reaches 1300 m, the properties of the homogeneous layer can be found at 1300 m depth on the diagram, computed with a toolbox from Lilly et al. (2003).

Waldman et al. (2018), from model studies, and Ferron et al. (2017), from observations, both suggest that vertical mixing below coastal currents is more important than

previously inferred and, in the context of a changing Mediterranean with less deep convective events, this mixing may be more important then ever. The fact that the basin was covered in double diffusive thermohaline steps (associated with salt fingers) after 4 years without deep convection may confirm the role of boundary currents in ventilating the interior ocean, as they enhance these vertical gradients.

Conclusions & Perspectives

5.1 Main results

The conception and maintenance of a meta-database of over 600 000 temperature and salinity profiles in the Mediterranean Sea has enabled an extensive monitoring of intermediate and deep layers of the Northwestern Mediterranean Sea .

A focus was put on the 2012/2013 winter, which proved to be an intense convective year that was thoroughly observed. With the coordinated observational effort conducted, a new comprehension view for deep convection was suggested, complementing the Marshall and Schott (1999) description of deep convection. For the first time, as gliders crossed several convective plumes, the mixing they induce was characterised both in terms of their physical and biogeochemical properties. A scaling for the vertical velocities relative to the buoyancy loss from heat fluxes was inferred as $variance(w) = (B_0/f)^{0.86}$, and an equivalent vertical diffusion coefficient of 7 $m^2.s^{-1}$ for a parametrisation of the mixing induced by the plumes was deduced.

The intense warming (0.06°C .$year^{-1}$) and salinification (0.08.$year^{-1}$) representative trends of the LIW in the Western Mediterranean was observed, at similar rates as in the Eastern Basin [Ozer et al., 2016] and in the Sicily Channel [Schroeder et al., 2017]. Indexes were built to monitor the heat and salt contents at intermediate depths. The observational strategy was tested in an OSSE context. The very high temporal and spatial resolution of the profiles collected enabled the detection of a new state of the basin since the winter 2012/2013 which last saw deep convection (until the winter 2017/2018). The crucial role of deep convective events in regulating the Northwestern basin was evidenced, and the respective impacts of changing preconditioning and atmospheric forcing were discussed. In this framework, the future occurrence of deep convective events was discussed, and a prediction tool for the deep water properties was tested with the 2017/2018 deep convection event.

5.2 Perspectives

Of course, this dataset has to be preserved and pursued, and projects monitoring the basin like the French MOOSE or the Spanish "RADMED" and SOCIB "Canales" observational networks have to be sustained, not only to continue time series but also to discover new phenomena. Their continuation will be key for expanding the LIW monitoring to also include biogeochemical parameters. The WIW, the least known Mediterranean water mass [Pinot and Ganachaud, 1999], can now also be easily tracked and characterised

thanks to the automatic detection tool that was devised, and the understanding of their circulation could be investigated. A new glider endurance line between Menorca and Sardinia will help to close the Northwestern Basin and investigate the North Balearic Front's role in preserving the waters formed from one year to the next as preconditioning. This new SMART (Sardinia MAllorca Repeated Transect) program conducted jointly by Italy and Spain will perform the transect twice a year, thus enabling not only the closing of the system previously mentioned but also the monitoring of submesoscale structures as the gliders are equipped with microstructure and biogeochemical sensors. Mooring lines deployed on this same transect could help explore the spreading of the newly formed WMDW, which form a series of layers covering the Western Mediterraneans' floor, but the propagation and mixing of which are not yet fully understood. Furthermore, in this warming and salinifying context, tracking the outflow exiting at Gibraltar and feeding the global ocean will be of central importance. If the waters exiting at Gibraltar change their neutral buoyancy depth because of a potential subsequent change in density, it could have important consequences on the Atlantic circulation. That is why OSSE will be key in the future to assess and sustain programs with global frameworks such as MOOSE.

A special mention has to be made that the observational effort remains coherent and shared, as too much data is lost due to lack of meta-data. With science going in the direction of freely shared data, the effort conducted in collective projects (Coriolis, Argo, EGO...) to harmonise and standardise the data collected is going to be of central importance. With the development of autonomous platforms, more and more data is going to be available. More data means the effort has to be sustained to make the data available and useful, through metadata standards as well as harmonisation.

New sensors (notably biogeochemical) and new instruments will offer opportunities to explore the Mediterranean Sea in more detail. For instance, the convective plumes were only characterised down to the current glider depth limit of 1000 m. With new deep glider technologies (down to 6000 m depth), the vertical structure of the plumes could also be investigated. The deep waters would also be more easily tracked and the deep circulation patterns could be explored (with deep Argo floats as well). Moreover, with the development of microstructure measurements (on gliders and on Vertical Microstructure Profilers), we could be able to quantify the erosion rate of the LIW between the investigated regional boxes.

In the context of a changing Mediterranean, it is essential to assess the observed regime shift over longer periods of time to extract a broader pattern out of it. Are double diffusive steps appearing preferentially after years without deep convection ? Can the changes in stratification possibly too important for deep convection to be triggered ? This case study with only one regime shift observed has to be put in context and winter 2017/2018 having also been a deep convective one, tracking how this episode will impact the basin after 4 years without deep convection will be key in better understanding the regulating role of deep convection. As the deep water properties were effectively predicted, an observational tool could be devised to predict the impact of deep convective years on the benthic population, highly sensitive to changes [Rastelli et al., 2018]. The

fact that convection also occurred in the Ligurian Sea and significantly ventilated the intermediate layers will likely have implications that are worth close monitoring over the upcoming year. With the updated atmospheric forcing, the different years' forcings could be tested on different statuses of the water column in order to predict deep convection or to better characterise the respective roles of preconditioning and atmospheric fluxes in determining the convective depth. The 2017/2018 also seems to have formed localised intermediate waters prior to the bottom reaching event, and understanding how this first episode could have triggered the deep convection later could also be investigated. The numerous observed changes in the different water mass properties could also affect water formation and circulation as a whole and this has to be more thoroughly investigated.

Models at higher resolution than Nemo-Med12 used in this work are also under way and should better represent the deep waters. Process studies as well as climate predictions for deep convection will be more reliable with more trustworthy parameterisations that are currently being devised. In process oriented simulations such as MARS3D, the representation of the convective plumes is promising and should enable more realistic deep water formation. This should also help, jointly with the observations, quantify the forcing versus advection relation in the mixed patch.

The PERLE oceanographic project, at sea as these words are being written, will also be of primal importance, as it will provide premiere observations offering novel perspectives. Thoroughly investigating the formation of the LIW will not only allow an analysis similar to that of deep convection with the DOWEX/DEWEX missions, but also offer an opportunity to use the same LIW tracking strategy that was used in the Northwestern Mediterranean Sea. The considerable increase in the number of profiles should indeed allow such an approach.

Bibliography

[Ambar and Howe, 1979] Ambar, Isabel and M.R. Howe (1979). "Observations of the Mediterranean outflow: mixing in the Mediterranean outflow". In: *Deep Sea Research Part A. Oceanographic Research Papers* 26, pp. 535–554.

[Armi and Zenk, 1984] Armi, Laurence and Walter Zenk (1984). "Large Lenses of Highly Saline Mediterranean Water". In: *Journal of Physical Oceanography* 14.10, pp. 1560–1576. ISSN: 0022-3670, 1520-0485. DOI: 10.1175/1520-0485(1984)014<1560:LLOHSM>2.0.CO;2.

[Armi et al., 1988] Armi, Laurence et al. (1988). "The history and decay of a Mediterranean salt lens". In: *Nature* 333, pp. 649–651. ISSN: 0028-0836. DOI: 10.1038/333649a0.

[Béthoux et al., 1990] Béthoux, J.-P. et al. (1990). "Warming trend in the western Mediterranean deep water". In: *Nature* 347, pp. 660–662. ISSN: 0028-0836. DOI: 10.1038/347660a0.

[Béthoux et al., 1998] Béthoux, J.-P., Bernard Gentili, and Dominique Tailliez (1998). "Warming and freshwater budget change in the Mediterranean since the 1940s, their possible relation to the greenhouse effect". In: *Geophysical Research Letters* 25.7, p. 1023. ISSN: 0094-8276. DOI: 10.1029/98GL00724.

[Béthoux et al., 2002] Béthoux, J.-P. et al. (2002). "Deep water in the western Mediterranean: Peculiar 1999 and 2000 characteristics, shelf formation hypothesis, variability since 1970 and geochemical inferences". In: *Journal of Marine Systems* 33-34, pp. 117–131. ISSN: 09247963. DOI: 10.1016/S0924-7963(02)00055-6.

[Beuvier et al., 2012] Beuvier, Jonathan et al. (2012). "Spreading of the Western Mediterranean Deep Water after winter 2005: Time scales and deep cyclone transport". In: *Journal of Geophysical Research: Oceans* 117, pp. 1–70. ISSN: 21699291. DOI: 10.1029/2011JC.

[Bianchi and Morri, 2000] Bianchi, N and C Morri (2000). "Marine biodiversity of the Mediterranean Sea: situation, problems and prospects for future research". In: *Marine Pollution Bulletin* 40.5, pp. 367–376. ISSN: 0025326X. DOI: 10.1016/S0025-326X(00)00027-8.

[Birol et al., 2010] Birol, Florence, M. Cancet, and Claude Estournel (2010). "Aspects of the seasonal variability of the Northern Current (NW Mediterranean Sea) observed by altimetry". In: *Journal of Marine Systems* 81.4, pp. 297–311. ISSN: 0924-7963. DOI: 10.1016/j.jmarsys.2010.01.005.

[Borzelli et al., 2009] Borzelli, Gian Luca Eusebi et al. (2009). "Eastern mediterranean transient and reversal of the Ionian Sea circulation". In: *Geophysical Research Letters* 36.15. ISSN: 00948276. DOI: 10.1029/2009GL039261.

[Bosse, thesis, 2015] Bosse, Anthony (thesis, 2015). "Circulation générale et couplage physique-biogéochimie à (sous-)mésoéchelle en Méditerranée Nord-occidentale à partir de données in situ". PhD thesis. Université Pierre et Marie Curie, Paris. URL: http://www.theses.fr/2015PA066451/document.

[Bosse et al., 2015] Bosse, Anthony et al. (2015). "Spreading of Levantine Intermediate Waters by submesoscale coherent vortices in the northwestern Mediterranean Sea as observed with gliders". In: *Journal of Geophysical Research: Oceans* 120, pp. 1599–1622. ISSN: 2169-9291. DOI: 10.1002/2014JC010263.

[Bosse et al., 2016] Bosse, Anthony et al. (2016). "Scales and dynamics of submesoscale coherent vortices formed by deep convection in the northwestern Mediterranean Sea". In: *Journal of Geophysical Research: Oceans*, n/a–n/a. ISSN: 2169-9291. DOI: 10.1002/2016JC012144. URL: http://dx.doi.org/10.1002/2016JC012144.

[Bosse et al., 2017] Bosse, Anthony et al. (2017). "A submesoscale coherent vortex in the Ligurian Sea: From dynamical barriers to biological implications". In: *Journal of Geophysical Research: Oceans*.

[Broecker, 1991] Broecker, Wallace S. (1991). "The great ocean conveyer". In: *Oceanography* 4, pp. 79–89. ISSN: 19448007. DOI: 10.1002/2014GL059707.

[Bryden et al., 1994] Bryden, Harry L., Julio Candela, and Thomas H. Kinder (1994). "Exchange through the Strait of Gibraltar". In: *Progress in Oceanography* 33, pp. 201–248. ISSN: 00796611. DOI: 10.1016/0079-6611(94)90028-0.

[Canals et al., 2006] Canals, Miquel et al. (2006). "Flushing submarine canyons." In: *Nature* 444.7117, pp. 354–357. ISSN: 0028-0836. DOI: 10.1038/nature05271.

[Candela, 2001] Candela, Julio (2001). "Chapter 5.7 Mediterranean water and global circulation". In: *International Geophysics* 77.C. ISSN: 00746142. DOI: 10.1016/S0074-6142(01)80132-7.

[Carniel et al., 2008] Carniel, Sandro et al. (2008). "Double-diffusive layers in the Adriatic Sea". In: *Geophysical Research Letters* 35.

[Cauchy et al., 2014] Cauchy, Pierre et al. (2014). "Passive acoustics embedded on gliders : Weather observation through ambient noise". In: *The Journal of the Acoustical Society of America* 135.4.

[Cauchy et al., 2018] Cauchy, Pierre et al. (2018). "Wind speed measured from underwater gliders using passive acoustics". In: *Journal of Atmospheric and Oceanic Technology*.

[Conan et al., 2018] Conan, Pascal et al. (2018). "Preface to the Special Section: Dense water formations in the North Western Mediterranean: from the physical forcings to the biogeochemical consequences". In: *Journal of Geophysical Research: Oceans*.

[Conkright et al., 2002] Conkright, M et al. (2002). "World Ocean Database 2001 and World Ocean Atlas 2001". In: *AGU Fall Meeting Abstracts* -1, p. 0220.

[Coppola et al., 2017] Coppola, Laurent et al. (2017). "Observation of oxygen ventilation into deep waters through targeted deployment of multiple Argo-O 2 floats in the north-western Mediterranean Sea in 2013". In: *Journal of Geophysical Research: Oceans* 122.

[Cowley et al., 2013] Cowley, Rebecca et al. (2013). "Biases in Expendable Bathythermograph Data: A New View Based on Historical Side-by-Side Comparisons". In: *Journal of Atmospheric and Oceanic Technology* 30, pp. 1195–1225.

[Damien et al., 2017] Damien, Pierre et al. (2017). "Modeling postconvective submesoscale coherent vortices in the northwestern Mediterranean Sea". In: *Journal of Geophysical Research: Oceans*.

[Davis et al., 2002] Davis, Russ E., Charles C. Eriksen, and Clayton P. Jones (2002). "Autonomous Buoyancy-driven underwater gliders". In: *G. Griffiths [ed.], The technology and applications of autonomous underwater vehicles. Taylor and Francis*, pp. 37–58. DOI: doi:10.1201/9780203522301.ch3.

[Domingues et al., 2008] Domingues, Catia et al. (2008). "Improved estimates of upper-ocean warming and multi-decadal sea-level rise". In: *Nature* 453, pp. 1090–3.

[Donoso et al., 2017] Donoso, Katty et al. (2017). "Zooplankton community response to the winter 2013 deep convection process in the NW Mediterranean Sea". In: *Journal of Geophysical Research: Oceans*.

[D'Ortenzio and Ribera d'Alcalà, 2008] D'Ortenzio, F. and M. Ribera d'Alcalà (2008). "On the trophic regimes of the Mediterranean Sea: a satellite analysis". In: *Biogeosciences Discussions* 5.4, pp. 2959–2983. ISSN: 17264189. DOI: 10.5194/bgd-5-2959-2008.

[D'Ortenzio et al., 2005] D'Ortenzio, Fabrizio et al. (2005). "Seasonal variability of the mixed layer depth in the Mediterranean Sea as derived from in situ profiles". In: *Geophysical Research Letters* 32, pp. 1–4. ISSN: 00948276. DOI: 10.1029/2005GL022463.

[D'Ortenzio et al., 2014] D'Ortenzio, Fabrizio et al. (2014). "Observing mixed layer depth, nitrate and chlorophyll concentrations in the northwestern Mediterranean: A combined satellite and NO3 profiling floats experiment". In: *Geophysical Research Letters* 41.18, pp. 6443–6451. ISSN: 00948276. DOI: 10.1002/2014GL061020. URL: http://doi.wiley.com/10.1002/2014GL061020.

[Drobinski et al., 2016] Drobinski, Philippe et al. (2016). "Lagrangian dynamics of the mistral during the HyMeX SOP2". In: *Journal of Geophysical Research: Atmospheres* 122.

[Durante et al., 2016] Durante, Sara et al. (2016). "Deep circulation and mixing in the Tyrrhenian sea: more than 10 years of data". In: *CIESM 2016 conference*.

[Durrieu de Madron et al., 2005] Durrieu de Madron, X. et al. (2005). "Comments on "Cascades of dense water around the world ocean"". In: *Progress in Oceanography* 64.1, pp. 83–90. ISSN: 00796611. DOI: 10.1016/j.pocean.2004.08.004. URL: http://linkinghub.elsevier.com/retrieve/pii/S0079661105000200.

[Durrieu de Madron et al., 2013] Durrieu de Madron, X. et al. (2013). "Interaction of dense shelf water cascading and open-sea convection in the northwestern Mediterranean during winter 2012". In: *Geophysical Research Letters* 40.7, pp. 1379–1385. ISSN: 1944-8007. DOI: 10.1002/grl.50331. URL: http://dx.doi.org/10.1002/grl.50331.

[Durrieu de Madron et al., 2011] Durrieu de Madron, Xavier et al. (2011). "Marine ecosystems' responses to climatic and anthropogenic forcings in the Mediterranean".

In: *Progress in Oceanography* 91.2, pp. 97–166. ISSN: 00796611. DOI: 10.1016/j.pocean.2011.02.003.

[E. Gill, 1982] E. Gill, Adrian (1982). *Atmosphere-Ocean Dynamic*. Vol. 30, p. 662.

[Estournel et al., 2016a] Estournel, C et al. (2016a). "High resolution modeling of dense water formation in the north-western Mediterranean during winter 2012-2013: Processes and budget". In: *Journal of Geophysical Research: Oceans*.

[Estournel et al., 2016b] Estournel, Claude et al. (2016b). "HyMeX-SOP2, the field campaign dedicated to dense water formation in the north-western Mediterranean". In: *Oceanography*.

[Ferron et al., 2017] Ferron, Bruno et al. (2017). "How important are diapycnal mixing and geothermal heating for the deep circulation of the Western Mediterranean?: Mixing and Mediterranean overturning". In: *Geophysical Research Letters*.

[Fieux, 2010] Fieux, Michèle (2010). *L'Océan planétaire*, pp. 190–208.

[Font et al., 2007] Font, Jordi et al. (2007). "Sequence of hydrographic changes in NW Mediterranean deep water due to the exceptional winter of 2005". In: *Scientia Marina* 71.

[Frajka-Williams et al., 2014] Frajka-Williams, Eleanor, Peter B. Rhines, and Charles C. Eriksen (2014). "Horizontal Stratification during Deep Convection in the Labrador Sea". In: *Journal of Physical Oceanography*. ISSN: 0022-3670. DOI: 10.1175/JPO-D-13-069.1.

[Gacic et al., 2010] Gacic, M. et al. (2010). "Can internal processes sustain reversals of the ocean upper circulation? The Ionian Sea example". In: *Geophysical Research Letters* 37.9. ISSN: 00948276. DOI: 10.1029/2010GL043216.

[Garau et al., 2011] Garau, Bartolomé et al. (2011). "Thermal Lag Correction on Slocum CTD Glider Data". In: *Journal of Atmospheric and Oceanic Technology* 28.9, pp. 1065–1071. ISSN: 0739-0572. DOI: 10.1175/JTECH-D-10-05030.1. URL: http://journals.ametsoc.org/doi/abs/10.1175/JTECH-D-10-05030.1.

[Gascard and Richez, 1985] Gascard, J.C. and C. Richez (1985). "Water masses and circulation in the Western Alboran sea and in the Straits of Gibraltar". In: *Progress in Oceanography* 15.3, pp. 157–216. ISSN: 00796611. DOI: 10.1016/0079-6611(85)90031-X. URL: http://www.sciencedirect.com/science/article/pii/007966118590031X.

[Gascard, 1978] Gascard, Jean-Claude (1978). "Mediterranean deep water formation baroclinic instability and oceanic eddies". In: *Oceanologica Acta* 1.3, pp. 315–330.

[Gascard and Clarke, 1983] Gascard, Jean-Claude and R. Allyn Clarke (1983). "The Formation of Labrador Sea Water. Part II. Mesoscale and Smaller-Scale Processes". In: *Journal of Physical Oceanography* 13, pp. 1779–1797. ISSN: 0022-3670. DOI: 10.1175/1520-0485(1983)013$<$1779:TFOLSW$>$2.0.CO;2.

[Gasparini et al., 2005] Gasparini, Gian Pietro et al. (2005). "The effect of the Eastern Mediterranean Transient on the hydrographic characteristics in the Strait of Sicily and in the Tyrrhenian Sea". In: *Deep-Sea Research Part I: Oceanographic Research Papers* 52.6, pp. 915–935. ISSN: 09670637. DOI: 10.1016/j.dsr.2005.01.001. URL: http://www.sciencedirect.com/science/article/pii/S0967063705000348.

[Gačić et al., 2011] Gačić, Miroslav et al. (2011). "On the relationship between the decadal oscillations of the northern Ionian Sea and the salinity distributions in the eastern Mediterranean". In: *Journal of Geophysical Research: Oceans* 116, pp. 1–9. ISSN: 21699291. DOI: 10.1029/2011JC007280.

[Giordani et al., 2017] Giordani, Herve et al. (2017). "A PV-approach for dense water formation along fronts: Application to the Northwestern Mediterranean". In: *Journal of Geophysical Research: Oceans* 122, pp. 995–1015.

[Giorgi, 2006] Giorgi, F (2006). "Climate change Hot-Spots". In: *Geophys. Res. Let* 33doi, pp. 101029/.

[Gouretski and Franco, 2010] Gouretski, Viktor and Reseghetti Franco (2010). "On depth and temperature biases in bathythermograph data: Development of a new correction scheme based on analysis of a global ocean database". In: *Deep Sea Research Part I: Oceanographic Research Papers* 57, pp. 812–833.

[Gouretski and Koltermann, 2007] Gouretski, Viktor and K Koltermann (2007). "How much is ocean really warming?" In: *Geophys. Res. Lett* 34.

[Gower, 2015] Gower, Jim (2015). "A sea surface height control dam at the Strait of Gibraltar". In: *Natural Hazards* 78.

[Grignon et al., 2010] Grignon, L. et al. (2010). "Importance of the variability of hydrographic preconditioning for deep convection in the Gulf of Lion, NW Mediterranean". In: *Ocean Science* 6.2, pp. 573–586. DOI: 10.5194/os-6-573-2010. URL: http://www.ocean-sci.net/6/573/2010/.

[Hamon et al., 2012] Hamon, Mathieu, Gilles Reverdin, and Pierre-Yves Traon (2012). "Empirical Correction of XBT Data". In: *Journal of Atmospheric and Oceanic Technology* 29, pp. 960–973.

[Herrmann et al., 2017] Herrmann, Marine et al. (2017). "Long-term monitoring of ocean deep convection using multisensors altimetry and ocean color satellite data". In: *Journal of Geophysical Research: Oceans*.

[Heslop et al., 2012] Heslop, Emma E. et al. (2012). "Autonomous underwater gliders monitoring variability at choke points in our ocean system: A case study in the Western Mediterranean Sea". In: *Geophysical Research Letters* 39, pp. 1–6. ISSN: 00948276. DOI: 10.1029/2012GL053717.

[Houpert et al., 2015] Houpert, L. et al. (2015). "Seasonal cycle of the mixed layer, the seasonal thermocline and the upper-ocean heat storage rate in the Mediterranean Sea derived from observations". In: *Progress in Oceanography* 132, pp. 333–352. ISSN: 0079-6611. DOI: 10.1016/j.pocean.2014.11.004. URL: http://www.sciencedirect.com/science/article/pii/S0079661114001797.

[Houpert et al., 2016] Houpert, L. et al. (2016). "Observations of open-ocean deep convection in the northwestern Mediterranean Sea: Seasonal and interannual variability of mixing and deep water masses for the 2007-2013 period". In: *Journal of Geophysical Research: Oceans*, n/a–n/a. ISSN: 2169-9291. DOI: 10.1002/2016JC011857. URL: http://dx.doi.org/10.1002/2016JC011857.

[Houpert, 2013] Houpert, Loïc (2013). "Contribution to the Study of Transfer Processes from the Surface to the Deep Ocean in the Mediterranean Sea using in situ Measurements". PhD thesis. Université de Perpignan.

[Hurrell et al., 2001] Hurrell, J.W, Yochanan Kushnir, and Martin Visbeck (2001). "The North Atlantic Oscillation". In: *Science (New York, N.Y.)* 291, pp. 603–5. DOI: 10.1126/science.1058761.

[Ishii and Kimoto, 2009] Ishii, Masayoshi and Masahide Kimoto (2009). "Reevaluation of historical ocean heat content variations with time-varying XBT and MBT depth bias". In: *Journal of Oceanography* 65, pp. 287–299.

[Iudicone, 2003] Iudicone, Daniele (2003). "Distribution and mixing of intermediate water masses in the Channel of Sicily (Mediterranean Sea)". In: *Journal of Geophysical Research* 108. ISSN: 0148-0227. DOI: 10.1029/2002JC001647.

[Ivanov et al., 2004] Ivanov, V. V. et al. (2004). "Cascades of dense water around the world ocean". In: *Progress in Oceanography* 60.1, pp. 47–98. ISSN: 00796611. DOI: 10.1016/j.pocean.2003.12.002.

[J. Rohling and L. Bryden, 1992] J. Rohling, E and Harry L. Bryden (1992). "Man-Induced Salinity and Temperature Increases in Western Mediterranean Deep Water". In: *Journal of Geophysical Research* 97, pp. 11191–11198.

[Jones and Marshall, 1997] Jones, Helen and John Marshall (1997). "Restratification after Deep Convection". In: *Journal of Physical Oceanography* 27, pp. 2276–2287. ISSN: 0022-3670. DOI: 10.1175/1520-0485(1997)027$<$2276:RADC$>$2.0.CO;2.

[Jordà et al., 2017] Jordà, Gabriel et al. (2017). "The Mediterranean Sea Heat and Mass Budgets : Estimates, Uncertainties and Perspectives". In: *Progress in Oceanography* 156.

[Juza et al., 2013] Juza, Mélanie et al. (2013). "Origin and pathways of Winter Intermediate Water in the Northwestern Mediterranean Sea using". In: *J. Geophys. Res.* DOI: 10.1002/2013JC009231.

[Juza et al., 2018] Juza, Mélanie et al. (2018). "Characterization of changes in Western Intermediate Water properties enabled by an innovative geometry-based detection approach". In: *Journal of Marine Systems* 191. DOI: 10.1016/j.jmarsys.2018.11.003.

[Kessouri et al., 2018] Kessouri, Faycal et al. (2018). "Vertical Mixing Effects on Phytoplankton Dynamics and Organic Carbon Export in the Western Mediterranean Sea". In: *Journal of Geophysical Research: Oceans*.

[Killworth, 1983] Killworth, P. D. (1983). "Deep convection in the world ocean". In: *Reviews of Geophysics and Space Physics* 21.1, pp. 1–26.

[Kinder and Parrilla, 1987] Kinder, T. H. and G. Parrilla (1987). "Yes, some of the Mediterranean outflow does comes from great depth". In: *Journal of Geophysical Research* 92.6, pp. 2901–2906.

[Lacombe et al., 1985] Lacombe, H., P. Tchernia, and L. Gamberoni (1985). "Variable bottom water in the Western Mediterranean basin". In: *Prog. Oceanogr.* 14, pp. 319–338.

[Lascaratos et al., 1999] Lascaratos, Alex et al. (1999). "Recent changes in deep water formation and spreading in the eastern Mediterranean Sea: a review". In: *Prog.*

Oceanogr. 44.1–3, pp. 5–36. ISSN: 0079-6611. DOI: 10.1016/S0079-6611(99)00019-1. URL: http://www.sciencedirect.com/science/article/pii/S0079661199000191.

[Lavigne et al., 2012] Lavigne, H. et al. (2012). "Towards a merged satellite and in situ fluorescence ocean chlorophyll product". In: *Biogeosciences* 9.6, pp. 2111–2125. ISSN: 17264170. DOI: 10.5194/bg-9-2111-2012.

[Lavigne et al., 2013] Lavigne, Héloïse et al. (2013). "Enhancing the comprehension of mixed layer depth control on the Mediterranean phytoplankton phenology". In: *Journal of Geophysical Research: Oceans* 118, pp. 3416–3430. ISSN: 21699291. DOI: 10.1002/jgrc.20251.

[Leaman and Schott, 1991] Leaman, Kevin D. and Friedrich a. Schott (1991). "Hydrographic Structure of the Convection Regime in the Gulf of Lions: Winter 1987". In: *Journal of Physical Oceanography* 21.4, pp. 575–598. ISSN: 0022-3670. DOI: 10.1175/1520-0485(1991)021$<$0575:HSOTCR$>$2.0.CO;2.

[Lebeaupin Brossier et al., 2017] Lebeaupin Brossier, Cindy et al. (2017). "Dense Water Formation in the North-Western Mediterranean area during HyMeX-SOP2 in 1/36 ocean simulations: Ocean-atmosphere coupling impact". In: *Journal of Geophysical Research: Oceans* 122, pp. 5749–5773.

[Legg and McWilliams, 2001] Legg, Sonya and James C. McWilliams (2001). "Convective Modifications of a Geostrophic Eddy Field". In: *Journal of Physical Oceanography* 31, pp. 874–891. ISSN: 0022-3670. DOI: 10.1175/1520-0485(2001)031<0874:CMOAGE>2.0.CO;2.

[Levitus et al., 2009] Levitus, S et al. (2009). "Global ocean heat content 1955-2008 in light of recently revealed instrumentation problems". In: *Geophysical Research Letters - GEOPHYS RES LETT* 36.

[L'Hévéder et al., 2013] L'Hévéder, Blandine et al. (2013). "A glider network design study for a synoptic view of the oceanic mesoscale variability". In: *Journal of Atmospheric and Oceanic Technology* 30, pp. 1472–1493. ISSN: 07390572. DOI: 10.1175/JTECH-D-12-00053.1.

[Lilly et al., 2003] Lilly, Jonathan et al. (2003). "Observations of the Labrador Sea eddy field [review article]". In: *Progress in Oceanography* 59, pp. 75–176.

[López-Jurado et al., 2005] López-Jurado, José Luís, Cesar González-Pola, and Pedro Vélez-Belchi (2005). "Observation of an abrupt disruption of the long-term warming trend at the Balearic Sea, western Mediterranean Sea, in summer 2005". In: *Geophysical Research Letters* 32.July, pp. 1–4. ISSN: 00948276. DOI: 10.1029/2005GL024430.

[Madec and NEMO Team, 2008] Madec, G. and the NEMO Team (2008). *NEMO ocean engine*. Note du Pôle de modélisation, Institut Pierre-Simon Laplace (IPSL), France.

[Madec et al., 1996] Madec, G. et al. (1996). "Large-Scale Preconditioning of Deep-Water Formation in the Northwestern Mediterranean Sea". In: *Journal of Physical Oceanography* 26, pp. 1393–1408.

[Madec et al., 1991] Madec, Gurvan et al. (1991). "A three-dimensional numerical study of deep-water formation in the northwestern Mediterranean Sea". In: *Journal*

of Physical Oceanography 21, pp. 1349–1371. URL: http://cat.inist.fr/?aModele=afficheN\&cpsidt=5149571.

[Madron et al., 2017] Madron, X. Durrieu de et al. (2017). "Deep sediment resuspension and thick nepheloid layer generation by open-ocean convection". In: *Journal of Geophysical Research: Oceans* 122.3, pp. 2291–2318. ISSN: 2169-9291. DOI: 10.1002/2016JC012062. URL: http://dx.doi.org/10.1002/2016JC012062.

[Malanotte-rizzoli, 2001] Malanotte-rizzoli, Paola (2001). "Current systems in the mediterranean sea". In: *Encyclopedia of Ocean Sciences*, pp. 744–751.

[Mann and Lazier, 2005] Mann, K.H. and J.R.N. Lazier (2005). *Dynamics of marine ecosystems: biological-physical interactions in the oceans*, p. 196.

[Marco Luna et al., 2016] Marco Luna, Gian et al. (2016). "Dense water plumes modulate richness and productivity of deep sea microbes". In: *Environmental Microbiology* 18.

[Margirier et al., 2017] Margirier, Félix et al. (2017). "Characterization of Convective Plumes Associated With Oceanic Deep Convection in the Northwestern Mediterranean From High-Resolution In Situ Data Collected by Gliders". In: *Journal of Geophysical Research: Oceans*.

[Marshall and Schott, 1999] Marshall, John and Friedrich Schott (1999). "Open-ocean convection: Observations, theory, and models". In: *Reviews of Geophysics* 37.1, pp. 1–64. ISSN: 1944-9208. DOI: 10.1029/98RG02739.

[MEDAR, 2002] MEDAR, Group (2002). "MEDATLAS/2002 database: Mediterranean and Black Sea database of temperature salinity and bio-chemical parameters". In:

[MEDOC-Group, 1970] MEDOC-Group, The (1970). "Observation of Formation of Deep Water in the Mediterranean Sea, 1969". In: *Nature* 225, pp. 1037–1040. ISSN: 0028-0836. DOI: 10.1038/2271037a0.

[Mertens and Schott, 1998] Mertens, C. and Friedrich Schott (1998). "Interannual Variability of Deep-Water Formation in the Northwestern Mediterranean". In: *Journal of Physical Oceanography* 28.7, pp. 1410–1424. ISSN: 0022-3670. DOI: 10.1175/1520-0485(1998)028$<$1410:IVODWF$>$2.0.CO;2. URL: http://journals.ametsoc.org/doi/abs/10.1175/1520-0485\%281998\%29028\%3C1410\%3AIVODWF\%3E2.0.CO\%3B2.

[Millot, 1999] Millot, Claude (1999). "Circulation in the Western Mediterranean Sea". In: *J. Mar. Syst.* 20.1-4, pp. 423–442. ISSN: 09247963. DOI: 10.1016/S0924-7963(98)00078-5. URL: http://linkinghub.elsevier.com/retrieve/pii/S0924796398000785.

[Millot, 2013] Millot, Claude (2013). "Levantine Intermediate Water characteristics: an astounding general misunderstanding!" In: *Scientia Marina* 77.June, pp. 217–232. ISSN: 1886-8134. DOI: 10.3989/scimar.03518.13A. URL: http://scientiamarina.revistas.csic.es/index.php/scientiamarina/article/view/1454/1569.

[Millot and Taupier-Letage, 2005a] Millot, Claude and Isabelle Taupier-Letage (2005a). "Additional evidence of LIW entrainment across the Algerian subbasin by mesoscale

eddies and not by a permanent westward flow". In: *Progress in Oceanography* 66.2–4, pp. 231–250. ISSN: 00796611. DOI: 10.1016/j.pocean.2004.03.002. URL: http://www.sciencedirect.com/science/article/pii/S0079661105000728.

[Millot and Taupier-Letage, 2005b] Millot, Claude and Isabelle Taupier-Letage (2005b). "Circulation in the Mediterranean Sea". In: *Hanbook of Environmental Chemistry* 5K, pp. 29–66. DOI: 10.1007/b107143.

[Millot et al., 2006] Millot, Claude et al. (2006). "Large warming and salinification of the Mediterranean outflow due to changes in its composition". In: *Deep-Sea Research Part I: Oceanographic Research Papers* 53, pp. 656–666. ISSN: 09670637. DOI: 10.1016/j.dsr.2005.12.017.

[Ozer et al., 2016] Ozer, Tal et al. (2016). "Interannual thermohaline (1979-2014) and nutrient (2002-2014) dynamics in the Levantine surface and intermediate water masses, SE Mediterranean Sea". In: *Global and Planetary Change*.

[Pinardi and Masetti, 2000] Pinardi, N. and E. Masetti (2000). "Variability of the large scale general circulation of the Mediterranean Sea from observations and modelling: a review". In: *Palaeogeography, Palaeoclimatology, Palaeoecology* 158.3-4, pp. 153–173. ISSN: 00310182. DOI: 10.1016/S0031-0182(00)00048-1. URL: http://linkinghub.elsevier.com/retrieve/pii/S0031018200000481.

[Pinot and Ganachaud, 1999] Pinot, J.-M and A Ganachaud (1999). "The role of winter intermediate waters in the spring-summer circulation of the Balearic Sea - 1. Hydrography and inverse box modeling". In: *Journal of Geophysical Research* 1042, pp. 29843–29864.

[Pinot et al., 1999] Pinot, Jean-Michel et al. (1999). "The role of winter intermediate waters in the spring-summer circulation of the Balearic Sea 2. A sensitivity numerical study". In: *Journal of Geophysical Research* 104, pp. 865–884.

[Poulain et al., 2012] Poulain, Pierre-Marie, Milena Menna, and Elena Mauri (2012). "Surface Geostrophic Circulation of the Mediterranean Sea Derived from Drifter and Satellite Altimeter Data". In: *Journal of Physical Oceanography* 42.6, pp. 973–990. ISSN: 0022-3670. DOI: 10.1175/JPO-D-11-0159.1. URL: http://journals.ametsoc.org/doi/abs/10.1175/JPO-D-11-0159.1.

[Puig et al., 2013] Puig, Pere et al. (2013). "Thick bottom nepheloid layers in the western Mediterranean generated by deep dense shelf water cascading". In: *Progress in Oceanography* 111, pp. 1–23. ISSN: 00796611. DOI: 10.1016/j.pocean.2012.10.003.

[Rastelli et al., 2018] Rastelli, Eugenio et al. (2018). "Rapid response of benthic deep-sea microbes (viruses and prokaryotes) to an intense dense shelf water cascading event in a submarine canyon of the NW Mediterranean Sea". In: *Progress in Oceanography*.

[Roemmich et al., 2009] Roemmich, Dean et al. (2009). "Argo: The Challenge of Continuing 10 Years of Progress". In: *Oceanography* 22.3, pp. 46–55. ISSN: 10428275. DOI: 10.5670/oceanog.2009.65.

[Roether et al., 1996] Roether, Wolfgang et al. (1996). "Recent Changes in Eastern Mediterranean Deep Waters". In: *Science* 271.

[Sabine et al., 2004] Sabine, Christopher L et al. (2004). "The oceanic sink for anthropogenic CO2." In: *Science (New York, N.Y.)* 305.5682, pp. 367–371. ISSN: 0036-8075. DOI: 10.1126/science.1097403.

[Sanchez-Gomez et al., 2011] Sanchez-Gomez, E. et al. (2011). "Evaluation of Mediterranean Sea water and heat budgets simulated by an ensemble of high resolution regional climate models". In: *Climate Dynamics* 37.9-10, pp. 2067–2086. ISSN: 09307575. DOI: 10.1007/s00382-011-1012-6.

[Sánchez-Muros et al., 2018] Sánchez-Muros, Maria et al. (2018). "Mercury contents in relation to biometrics and proximal composition and nutritional levels of fish eaten from the Western Mediterranean Sea (Almería bay)". In: *Marine Pollution Bulletin* 135, pp. 783–789.

[Sanchez-Roman et al., 2018] Sanchez-Roman, Antonio et al. (2018). "Improvements of CMEMS altimetry gridded products on estimates of mesoscale activity in the Mediterranean Sea". In:

[Schroeder et al., 2008a] Schroeder, K. et al. (2008a). "An extensive western Mediterranean deep water renewal between 2004 and 2006". In: *Geophysical Research Letters* 35.18, pp. 1–7. ISSN: 0094-8276. DOI: 10.1029/2008GL035146. URL: http://www.agu.org/pubs/crossref/2008/2008GL035146.shtml.

[Schroeder et al., 2008b] Schroeder, Katrin et al. (2008b). "The circulation of the western Mediterranean Sea in spring 2005 as inferred from observations and from model outputs". In: *Deep-Sea Research Part I: Oceanographic Research Papers* 55, pp. 947–965. ISSN: 09670637. DOI: 10.1016/j.dsr.2008.04.003.

[Schroeder et al., 2010] Schroeder, Katrin et al. (2010). "Abrupt warming and salting of the Western Mediterranean Deep Water after 2005: Atmospheric forcings and lateral advection". In: *Journal of Geophysical Research: Oceans* 115.C8. ISSN: 21699291. DOI: 10.1029/2009JC005749.

[Schroeder et al., 2012] Schroeder, Katrin et al. (2012). "Circulation of the mediterranean sea and its variability". In: *The Climate of the Mediterranean Region*, pp. 187–256. ISBN: 9780124160422. DOI: 10.1016/B978-0-12-416042-2.00003-3.

[Schroeder et al., 2017] Schroeder, Katrin et al. (2017). "Rapid response to climate change in a marginal sea". In: *Scientific Reports* 7.

[Send et al., 1996] Send, Uwe, Jordi Font, and C. Mertens (1996). "Recent observation indicates convection's role in deep water circulation". In: *Eos* 77.7, pp. 61–65. ISSN: 00963941.

[Severin et al., 2017] Severin, Tatiana et al. (2017). "Open-ocean convection process: A driver of the winter nutrient supply and the spring phytoplankton distribution in the Northwestern Mediterranean Sea". In: *Journal of Geophysical Research: Oceans*.

[Shapiro et al., 2003] Shapiro, Ge, J Huthnance, and Vladimir Ivanov (2003). "Dense Water Cascading off the Continental Shelf". In: *Journal of Geophysical Research* 108.

[Smith and Sandwell, 1997] Smith, Walter and David Sandwell (1997). "Global Sea Floor Topography from Satellite Altimetry and Ship Depth Soundings". In: *Science* 277, pp. 1956–1962.

[Somot et al., 2006] Somot, Samuel, F. Sevault, and M. Déqué (2006). "Transient climate change scenario simulation of the Mediterranean Sea for the twenty-first century using a high-resolution ocean circulation model". In: *Climate Dynamics* 27.7-8, pp. 851–879. ISSN: 09307575. DOI: 10.1007/s00382-006-0167-z.

[Somot et al., 2016] Somot, Samuel et al. (2016). "Characterizing, modelling and understanding the climate variability of the deep water formation in the North-Western Mediterranean Sea". In: *Climate Dynamics*. DOI: 10.1007/s00382-016-3295-0.

[Soto-Navarro et al., 2015] Soto-Navarro, J. et al. (2015). "Evaluation of regional ocean circulation models for the Mediterranean Sea at the Strait of Gibraltar: volume transport and thermohaline properties of the outflow". In: *Climate Dynamics* 44, pp. 1277–1292. DOI: 10.1007/s00382-014-2179-4.

[Stommel, 1989] Stommel, H (1989). "The Slocum Mission". In: *Oceanography*, pp. 1–3.

[Stommel et al., 1973] Stommel, Henry, Harry Bryden, and Paul Mangelsdorf (1973). "Does some of the Mediterranean outflow come from great depth?" In: *Pure and Applied Geophysics* 105, pp. 879–889.

[Straneo and Kawase, 1999] Straneo, Fiammetta and Mitsuhiro Kawase (1999). "Comparisons of Localized Convection due to Localized Forcing and to Preconditioning". In: *Journal of Physical Oceanography* 29.1996, pp. 55–68. ISSN: 0022-3670. DOI: 10.1175/1520-0485(1999)029<0055:COLCDT>2.0.CO;2.

[Sverdrup, 1947] Sverdrup, HU (1947). "Wind-Driven Currents in a Baroclinic Ocean; with Application to the Equatorial Currents of the Eastern Pacific". In: *Proceedings of the National Academy of Sciences of the United States of America* 11, pp. 316–326. DOI: 10.1073/pnas.33.11.318.

[Testor and Gascard, 2006] Testor, Pierre and J.-C. C Gascard (2006). "Post-convection spreading phase in the Northwestern Mediterranean Sea". In: *Deep Sea Research Part I* 53.5, pp. 869–893. ISSN: 09670637. DOI: 10.1016/j.dsr.2006.02.004. URL: www.elsevier.com/locate/dsrhttp://linkinghub.elsevier.com/retrieve/pii/S0967063706000550.

[Testor et al., 2010] Testor, Pierre et al. (2010). "Gliders as a component of future observing systems". In: *Proceedings of OceanObs'09: Sustained Ocean Observations and Information for Society (Vol. 2), Venice, Italy, 21-25 September 2009, J. Hall, D.E. Harrison & D. Stammer Eds.* 1. DOI: 10.5270/OceanObs09.cwp.89.

[Testor et al., 2017] Testor, Pierre et al. (2017). "Multi-scale observations of deep convection in the northwestern Mediterranean Sea during winter 2012-2013 from a multi-platform approach". In: *Journal of Geophysical Research: Oceans*.

[Vaquer-Sunyer and Duarte, 2013] Vaquer-Sunyer, Raquel and Carlos Duarte (2013). "Experimental Evaluation of the Response of Coastal Mediterranean Planktonic and Benthic Metabolism to Warming". In: *Estuaries and Coasts* 36, pp. 697–707.

[Visbeck et al., 1996] Visbeck, Martin, John Marshall, and Helen Jones (1996). "Dynamics of Isolated Convective Regions in the Ocean". In: *Journal of Physical Oceanography*. ISSN: 0022-3670. DOI: 10.1175/1520-0485(1996)026<1721:DOICRI>2.0.CO;2.

[Vladoiu et al., 2018] Vladoiu, Anda et al. (2018). "Turbulence in the Sicily Channel from microstructure measurements". In: *Deep Sea Research Part I: Oceanographic Research Papers*.

[Von Schuckmann et al., 2016] Von Schuckmann, Karina et al. (2016). "An imperative to monitor Earth's energy imbalance". In: *Nature Climate Change* 6, pp. 138–144.

[Waldman et al., 2016a] Waldman, Robin et al. (2016a). "Estimating dense water volume and its evolution for the year 2012–2013 in the North-western Mediterranean Sea: An observing system simulation experiment approach". In: *Journal of Geophysical Research: Oceans*. ISSN: 2169-9291. DOI: 10.1002/2016JC011694. URL: http://dx.doi.org/10.1002/2016JC011694.

[Waldman et al., 2016b] Waldman, Robin et al. (2016b). "Modelling the intense 2012–2013 dense water formation event in the northwestern Mediterranean Sea: evaluation with an ensemble simulation approach". In: *Journal of Geophysical Research: Oceans*.

[Waldman et al., 2017] Waldman, Robin et al. (2017). "How does mesoscale impact dense water formation? Answers from an ensemble simulation of the intense 2012–2013 event in the northwestern Mediterranean sea". In: *Journal of Geophysical Research: Oceans*.

[Waldman et al., 2018a] Waldman, Robin et al. (2018a). "On the Chaotic Variability of Deep Convection in the Mediterranean Sea". In: *Geophysical Research Letters* 45.

[Waldman et al., 2018b] Waldman, Robin et al. (2018b). "Overturning the Mediterranean Thermohaline Circulation". In: *Geophysical Research Letters*.

[Wijffels et al., 2008] Wijffels, Susan et al. (2008). "Changing Expendable Bathythermograph Fall Rates and Their Impact on Estimates of Thermosteric Sea Level Rise". In: *Journal of Climate - J CLIMATE* 21, pp. 5657–5672.

[Wolk et al., 2009] Wolk, F et al. (2009). "Turbulence Measurements from a Glider". In: *OCEANS 2009, MTS/IEEE Biloxi - Marine Technology for Our Future: Global and Local Challenges*, pp. 1 –6. ISBN: 9781424449606.

Appendix A

Multiscale Observations of Deep Convection in the Northwestern Mediterranean Sea During Winter 2012-2013 Using Multiple Platforms, Testor P. et al., 2017

AGU PUBLICATIONS

JGR

Journal of Geophysical Research: Oceans

RESEARCH ARTICLE

10.1002/2016JC012671

Special Section:
Dense Water Formations in the North Western Mediterranean: From the Physical Forcings to the Biogeochemical Consequences

Multiscale Observations of Deep Convection in the Northwestern Mediterranean Sea During Winter 2012–2013 Using Multiple Platforms

Pierre Testor[1], Anthony Bosse[2], Loïc Houpert[3], Félix Margirier[1], Laurent Mortier[4], Hervé Legoff[1], Denis Dausse[1], Matthieu Labaste[1], Johannes Karstensen[5], Daniel Hayes[6], Antonio Olita[7], Alberto Ribotti[7], Katrin Schroeder[8], Jacopo Chiggiato[8], Reiner Onken[9], Emma Heslop[10], Baptiste Mourre[10], Fabrizio D'ortenzio[11], Nicolas Mayot[11], Héloise Lavigne[11], Orens de Fommervault[11,12], Laurent Coppola[11], Louis Prieur[11], Vincent Taillandier[11], Xavier Durrieu de Madron[13], Francois Bourrin[13], Gael Many[13], Pierre Damien[14], Claude Estournel[14], Patrick Marsaleix[14], Isabelle Taupier-Letage[15], Patrick Raimbault[15], Robin Waldman[16], Marie-Noelle Bouin[16,17], Hervé Giordani[16], Guy Caniaux[16], Samuel Somot[16], Véronique Ducrocq[16], and Pascal Conan[18]

[1]CNRS-Sorbonne Universités (UPMC Univ. Pierre et Marie Curie, Paris 06)-CNRS-IRD-MNHN, UMR 7159, Laboratoire d'Océanographie et de Climatologie (LOCEAN), Institut Pierre Simon Laplace (IPSL), Observatoire Ecce Terra, Paris, France, [2]Geophysical Institute, University of Bergen and Bjerknes Center for Climate Research, Bergen, Norway, [3]Scottish Association for Marine Science, Oban, Argyll, Scotland, [4]ENSTA–Paristech, Laboratoire d'Océanographie et de Climatologie (LOCEAN), Palaiseau, France, [5]GEOMAR, Kiel, Germany, [6]Oceanography Center, University of Cyprus, Nicosia, Cyprus, [7]Consiglio Nazionale delle Ricerche - Istituto per l'ambiente Marino Costiero (CNR-IAMC) Oristano, Oristano, Italy, [8]Consiglio Nazionale delle Ricerche - Istituto di Scienze Marine (CNR-ISMAR), Venezia, Italy, [9]Helmholtz-Zentrum Geesthacht, Geesthacht, Germany, [10]SOCIB, Mallorca, Spain, [11]Sorbonne Universités (UPMC Univ. Pierre et Marie Curie, Paris 06), UMR 7093, Laboratoire d'Océanographie de Villefranche (LOV), Observatoire Océanologique de Villefranche/mer, France, [12]Departamento de Oceanografa Fisica, Centro de Investigacion Cientfica y de Educacion Superior de Ensenada, Ensenada, Baja California, Mexico, [13]CNRS-Université de Perpignan, Centre de Formation et de Recherche sur les Environnements Mditerranens (CEFREM), Perpignan, France, [14]CNRS-Universit de Toulouse, Laboratoire d'Aerologie (LA), Observatoire Midi-Pyrénées, Toulouse, France, [15]Aix-Marseille Université, Université de Toulon, CNRS, IRD, MIO UM 110, Marseille, France, [16]MétéoFrance/CNRS, CNRM, UMR 3589, Toulouse, France, [17]Ifremer-CNRS-IRD-UBO, LOPS, IUEM, Plouzané, France, [18]Sorbonne Universités (UPMC Univ. Pierre et Marie Curie, Paris 06), UMR 7093, Laboratoire d'Océanographie Microbienne (LOMIC), Observatoire Océanologique de Banyuls/mer, France

Abstract During winter 2012–2013, open-ocean deep convection which is a major driver for the thermohaline circulation and ventilation of the ocean, occurred in the Gulf of Lions (Northwestern Mediterranean Sea) and has been thoroughly documented thanks in particular to the deployment of several gliders, Argo profiling floats, several dedicated ship cruises, and a mooring array during a period of about a year. Thanks to these intense observational efforts, we show that deep convection reached the bottom in winter early in February 2013 in a area of maximum $28 \pm 3\ 10^9 m^2$. We present new quantitative results with estimates of heat and salt content at the subbasin scale at different time scales (on the seasonal scale to a 10 days basis) through optimal interpolation techniques, and robust estimates of the deep water formation rate of 2.0 ± 0.2 Sv. We provide an overview of the spatiotemporal coverage that has been reached throughout the seasons this year and we highlight some results based on data analysis and numerical modeling that are presented in this special issue. They concern key circulation features for the deep convection and the subsequent bloom such as Submesoscale Coherent Vortices (SCVs), the plumes, and symmetric instability at the edge of the deep convection area.

Key Points:
- We study deep convection and subsequent bloom in the northwestern Mediterranean Sea based on modern observation techniques
- We provide estimates of mass and energy fluxes over a period of a year in the deep convection area and deep water formation rates
- We highlight small-scale circulation features that are important for deep convection and subsequent bloom and introduce this special issue

Correspondence to:
P. Testor,
testor@locean-ipsl.upmc.fr

Citation:
Testor, P., Bosse, A., Houpert, L., Margirier, F., Mortier, L., Legoff, H., . . . Conan, P. (2018). Multiscale observations of deep convection in the northwestern Mediterranean Sea during winter 2012–2013 using multiple platforms. *Journal of Geophysical Research: Oceans*, *123*, 1745–1776. https://doi.org/10.1002/2016JC012671

Received 30 DEC 2016
Accepted 15 NOV 2017
Accepted article online 14 DEC 2017
Published online 5 MAR 2018

1. Introduction

Open-ocean deep convection is a key process that materially exchanges heat and salt, as well as momentum, between the surface layers and the deep ocean in localized regions of the global ocean and is a major contributor to the thermohaline circulation (Marshall & Schott, 1999). Open-ocean deep convection happens in winter and results in oceanic deep water formation. The Mediterranean Sea, the Weddell Sea, the

Appendix B

Additional figures

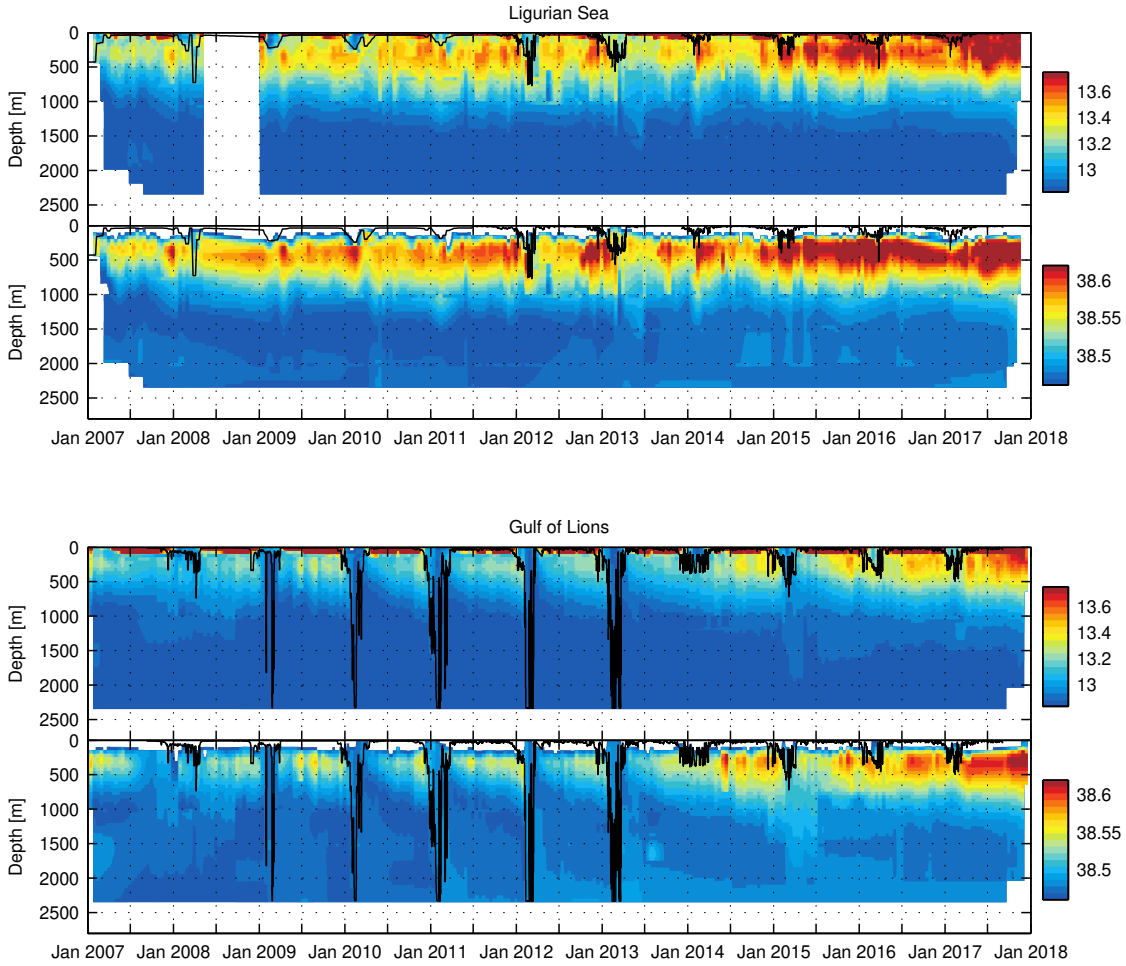

FIGURE B.1: Temperature and Salinity Hovmöller diagrams at the (top) DYFAMED (43.41 N 7.89 E) and (bottom) LION (42.04 N 4.68 E) mooring locations for the Ligurian Sea and the Gulf of Lions respectively (the salinity structure is similar). All the profiles within a 15 km radius of the mooring location are used, as well as the mooring line measurements for this interpolation. The black contour represent the mixed layer depth, computed as in Houpert et al.**Houpert2016** Since 2013 and the absence of deep convection, the LIW has invaded a larger portion of the water column.

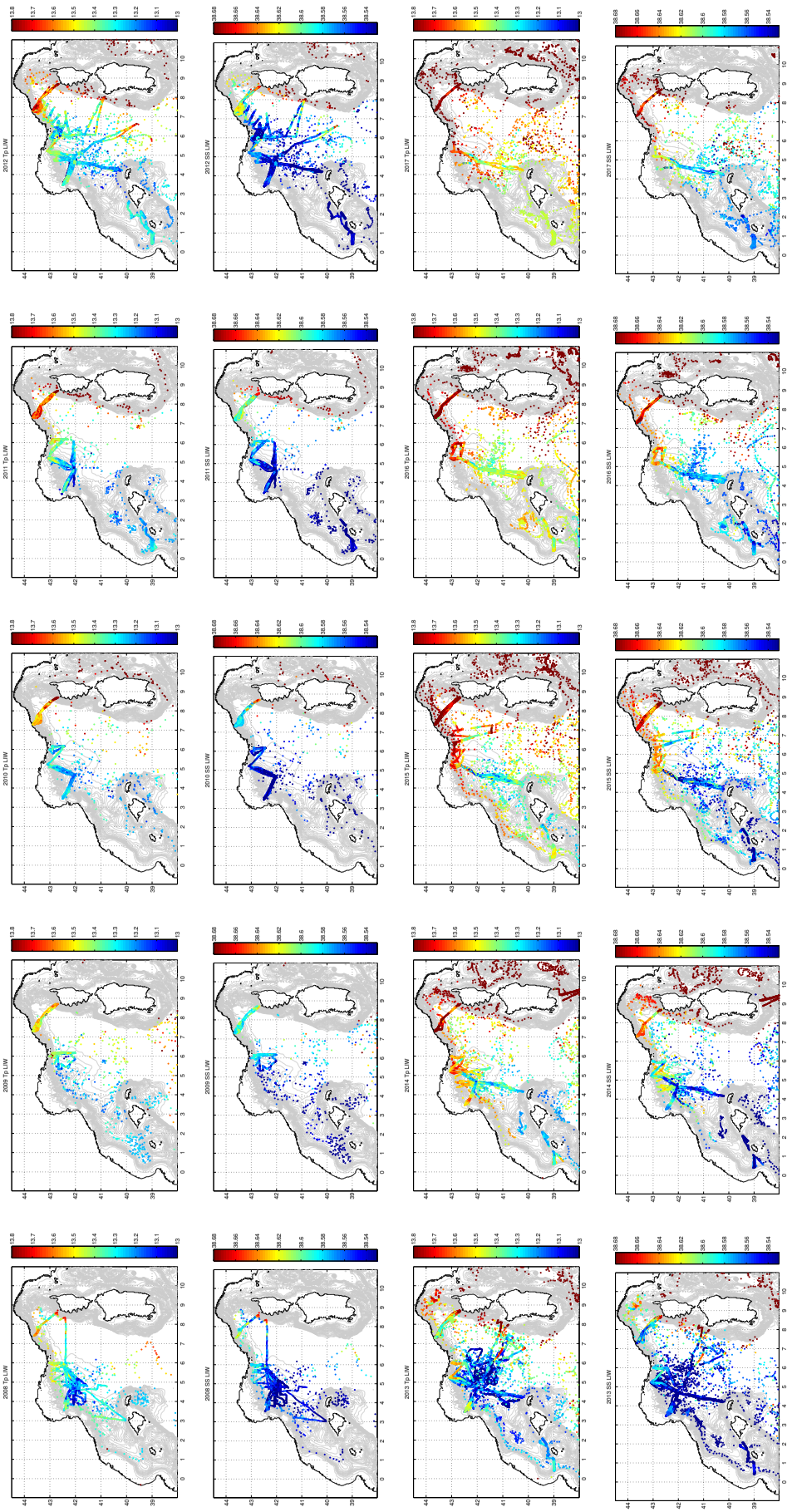

FIGURE B.2: Basinwide LIW temperature and salinity.

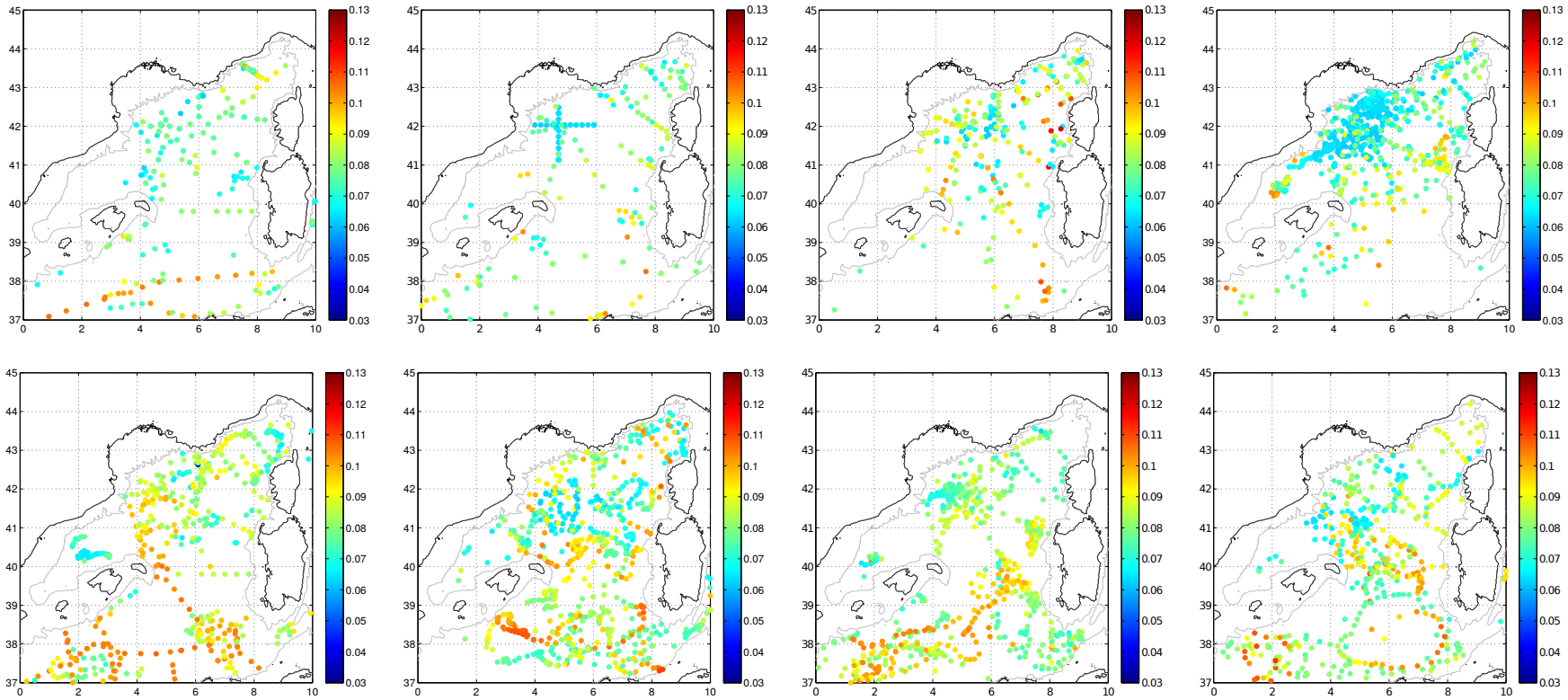

FIGURE B.3: Basinwide stratification index at 1500 m depth during the preconditioning phase, from 2010 top left to 2017 bottom right.

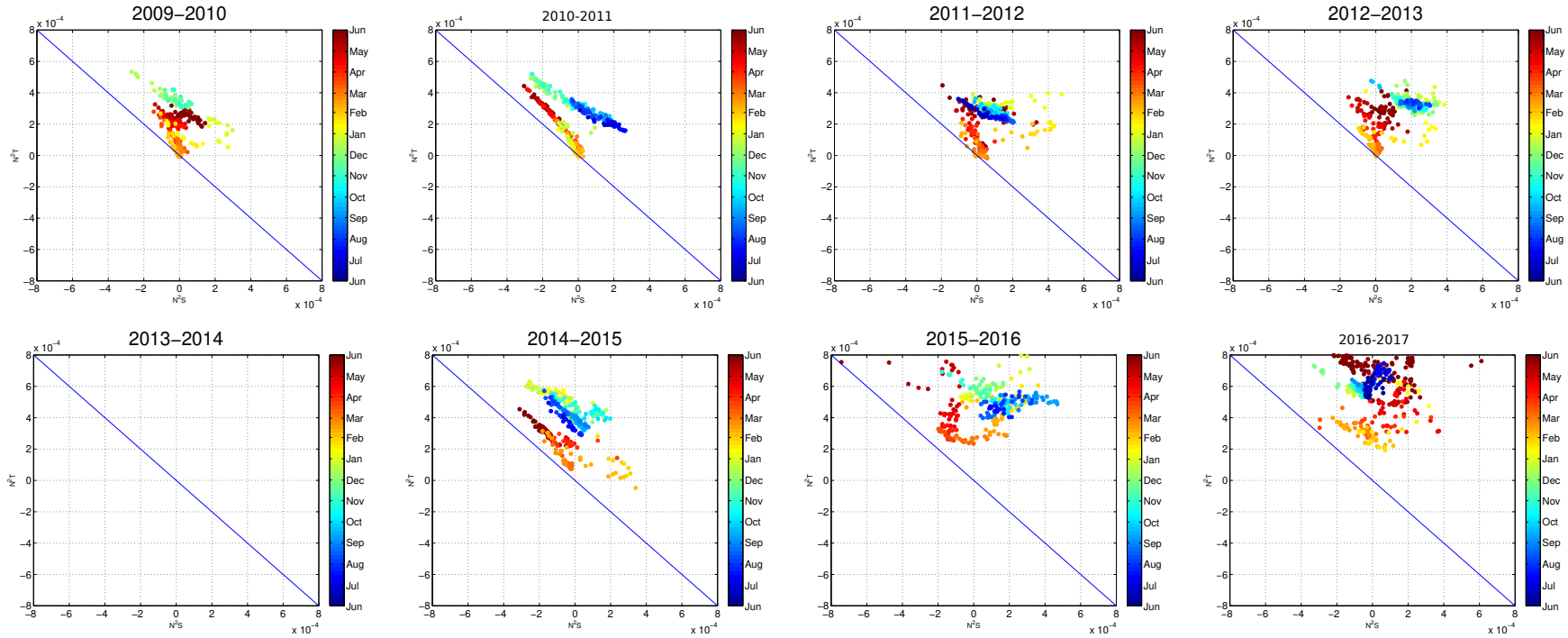

FIGURE B.4: Turner diagram of water column stability in temperature (N^2T) and salinity (N^2S) in the Gulf of Lions. Under the blue line, the water column is gravitationally unstable. Three stable scenarios are possible: if N^2T and N^2S are both positive the temperature and salinity both contribute in stabilising the water column, if N^2T is positive and N^2S negative the stabilising temperature gradient is accompanied by destabilising salinity gradient and vice-versa.

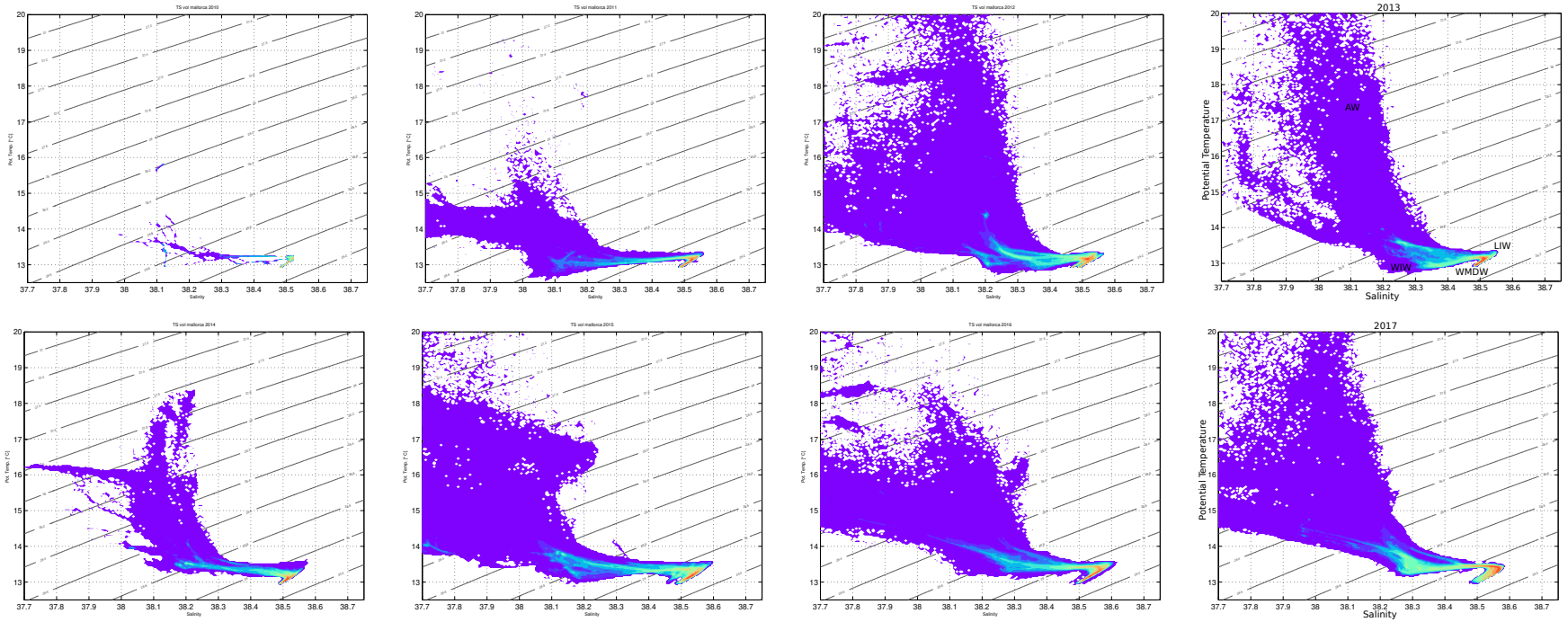

FIGURE B.5: Yearly volumetric θ/S diagrams in the Balearic Sea. Isopycnals are plotted in grey. The red colour vouches for a high concentration of points and thus a high volume of water at said characteristics, purple for a low concentration of points.

Félix MARGIRIER **29/11/2018**

Sujet : Étude de la variabilité physique et biogéochimique des masses d'eaux en Mer Méditerranée

Résumé : L'explosion du nombre d'observations in-situ collectées en Mer Méditerrranée au cours des 15 dernières années offre de nouveaux moyens d'analyse et de suivi des masses d'eaux. L'accent a été mis sur la Méditerranée Nord-Occidentale, siège du phénomène dit de convection profonde et plus intensément observée. Notemment grâce aux observations à hautes résolutions temporelles et spatiales de gliders, un réchauffement et une salinification intense des Eaux Levantines Intermédiaires (LIW) a été mis en évidence. Des indicateurs de variabilité de la LIW ont été construits et sa circulation a été détaillée. En l'absence de convection profonde depuis l'hiver 2012/2013, le bassin a été envahi par ces eaux non diluées dans les eaux profondes et un nouvel état du bassin est observé. Afin de mieux comprendre comment la convection profonde régule la Méditerranée Occidentale, une étude de processus a été effectuée et les importances relatives du préconditionnement océanique et des flux atmosphériques ont été évaluées afin de discuter la possibilité d'évènements convectifs profonds futurs. Pour la première fois, les propriétés physiques et biogéochimiques des plumes convectives ont été caractérisées et s'inscrivent dans le nouveau paradigme de la convection profonde proposé.

Mots clés : Mer Méditerranée, convection profonde, series temporelles, gliders, plumes convectives, vitesses verticales, observations oceanographiques in-situ

Subject : Study of the physical and biogeochemical variability of water masses in the Mediterranean Sea

Abstract : The numerous in-situ observations collected in the Mediterranean Sea over the past 15 years enable a new analysis, and the monitoring of water masses is now possible. A focus has been put on the North-Western Mediterranean Sea where deep convection occurs. Thanks to the numerous high resolution temporal and spatial data collected notably by gliders, an intense warming and salinification of the Levantine Intermediate Water (LIW) was evidenced. Indexes have been built to monitor the LIW and its spreading pattern was further described. This warming and salinification concurs with the absence of deep convective events since winter 2012/2013 and the basin has been invaded at intermediate depth by the new waters. The interplay between the key deep convection phenomenon and the warming at intermediate levels was explored through the mixing agents: for the first time, the physical and biogeochemical properties of convective plumes were characterised and have been integrated in the new paradigm for deep convection. In order to better understand how the deep convective events regulate the basin, the relative importance of oceanic preconditioning and of atmospheric fluxes, as well as the possibility of future deep convective events were discussed.

Keywords : Mediterranean Sea, deep convection, time series, gliders, convective plumes, vertical velocities, oceanographic in-situ observations